

personal buildup for

# Force Motors Ltd.



MTZ worldwide 4/2009, as epaper released on 10.03.2009  
<http://www.mtz-worldwide.com>

content:

page 1: Titelseite. p.1

page 2: Content. p.2

page 3: Editorial. p.3

page 4: F. Kloiber: W\_Abgaswärme\_BMW. p.4-11

page 12: Kai Kuhlbach: Zylinderkopf mit integriertem Abgaskrümmer für Downsizing-Konzepte. p.12-17

page 18: Georg Stampf: Aspects of Gasoline Controlled Auto Ignition Development of a Controller Concept. p.18-25

page 26: F. Thiel: Cylinder Deactivation for Valve Trains with Roller Finger Follower. p.26-31

page 32: H. Büttner: Variable Valve Timing Complementing Hybrid-EGR at Diesel Engines. p.32-39

page 40: F. Schwarzer: Two-stroke/Four-stroke Multicylinder Gasoline Engine for Downsizing Applications. p.40-45

page 46: Less Wear and Oil Consumption through Helical Slide Honing of Engines by Deutz. p.46-51

page 52: Research\_News. p.52-53

page 54: Gunter Knoll, Michael Bargende, Jochen Lang, Ulrich Philipp, Maik Lazzara: Piston Pin in Mixed Friction Contact - Elasto-Hydrodynamic Simulation Theory for Support Analysis. p.54-60

**copyright**

The PDF download of contributions is a service for our subscribers. This compilation was

created individually for Force Motors Ltd.. Any duplication, renting, leasing, distribution and publicreproduction of the material supplied by the publisher, as well as making it publicly available, is prohibited without his permission.

## Thermoelectrics in Automobiles

**Cylinder Head with Integrated Exhaust Manifold**

**Aspects of Gasoline Controlled Auto Ignition**

**Cylinder Deactivation for Valve Trains with Roller Finger Follower**

**Variable Valve Timing Complementing Hybrid-EGR at Diesel Engines**

**Two-stroke/Four-stroke Multicylinder Gasoline Engine**

**Less Wear and Oil Consumption through Helical Slide Honing**

**Simulation Theory of Piston Pin in Mixed Friction Contact**

personal buildup for Force Motors Ltd.



For more information visit:  
[www.MTZ-online.com](http://www.MTZ-online.com)

## COVER STORY

## Thermoelectrics in Automobiles



4

In combustion engines, the majority of the energy is converted into wasted heat. With a thermoelectric generator, a part of this wasted energy can be converted into electric energy. The BMW Group decided to develop a prototype vehicle with a **Thermoelectric Generator** in order to investigate the interactions of this technology with the powertrain as well as further fundamental topics.

## COVER STORY

**Thermo Management:**

- 4 **The Thermoelectric Generator from BMW is Making Use of Waste Heat**  
 Johannes Liebl, Stephan Neugebauer, Andreas Eder, Matthias Linde, Boris Mazar, Wolfgang Stütz

## DEVELOPMENT

**Cylinder Head:**

- 12 **Cylinder Head with Integrated Exhaust Manifold for Downsizing Concepts**  
 Kai Kuhlbach, Jan Mehring, Dirk Borrmann, Rainer Friedfeldt

**Controlling:**

- 18 **Aspects of Gasoline Controlled Auto Ignition – Development of a Controller Concept**  
 Karl Georg Stapf, Dieter Seebach, Stefan Pischinger, Kai Hoffmann, Dirk Abel

**Valve Gear:**

- 26 **Cylinder Deactivation for Valve Trains with Roller Finger Follower**  
 Hermann Hoffmann, Adam Loch, Richard Widmann, Gerhard Kreusen, Daniel Meehsen, Martin Rebbert

- 32 **Variable Valve Timing Complementing Hybrid-EGR at Diesel Engines**  
 Olaf Weber, Volker Jörgl, Wolfgang Bullmer, Steve Wyatt

**New Engines:**

- 40 **Two-stroke/Four-stroke Multicylinder Gasoline Engine for Downsizing Applications**  
 Martin Rebban, John Stokes

**Tribology:**

- 46 **Less Wear and Oil Consumption through Helical Slide Honing of Engines by Deutz**  
 Thomas Hoen, Josef Schmid, Walter Stumpf

## RESEARCH

52 **Research News****Bearing:**

- 54 **Piston Pin in Mixed Friction Contact – Elasto-hydrodynamic Simulation Theory for Support Analysis**  
 Gunter Knoll, Michael Bargende, Jochen Lang, Ulrich Philipp, Maik Lazzara

## RUBRICS

3 **Editorial**3 | 24 **Imprint**

# No End to Globalisation

Dear Reader,

There is no doubt that the economic crisis that we are currently experiencing is a global one. But does that also mean the end of globalisation, as some are predicting? Unfortunately, people tend to have short memories. They would otherwise recall that people were already preaching the “end of the world as we know it” after the collapse of the New Economy and the 9/11 terrorist attacks. In fact, the recession of 2001/2002 was followed by several years of prosperous growth, based to a large extent on emerging economies like China and India buying production resources in the triad in order to manufacture consumer goods for the whole world.

As a publishing house whose roots go far back into the past (the scientific publishing house Springer was founded in 1846, and the magazine ATZ in 1898), we tend to focus less on short-term events than on long-term trends. I believe that the growing together of the global economy will not be reversible as long as people throughout the world continue to strive for prosperity. Whether they are at the Ganges or the Ural, they do so with the same entitlement and the same energy as we did decades ago.

For that reason, we are also launching two new international products over the next few days. The first is the MTZ reference work “Gasoline Engine with Direct Injection”, the first English-language book to be published by Vieweg+Teubner (founded, by the way, in 1786). The book was written by our publisher, Dr. Richard van Basshuysen, an acclaimed expert in the field of direct injection for diesel and spark-ignition engines and one of its strongest proponents. The second new product is the very first edition of ATZ in Chinese, published to mark the Auto Shanghai car show. This will allow us to reach the growing numbers of Chinese car and engine developers – your business partners of tomorrow.

I wish you all the best – and hope that, in spite of all the talk of crisis, you keep your long-term objectives in mind, both professionally and personally.



Johannes Winterhagen  
Frankfurt/Main, 22 February 2009



Johannes Winterhagen  
Editor-in-Chief

**MTZ** WORLDWIDE  
04|2009

Founded 1939 by  
Prof. Dr.-Ing. E. h. Heinrich Buschmann and  
Dr.-Ing. E. h. Prosper L'Orange

Organ of the Fachverband Motoren und  
Systeme im VDMA, Verband Deutscher  
Maschinen- und Anlagenbau e. V.,  
Frankfurt/Main, for the areas combustion  
engines and gas turbines

Organ of the Forschungsvereinigung  
Verbrennungskraftmaschinen e. V. (FVV)

Organ of the Wissenschaftliche  
Gesellschaft für Kraftfahrzeug- und  
Motorentechnik e. V. (WKM)

Organ of the Österreichischer  
Verein für Kraftfahrzeugtechnik (ÖVK)

Cooperation with the STG,  
Schiffbautechnische Gesellschaft e. V.,  
Hamburg, in the area of ship drives  
by combustion engines

#### EDITORS-IN-CHARGE

Dr.-Ing. E. h. Richard van Basshuysen  
Wolfgang Siebenpfeiffer

#### SCIENTIFIC ADVISORY BOARD

Prof. Dr.-Ing. Michael Bargende  
Universität Stuttgart

Prof. Dr. techn. Christian Beidl  
TU Darmstadt

Dipl.-Ing. Wolfgang Dürheimer  
Dr. Ing. h. c. F. Porsche AG

Dr. Klaus Egger

Dipl.-Ing. Dietmar Goericke  
Forschungsvereinigung  
Verbrennungskraftmaschinen e. V.

Prof. Dr.-Ing. Uwe-Dieter Grebe  
GM Powertrain

Dipl.-Ing. Thorsten Herdan  
VDMA-Fachverband Motoren und Systeme

Prof. Dr.-Ing. Heinz K. Junker  
Mahle GmbH

Prof. Dr. Hans Peter Lenz  
ÖVK

Prof. Dr. h. c. Helmut List  
AVL List GmbH

Prof. Dr.-Ing. Stefan Pischinger  
FEV Motorentechnik GmbH

Prof. Dr. Hans-Peter Schmalzl  
BorgWarner Inc.

Prof. Dr.-Ing. Ulrich Seiffert  
TU Braunschweig

Prof. Dr.-Ing. Ulrich Spicher  
WKM

Dr.-Ing. Gerd-Michael Wolters  
MTU Friedrichshafen

# The Thermoelectric Generator from BMW is Making Use of Waste Heat

Even in a highly efficient, state-of-the-art internal combustion engine, the majority of the energy contained in the fuel is converted into wasted heat. With a thermoelectric generator, a part of this wasted energy can be converted into electric energy. So far there are no high temperature thermoelectric materials commercially available. The BMW Group decided to develop a prototype vehicle with a thermoelectric generator in order to investigate the interactions of this technology with the powertrain as well as further fundamental topics.

personal buildup for Force Motors Ltd.



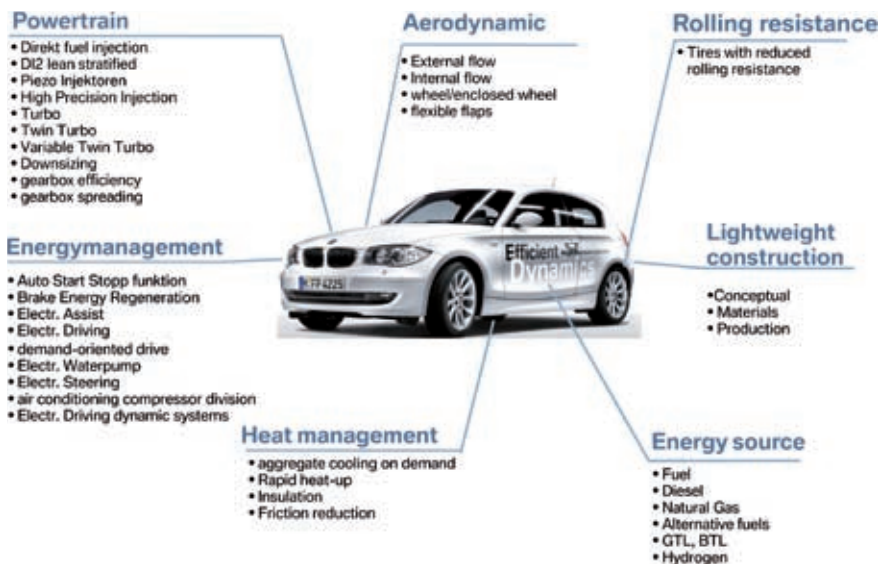


Figure 1: Physical levers for CO<sub>2</sub> reduction

## 1 BMW Efficient Dynamics

With BMW Efficient Dynamics, the BMW Group established a strategy that ensures that even in the future, driving pleasure and environmental sustainability are no contradiction. In the past, reductions were achieved by conventional methods of improving the powertrain. In order to achieve further significant reductions, a

function-oriented total vehicle approach is required.

In order to further reduce CO<sub>2</sub> emissions, the BMW Group began as early as in the year 2000 to consider all physical levers and their interactions with the total vehicle approach. A systematic procedure with corresponding priorities is a prerequisite for new approaches to the solution, **Figure 1**.



## The Authors



Dr.-Ing. E.h. Johannes Liebl is Head of Efficient Dynamics at the BMW Group in Munich (Germany).



Dr.-Ing. Stephan Neugebauer is Head of Thermal Management at the BMW Group in Munich (Germany).



Dr.-Ing. Andreas Eder is Head of Advanced Development and Simulation in the Thermal Management Department at the BMW Group in Munich (Germany).



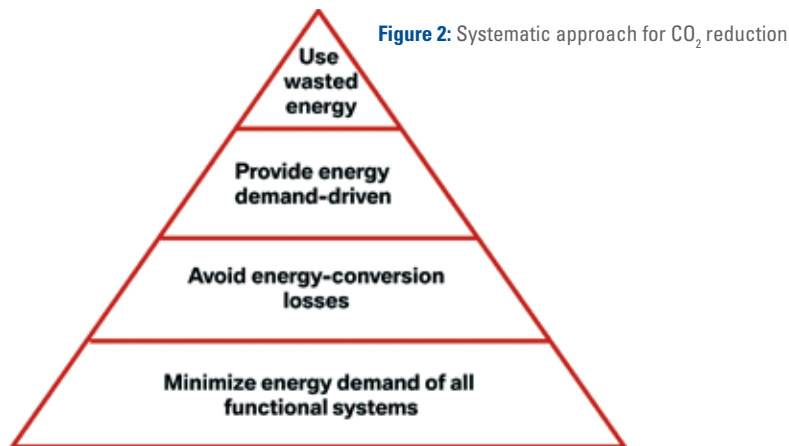
Dr. rer. nat. Matthias Linde is Project Manager for Thermoelectrics in the Thermal Management Department at the BMW Group in Munich (Germany).



Dipl.-Phys. Boris Mazar is a Doctoral Candidate in the Thermal Management Department within the Advanced Development and Simulation Group at the BMW Group in Munich (Germany).



Dipl.-Ing. Wolfgang Stütz is Head of Advanced Development of Diesel Engines at the BMW Group in Steyr (Austria).



What measures are considered for series production has to be decided by each individual car manufacturer. The market has a great influence in this respect with the realization of the product prices, and the chosen measure has to be verified for any interactions with the overall vehicle energy system. It is important to determine where the levers are applied in the functional process chain caused by energy demand, conversion and provision, **Figure 2**.

### 1.1 Examples of the Efficient Dynamics Strategy

The structured and systematic approach was the basis for BMW Efficient Dynamics. The BMW Group has compiled a customized package for each model that every customer receives with the standard equipment of the vehicle, **Figure 3**.

The consistent basis is the reduction of all resistances, such as low rolling resist-

ance and air resistance, in addition to active aerodynamics that control the air intakes, depending on the cooling requirements of the engine or the brakes. Gasoline and diesel engines have been equipped with high-pressure injection systems. An intelligent energy management system provides energy only when it is required with a high priority. For example, an electric pump only circulates the coolant when cooling is actually necessary. Conventional, mechanically driven water pumps, on the other hand, are pumping continuously. In contrast to hydraulic power steering, electrically operated power steering only demands energy when the driver is actually changing direction and not when driving in a straight line. If the air-conditioning compressor is not being used, it is completely disconnected from the engine by means of a clutch mechanism and does not run in idle mode via the belt drive.



**Figure 3:** BMW 1 series with Efficient Dynamics technology

Even in highly efficient engines it is more energy-efficient to switch them off completely when no mechanical energy is required, e.g. when stopped at traffic lights. By intelligently controlling the generator, it has further been possible to recover a portion of the kinetic energy during deceleration of the vehicle.

The products of the BMW Group have tailor-made CO<sub>2</sub> packages selected from this overall package to fit the individual model character. CO<sub>2</sub> reductions of over 20 % have been possible. The BMW Group has thus been setting the standard in the automotive industry for more than two years in this respect.

### 1.2 Customer Orientation

It is not enough, however, to verify these measures in the approval test. Eventually, it is important to proof the effectiveness of the measures during customer driving. Besides the type of road, the driving style, the traffic flow and the actual ambient conditions, the energy demanded by auxiliary consumer loads is an important factor. In order to offer the customers an efficient driving experience, the BMW Efficient Dynamics concept also offers a gearshift indicator for particularly low CO<sub>2</sub> emissions and efficient driving routes by means of the navigation system. In addition, the customer analyses show that the customers demand a not inconsiderable quantity of electrical energy, depending on the type of vehicle, which raises the CO<sub>2</sub> emissions.

On average, customers with a BMW 1-series car demand 330 W, those with a BMW 5-series car demand 750 W and those with a BMW 7-series car as much as 1000 W, **Figure 4**. This demand for electricity can add to the energy conversion chain with as much as one additional l fuel consumption per 100 km in normal customer driving operation. The standard brake energy regeneration system provides a proportion of this energy for free. It is the target to meet the remaining requirements with minimal impact on the environment.

## 2 Thermal Recuperation

Even in a highly efficient combustion engine of the latest generation a large proportion of the latent energy contained in the fuel is converted into unused thermal energy. The various ways of using and con-

verting this thermal energy have been discussed in detail in various publications covering basic principles ([1]). Especially the exhaust gas, with its very high temperature level, represents a considerable resource that is only exploited to a very limited extent today (e.g. in the exhaust gas turbocharging or to shorten the engine warm-up time). The conversion of thermal into mechanical energy (e.g. with a steam cycle, see [2]) provides high conversion efficiencies, however the complexity of vehicle integration is high as well. Due to the continually rising demand for electrical energy in the car already described in detail, the conversion of this thermal waste energy into electrical power is a very interesting step toward further efficiency gains of contemporary power trains – in particular in customer operation.

### 2.1 Potential Limits for Waste Heat Recovery

The efficiency of each conversion of thermal energy is physically limited. These limits are described with the 2<sup>nd</sup> law of thermodynamics, which results in the Carnot Process as a limiting process of a machine for the use of a defined amount of heat. From this ideal process you can determine what proportion of the available thermal energy can theoretically be converted, depending on the process temperatures  $T_{hot}$  and  $T_{cold}$ :

$$\eta = 1 - \frac{T_{cold}}{T_{hot}} \quad \text{Eq. (1)}$$

The exhaust temperatures represent the upper limit between 300 °C and 900 °C during operation, depending on the load requirements. In the European approval test NEDC (New European Driving Cycle), only low engine loads are demanded on average. For this reason, the potential limits for using the waste heat (i.e. the proportion of energy that can be converted from the exhaust heat into electrical energy) amount 30 %. In actual customer operation, additional higher load requirements are en-

countered. In this case the usable potential rises to over 60 %, assuming a coolant temperature of 80 °C as the lower limit.

The levels of efficiency of the Carnot process presented here cannot be fully converted for technical reasons. In order to extract the heat from the exhaust system, a heat exchanger is required which can operate at an efficiency of about 65 % assuming a backpressure of 30 mbar to be tolerated at medium-fast inter-urban cruise (approximately 130 km/h) and considering the package and weight limitations of a state-of-the-art vehicle. Considering all these losses, only a few percentage points for improving the consumption are left from the initial 30 to 60 %. If you consider, however, that the potential savings are doubled, provided the thermal loss energy is converted into electricity, as this would otherwise have to be generated via the crankshaft-drive belt-generator route with an efficiency of about 50 %, the potential savings become very attractive on further consideration. The technical potential therefore for this form of use, conversion of heat into electricity, is up to 8 %.

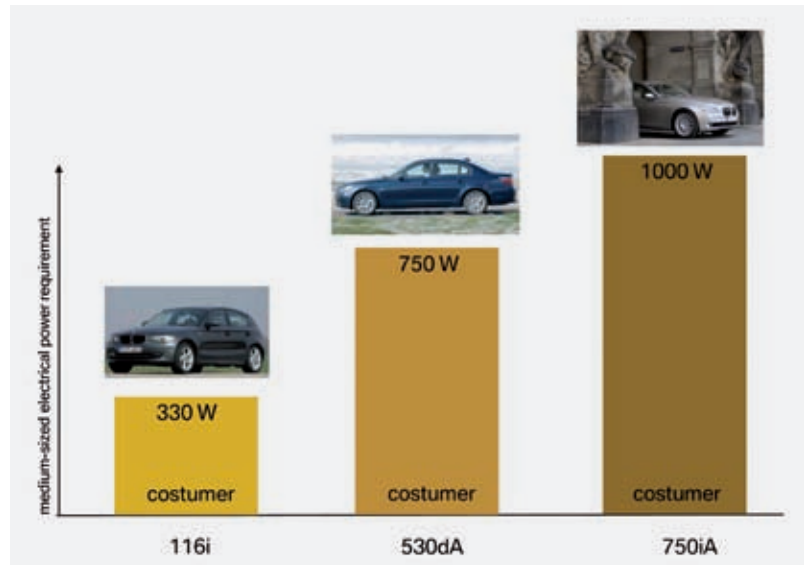


Figure 4: Electrical power demand of a BMW 1, BMW 5 and BMW 7 series

A thermoelectric generator is a suitable method of converting heat into electrical energy in a car. The particular advantage is that no moving parts have to be used for this solid state energy conversion.

### 2.2 The Thermoelectric Generator

The conversion of heat into electricity using a thermoelectric generator (TEG) is based on the effect discovered in 1821 by Thomas Seebeck. This effect describes the generation of an electrical voltage  $U_{therm}$  between the contacts of two conducting materials, provided that these are exposed to a temperature difference  $\Delta T = T_{hot} - T_{cold}$ . The reversal of the Seebeck effect is known as the Peltier effect and describes the creation of a temperature difference when a voltage is applied. The level of the voltage that can be generated per degree Kelvin for a specific material is described with the Seebeck coefficient  $\alpha$  [3], Figure 5.

$$\alpha = U_{thermo} / \Delta T \quad \text{Eq. (2)}$$

Applying the Seebeck coefficient, the dimensionless figure of merit  $ZT$  of a thermoelectric material can be determined depending on  $\alpha$ , the absolute temperature  $T$ , the electrical resistance  $\rho$ , and the thermal conductivity  $\kappa$ .

$$ZT = \alpha^2 T / \rho \kappa \quad \text{Eq. (3)}$$

This  $ZT$  number is a common variable for assessing the effectiveness of a thermo-

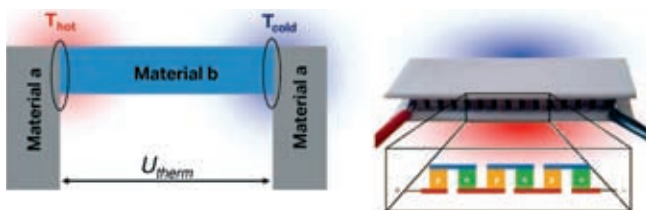
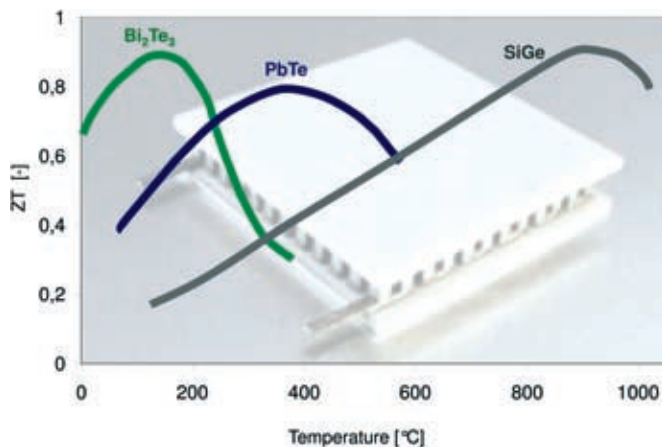


Figure 5: Thermo-electrical effect and technical implementation in a module



**Figure 6:**  
ZT values  
for different  
materials

electric material at a specific temperature  $T$  and contributes to the evaluation of the energy conversion efficiency when converting heat.

$$\eta_{TE} = \frac{(1 + ZT)^{1/2} - 1}{(1 + ZT)^{1/2} + \frac{T_{cold}}{T_{hot}}} \eta_{Carnot} \quad \text{Eq. (4)}$$

As can be seen from this equation, the efficiency approaches that of the Carnot efficiency described above, if the ZT value becomes infinitely large. The challenge facing the development of a high-efficiency thermoelectric material, as can be seen in the definition for ZT, is to combine the intrinsic properties of a good electrical conductivity with a low thermal conductivity. The optimum is achieved with semiconductor materials such as Bismuth telluride ( $\text{Bi}_2\text{Te}_3$ ) for low temperatures and lead telluride (PbTe), or silicon-germanium (SiGe) for higher temperatures, **Figure 6**.

These semiconductors are so heavily doped their transport properties resemble metals. In technical thermoelectric devices, p- and n-doped semiconductors are paired as one thermoelectric couple, **Figure 5**, and the heat flow drives the free electrons (n-doped material) and free holes (p-doped material) from the hot to the cold side and generate a voltage.

In the past 40 years thermoelectric generators have been successfully deployed in space travel (for power generation in space probes for deep-space missions on which sufficient energy can no longer be generated with solar energy). For the heat source a radioactive material has been used which provides sufficiently high thermal energy for several decades [5].

Until now, the low efficiency of the thermoelectric materials with ZT values

of up to 0,9 have limited the commercial use of this technology. Due to new material developments in recent years, in particular through the use of nanotechnology, however, it has been possible to increase significantly the performance of the thermoelectric modules, **Figure 7**.

ZT values of up to 1.7 have already been reported for individual PbTe-based materials [6]. In the development of materials, it is not only important that these materials generally proof a high efficiency, but in addition that they are not damaged by high exhaust gas temperatures and the consequent thermal loads. Although there are still no commercially available materials for the automotive application, the BMW Group has decided to develop a prototype car with a thermoelectric generator, in order to examine the interactions of the system with the powertrain and other important fundamental topics.

## 2.3 Vehicle Integration Concept

The integration of a thermoelectric generator in an exhaust system requires extensive adaptations, depending on the required electrical recuperation performance. The boundary condition for the overall system is represented here by the maximum exhaust backpressure and the maximum temperature to which the thermoelectric materials can be exposed to.

### 2.3.1 TEG Design Concept

The TEG prototype of the BMW Group, which was assembled at the Institute for Vehicle Concepts at the DLR in Stuttgart, consists of three hot gas heat exchangers, 24  $\text{Bi}_2\text{Te}_3$  thermoelectric modules and four coolant heat exchangers with an alternately layered construction, **Figure 8**.

This layered construction is fixed with a pressure of up to 2 MPa using clamps, in order to ensure a defined and reproducible thermal transfer between the hot exhaust side, the thermoelectric modules and the cold side. A diffuser at the TEG intake optimizes the thermal transfer by homogenizing the flow of the exhaust gas.

### 2.3.2 Integration of the TEG

The multi-plate TEG system was integrated as a prototype into the exhaust system of a BMW 535i US with automatic transmission. Due to their material properties, the  $\text{Bi}_2\text{Te}_3$  thermoelectric modules used can only be exposed continuously to a temperature of about 250 °C. In order not only to prevent overheating, but also excessive exhaust pressure due to the hot gas heat exchanger at high operating loads, a bypass was integrated in parallel to the TEG. By

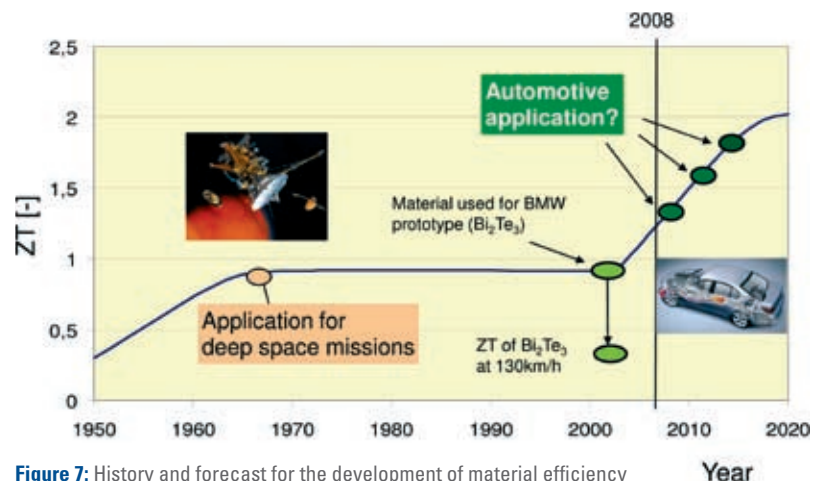


**Figure 7:** History and forecast for the development of material efficiency

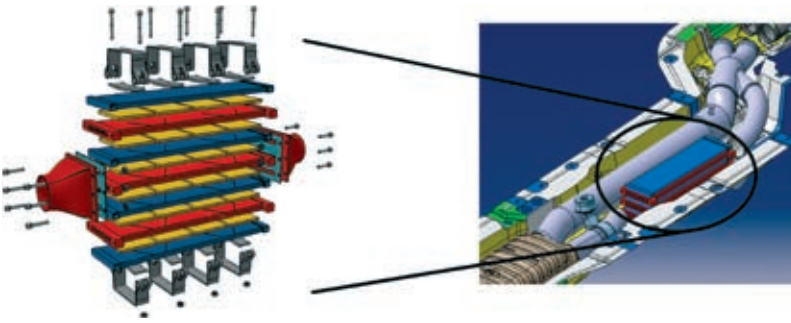


**Figure 8:** Design of the BMW Group TEG and location in the exhaust system

means of two exhaust flaps, one for each hot gas path, the exhaust mass flow is optimal divided between the two flows by means of an automated control, **Figure 9**.

The heat sink in this prototype vehicle was implemented by means of a separate coolant circuit and by two additional radiators installed in the wheelhouse. The decoupling of the TEG by means of an autonomous coolant circuit permits a reproducible analysis of the TEG behaviour during dynamic test drives.

With this setup a TEG output of up to 200 W has been achieved at a constant vehicle speed of 130 km/h. At this operating point and the corresponding exhaust gas temperatures, a temperature of 250 °C is achieved at the thermoelectric material. As shown in Figure 6, the ZT value of the  $\text{Bi}_2\text{Te}_3$  material is very low ( $ZT \approx 0,4$ ) at this temperature, i.e. that already today the power output could be significantly raised by using a PbTe material.

At the Motor Show Geneva 2009, a further developed TEG component was demonstrated in a Rolls-Royce concept vehicle which exhibited an improvement

of more than 50 % in power output with the application of high temperature thermoelectric materials. For this concept, no additional radiators were used and the waste heat of the TEG was directly fed into the main cooling system of the vehicle.

Due to the continuing fluctuating thermal boundary conditions depending on vehicle speed and the corresponding coolant temperature, the power output of a TEG is highly transient which results in significant requirements for the integration into the 12 V vehicle electric system.

The electricity feed of the recuperated thermal energy into the electric system of the vehicle with a nominal voltage of 12 V depends on several parameters. These are primarily the current voltage level, the state-of-charge of the battery or the instantaneous usage, the operating point of the TEG as well as the properties of the coupling device. The coupling device itself can consist of a diode or a DC/DC converter with an appropriate operating strategy in order to ensure a maximum power-point tracking [7].

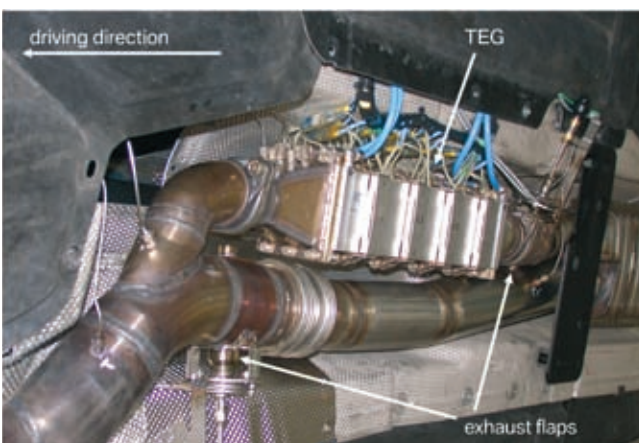


**Figure 9:** Integration of a thermoelectric generator into the exhaust system of a BMW 535i US

## 2.4 Simulation Models

The concept of a thermoelectric generator will only be applicable for series production in a car provided that the benefit is always considered in relation to the complexity in the form of volume, weight and costs. In addition, an increase of the recovered electrical power only results in a reduction of fuel consumption if a restrictive increase in the exhaust back pressure due to the exhaust gas heat exchanger is considered. The integration of a thermoelectric generator into the powertrain of a car thus offers a considerable number of parameters for an overall system optimization. Aspects to be considered include the position of integration in the exhaust system, the integration in the coolant system, the thermoelectric material used and the design of the exhaust heat exchanger, **Figure 10**.

Without the use of a flexible overall system simulation, it is impossible to assess and optimize the recuperation concept. Consequently, at the BMW Group in the course of the development process, a parameterized vehicle model was linked to a finite-volume model of a thermoelectric generator [8, 9]. By specifying a speed profile, and thus a default load for the combustion engine, the vehicle model calculates the thermal boundary conditions for the TEG on the basis of the engine characteristics. Necessary variables are the exhaust temperature and mass flow, as well as the coolant temperature and volume flow that are transferred to the TEG model. In the simulation, the thermoelectric generator is divided into control volumes, not only in flow direction, but also in all functional layers. By balancing all incoming and outgoing thermal fluxes for each control volume, the temperature matrix is solved, **Figure 11**.

On the basis of the determined hot side temperatures of the thermoelectric modules, as well as their conversion efficiency, the recovered electrical power is calculated and transferred back to the vehicle model. Further potential for reducing consumption is obtained by the accelerated warm-up of the powertrain. The heat flow extracted from the exhaust and transferred to the coolant causes the powertrain to reach its optimum operating temperature sooner. The hot gas heat exchanger fitted to the exhaust pipe can have a disadvantageous effect. The integrated fins cause an increase in the ex-

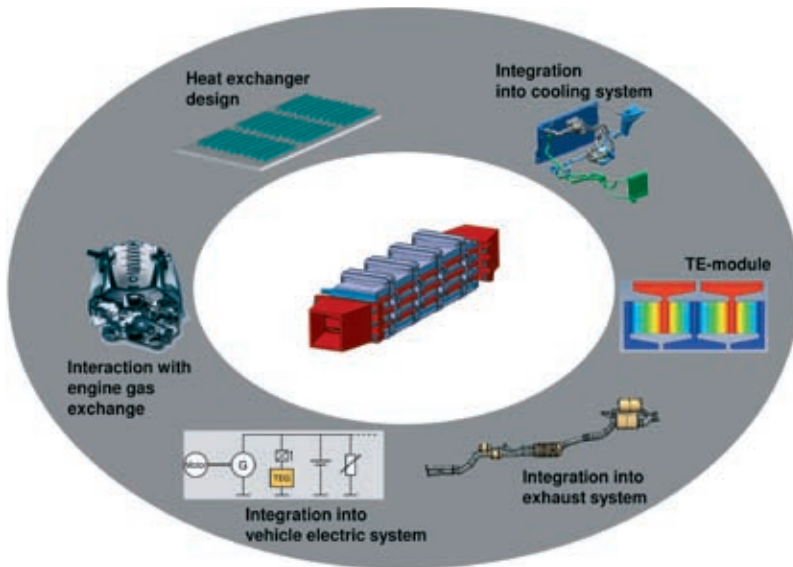


Figure 10: Relevant parameters of an overall system optimization

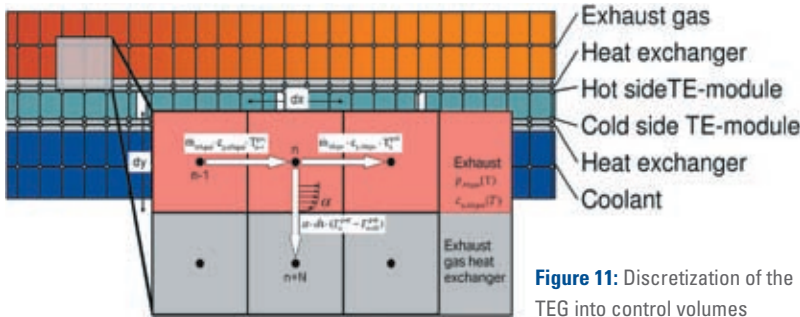


Figure 11: Discretization of the TEG into control volumes

haust gas backpressure which has a negative influence on the engine gas exchange. Accordingly, the fuel consumption map of the vehicle model is modified depending on the exhaust gas pressure rise.

All parts of the overall simulation model are validated by separate experiments and thus allow realistic assessments of the potentials. An optimization algorithm linked to the simulation tool automatically varies the available system parameters. In a short processing time, therefore, this tool enables the optimization of the cost-benefit ratio of a thermoelectric generator for any type of vehicle.

2.5 Potential in Driving Cycles and Constant Driving Points

By using the overall system simulation, the assessment of the fuel saving by using a thermoelectric generator in comparison with a reference vehicle without thermal recuperation can be achieved. The simulated potential consider, as described

above, the increased weight of the vehicle as well as the increased exhaust gas backpressure.

In Figure 12, the potential in fuel consumption reduction of a thermoelectric

generator for different implementations and different driving cycles or operating points is shown.

The characteristic figures of the thermoelectric material on which Figure 12 is based vary between  $ZT = 0,85$  and  $2,0$ . The feeding of the heat flow into the main coolant system permits the use of exhaust heat for a faster engine warm-up. In addition, the influence of exhaust pipe insulation for increasing the exhaust temperatures and the influence of the integration position of the TEG on the fuel consumption are shown. The “after flange” position is about 20 cm behind the catalytic converter, whereas “pre-tube” describes a position further downstream in front of the middle muffler, Figure 13.

Figure 12 clearly shows that for constant operating points, such as during a highway drive, a considerably higher effect on consumption can be achieved. Using currently available materials with material values of  $ZT = 0.85$ , savings of about 5 % can be expected, corresponding to a TEG-generated electrical output of about 600 W. The higher potentials as the  $ZT$  value rises are on the condition that the electric power generated by the TEG is actually required by the customer and would have to be provided by the conventional alternator if no TEG were fitted.

The NEDC started with a cold vehicle on the other hand offers, also due to lower engine loads, less potential for a system using exhaust gas heat in the region of 1 % to 2 %. In the US combined cycle

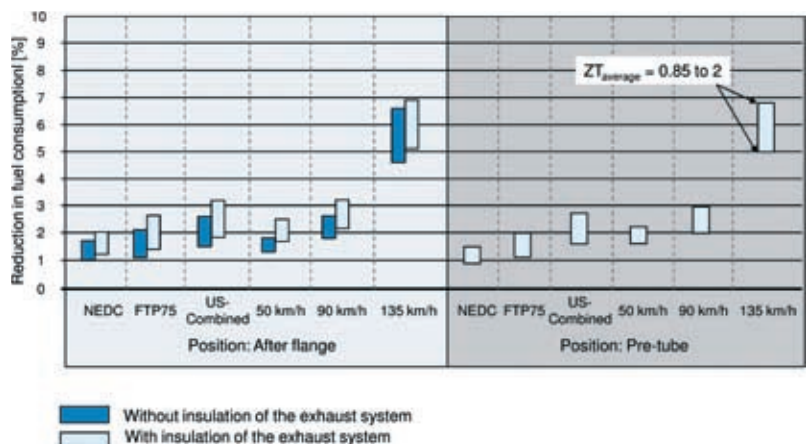
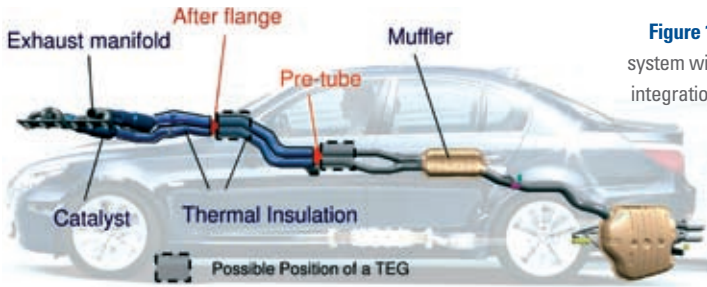


Figure 12: Potential consumption savings of a thermoelectric generator for different integration solutions; vehicle basis: BMW 530i

personal buildup for Force Motors Ltd.



**Figure 13:** Exhaust system with possible integration positions of a TEG

driven with higher loads and thus with a higher waste heat output, savings in the region of 2 % to 2.5 % are possible.

For cold-started driving cycles, depending on the cooling system integration, additional reductions of consumption can be achieved by reducing the friction; during constant speed driving, the influence of a faster engine warm-up is not applicable.

As can be seen from Figure 12, the thermoelectric generator makes a significant contribution to reducing fuel consumption, particularly on extra-urban roads and on highways, and thus represents an ideal addition to the BMW brake energy regeneration (BER). **Figure 14** is based on an example of a freeway drive with acceleration, constant speed and deceleration phases, and the generated power of the current TEGs at the prototype stage, a forecast of future performance and the electrical energy generated by means of brake energy regeneration are shown. It is obvious that the TEG performance is diminishing during the de-

celeration phases, as the engine is operating in the overrun fuel cut-off mode; this is however compensated by the brake energy regeneration, i.e. a car with both systems recuperates energy at every operating point: not only when braking, but also during acceleration and constant speed.

### 3 Outlook

The future of the thermoelectric generator depends mainly on the extent to which the efficiency of current materials demonstrated in the laboratory can be further developed so that they can be manufactured economically and can also withstand the harsh environment of an exhaust system. In this respect in particular, further important developments must be made in the joining technology between the thermoelectric semiconductor material and the heat exchanger structure so that the TEG components can be designed more efficiently in future.

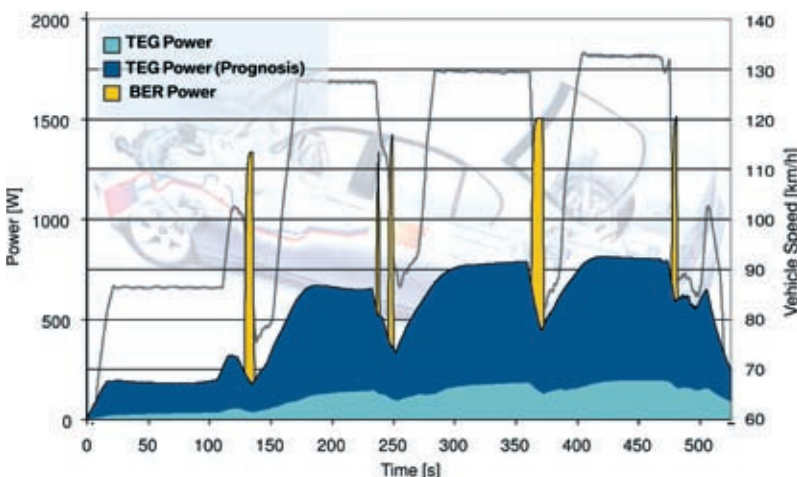


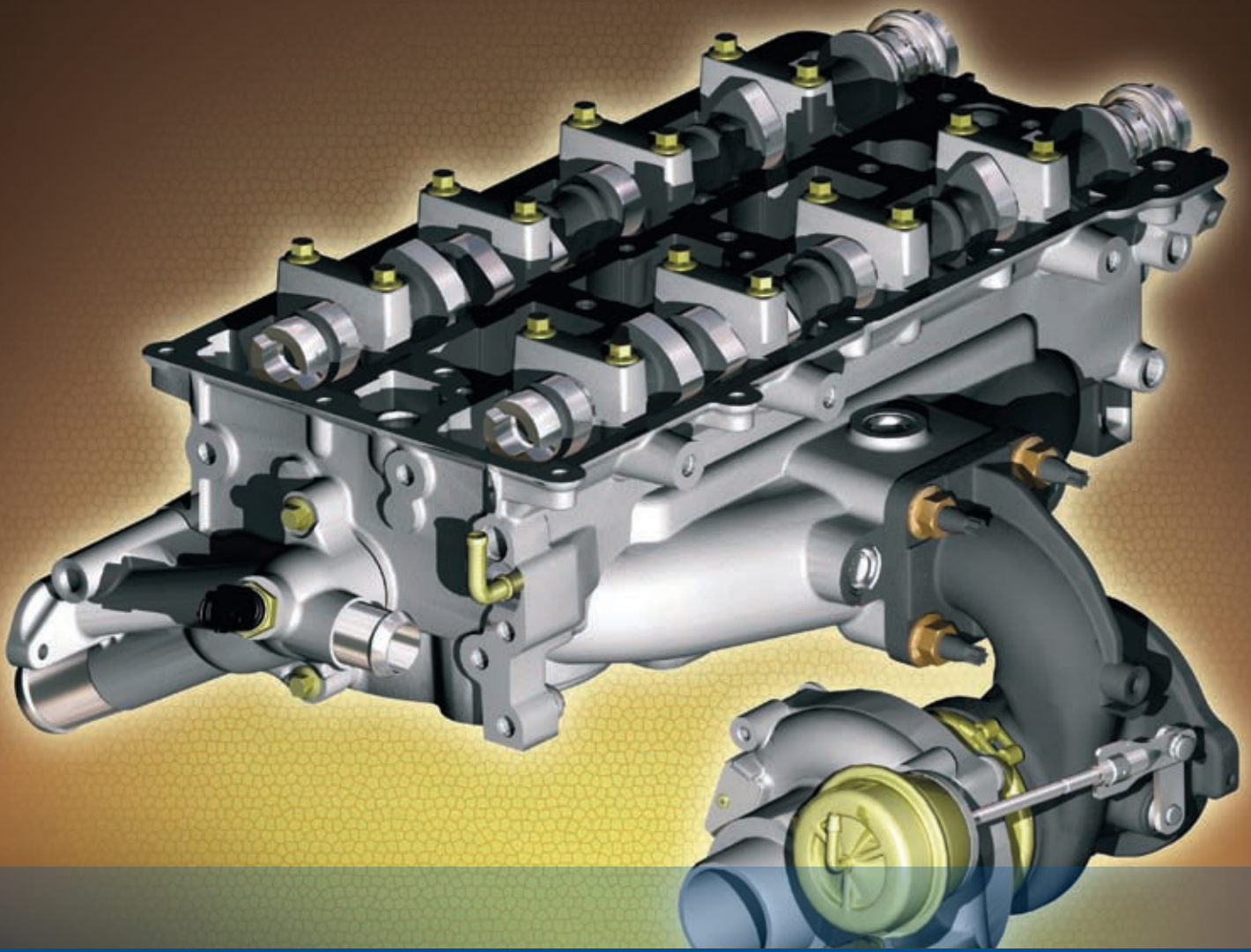
**Figure 14:** Thermoelectric generators and brake energy regeneration complement each other ideally, as show here in the case of a freeway drive

Particularly at the exhaust temperatures that occur in gasoline engines, thermoelectric materials already offer very good recuperation conditions. As thermoelectrics is particularly suitable for touring cars, integration in diesel-engined vehicles is favorable. Due to the lower exhaust temperatures, the potential of a thermoelectric generator is correspondingly smaller. In order to compensate for this, new integration approaches must be investigated, and the efficiency of the thermoelectric materials at lower temperatures must be increased considerably.

A further possibility for increasing performance in the long term is offered by the integration of a thermoelectric generator into an underhood catalytic converter. Due to the high temperatures prevailing there, the boundary conditions for converting heat into electrical energy are very favorable. Furthermore, additional effects could be exploited here through the multifunctionality of the TEG component: By applying current to the thermoelectric materials, for example, the heating of the catalytic converter or also local cooling could be supported by simply reversing the voltage polarity.

### References

- [1] Feulner, P.: Additional Energy-converters in Future Vehicles. In MTZ Worldwide Edition 2008 Nr. 9
- [2] Freymann, R.; Strobl, W.; Obieglo, A.: The Turbo-steamer: A System Introducing the Principle of Cogeneration in Automotive Applications. In MTZ worldwide Edition 2008 Nr. 5
- [3] Nolas, G.S., Sharp, J., Goldsmid, J.: Thermoelectrics – Basic Principles and New Material Development, Springer Publications Heidelberg 2001
- [4] Sommerlatte, J.; Nielsch, K.; Böttner, H.: Thermoelectric all-rounders (in German). Physik Journal 6 (2007) Nr. 5, 2007
- [5] Nasa Homepage, URL: <http://www.nasa.gov>
- [6] Degen, G.; Haaß, F.: Development of semiconductors for thermoelectric materials (in German); 1<sup>st</sup> Conference Thermoelectrics (IAV), Berlin 2008
- [7] Eder, A.; Fröschl, J.: Integration of a thermoelectric generator into the onboard electric system (in German). Submitted to: 7<sup>th</sup> "Powertrain Control Systems for Motor Vehicles" symposium, Berlin, June 2009
- [8] Mazar, B.; Richter, R.; Eder, A.: Potentials of Thermoelectric Waste Heat Utilization by Highly Efficient Powertrains (in German). 1<sup>st</sup> Conference Thermoelectrics (IAV), Berlin 2008
- [9] Treffinger et al., „Waste Heat Recovery by converting heat into usable energy“ (in German), VDI Conference on Innovative Vehicle Technologies, Dresden, 2008



# Cylinder Head with Integrated Exhaust Manifold for Downsizing Concepts

A study by the Ford European Powertrain Research department has shown that there is a significant potential to be tapped by using a cylinder head integrated exhaust manifold with turbo charged engines. It offers a win-win employment of technology providing improvements in the relevant attributes as well as a cost reduction.

## 1 Introduction

The European Union has defined its CO<sub>2</sub> emissions fleet target for 2015 as 130 g/km. From 2012 onwards the emission targets will be reduced step by step to meet this. The compliance with this limit is the key driver in the planning of powertrain portfolios at the car manufacturers. Important steps to achieve the targets are the introduction of new gasoline combustion methods such as stratified combustion or controlled auto ignition and through the introduction of downsizing for the European small and middle class car markets. Important for the breakthrough is meeting the customer expectations with regards to the fuel consumption under real world conditions, fun to drive, NVH and cost. Especially for downsizing concepts, where the intensive use of higher load areas is part of the concept, fuel enrichment in view of protecting components of the engine should be avoided as well as good transient response has to be ensured. Further the supply of sufficient heat in highly effective small car engines will be increasingly difficult. Put into this perspective the implementation of the cylinder head integrated exhaust manifold has been investigated and evaluated in view of the different functional effects and cost.

## 2 System Description

Key to the construction is the complete integration of the conventional external exhaust manifold into the aluminium cylinder head. The result of this is a single pipe feeding directly into the turbo charger. If necessary this can be made even more compact when vehicle package allows it, **Figure 1**.

In this instance, the overall cylinder head turned out to be only 32 mm wider and 200 g heavier than the conventional head. This is due to the fact that the flange area was significantly reduced. To be able to meet the durability requirements and as a result of high component and material temperatures, a totally new cooling concept in the cylinder head has been developed. This was proved out using CAE simulation to optimize the structure and fluid flow before being validated during the subsequent development phases on a test rig.

## 3 System Effects

### 3.1 System Cost

Downsizing with the aid of turbo technology, as well as the future introduction of Downsizing is going to mean changed load collectives for the gasoline engine. This turns out that a higher percentage of time will be spent at higher engine loads. In order to realize the most of the CO<sub>2</sub> potential the stoichiometric range at high loads needs to be expanded as far as possible, which leads to high temperature resistant material choices. Gas temperatures for such materials allow typically a maximum of 1050 °C. This subsequently increases the cost. Presently an austenitic steel with up to 37 % Nickel content is used in both the exhaust manifold and the turbo charger. The world market price for Nickel has risen considerably and was traded at around \$ 40 per kg. With an average weight of 3 to 4 kg, the elimination of an external exhaust manifold of an inline four cylinder engine creates a cost benefit on material costs alone. On top of this comes the elimination of the complicated and expensive machining of the external cast steel exhaust manifold. In comparison with this, the integrated exhaust manifold incurs a slightly higher cost by a potential upgrade to a larger vehicle cooler, **Table**. With respect to Downsizing of the gasoline architecture in a vehicle environment, the next larger cooling pack needs to be selected. That means within the same vehicle, the cooling pack for diesel engines or from the more powerful petrol engines needs to be used.

## The Authors



Dipl.-Ing. Kai Kuhlbach is Project Leader for Research and Advanced Gasoline Powertrain at Ford of Europe in Cologne (Germany).



Dipl.-Ing. Jan Mehring is Technical Specialist for Thermal Management at Research and Advanced Gasoline Powertrain at Ford of Europe in Cologne (Germany).



Dipl.-Ing. Dirk Borrmann is Department Manager for Research and Advanced Gasoline Powertrain at Ford of Europe in Cologne (Germany).



Dipl.-Ing. Rainer Friedfeldt is Supervisor for Design Concepts at Research and Advanced Gasoline Powertrain at Ford of Europe in Cologne (Germany).

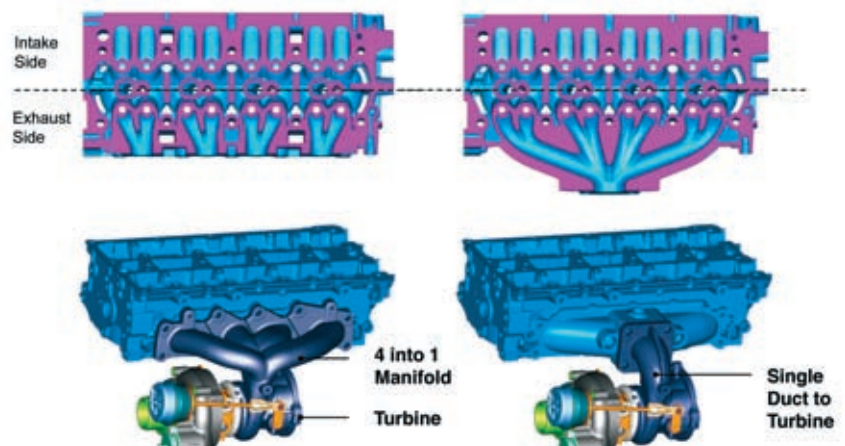


**Figure 1:** Section through the cylinder head (conventional and with integrated exhaust manifold)

**Table:** Cost saving on components

Components In-line 4 Gasoline Turbo	casted steel manifold + mating components = 100 %	
	case 1	case 2
Case 1: Eliminate 4 into 1 steel cast iron manifold (35 % Nickel)	- 95 %	-
Smaller heat shield and gasket, less bolts and nuts	- 5 %	- 5 %
Cylinder head add on	+ 5 %	+ 5 %
Next size radiator / fan (if required)	+ 15 %	+ 15 %
Case 2: Eliminate 4 into 1 sheet metal manifold	-	- 65 %
Case 1: Cost save vs. Steel cast manifold 1050 °C capable Engine weight save vs. steel cast manifold 3 kg	- 80 %	-
Case 2: Cost save vs. Steel sheet metal manifold Engine weight save vs. steel sheet manifold 1 kg	-	- 50 %
Further Potential: Eliminate electrical supplemental PTC heater	(- 60 %)	(- 60 %)

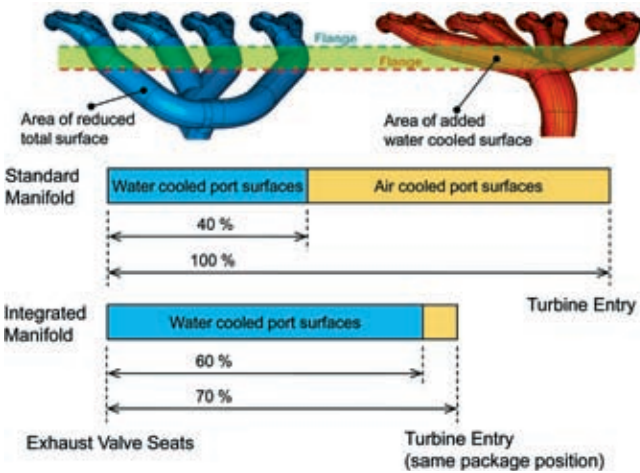


**Figure 2:** Comparison of the exhaust side port surfaces pre turbine (CAD model) and equivalent pipe surface schematics

As a general rule, the coolers usually have the same installation dimensions, simply increasing the cooler depth.

**3.2 Emissions**

The comparison of both systems (external and internal exhaust manifolds) with regards to the port wall surfaces from the exhaust valve seats to the entry of the turbine/catalyst lead to considerable difference. Using a normal four cylinder motor the following effects can be seen, **Figure 2:**

- a reduction by approximately 30 % of the overall surface area up to the turbo. (relevant e.g. for catalyst light-off)
- roughly a 50 % increase of the water-cooled surfaces (relevant for the air fuel ratio at higher loads and engine warm-up).

The main contributor that influences the quick starting of the catalyst conversion (reaching an operating temperature of 350 °C on the catalyst surface) is the size of the surface area on the exhaust

side all the way to the catalyst. In relation to the time frame required to heat the catalyst after a cold start it doesn't make a difference whether the surface is water or air cooled. According to results from the test rig, which used the same base engine but with different cylinder heads and the same position of the turbo, the integrated exhaust manifold delivered a 20 % reduction in the start time of the catalyst, **Figure 3.**

This results in a solid potential to reduce emissions and improve fuel economy after a cold start. Due to the reduced total port surface and port lengths with the integrated exhaust manifold, significantly increased exhaust gas temperatures pre-turbine and catalyst were observed in the first minutes after cold start, **Figure 4.** With increasing warming up state of the engine, when those walls that are water-cooled stay more and more cool in comparison to those that are air-cooled from the conventional system, the measured exhaust gas temperatures are getting closer and then equalize at a certain point in time (load dependent). Finally when the engine is fully up to normal operation temperature, the integrated exhaust manifold cylinder head delivers at steady state lower exhaust gas temperatures which make stoichiometric operation possible under all loads.

**3.3 Fuel Economy**

Through the integration of the exhaust manifold into the cylinder head, the engine achieves better fuel economy in the warm up phase and also at normal operating temperature. During the warm up phase the quicker catalyst light-off contributes as well as the reduced friction because of the added heating to cylinder

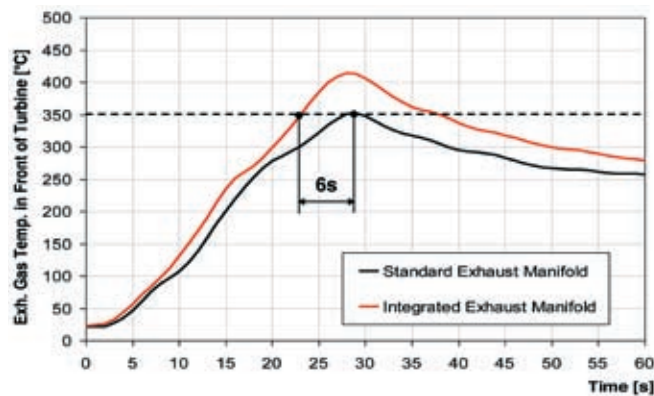


**Figure 3:** Exhaust gas temperature pre catalyst after cold start

head structure and coolant. Using the NEFZ, (New European Drive Cycle) fuel economy improvement between 1 to 2 % can be expected dependent on the warm-up relevant surface design as shown in Figure 2.

In the operating points near full load, depending on the materials used and temperature specs of the turbo housing, an improvement on fuel economy up to 15 % can be achieved. In the conventional design, even if the parts are made of heat resistant material, the exhaust gas temperatures at high load have to be decreased by over fueling significantly to avoid overheating and component damage. Typical temperature limit for high quality exhaust materials is 1050 °C.

The exhaust port lengths and diameters as well as the plenum surfaces represent the water cooled surface as a design parameter and can be optimized e.g. with 1D/3D simulation tools. Important factor is the amount which the exhaust gas needs to be cooled at full load to allow full stoichiometric Lambda 1 operation as well as the transient response requirements, Figure 5. This system provides a real contribution to decreasing the fuel consumption both for NEFZ as well as real world operation.

### 3.4 Warm-up Behavior

The heat input into the cylinder head and into the coolant at steady-state operating conditions increased approximately 20 % for the fully warmed up engine with integrated exhaust manifold. Figure 6 outlines the influence of the integrated exhaust manifold on the thermal load of the coolant in a part load operating point.

In the cold-start and warm-up phase the heat input increases as well. The heat flow can be quantified making use of the first law of thermodynamics, however the internal energy of the water jacket needs to be considered. Dyno tests proved that the additional usage of exhaust gas heat increases the heat input into the coolant during the warm-up phase up to 25 %.

$$\frac{dU}{dt} = m_{waterjacket} \cdot c_{cool} \cdot \frac{T_{cool-out}}{dt} =$$

$$\dot{Q} - \dot{m} \cdot c_{cool} \cdot (T_{cool-out} - T_{cool-in})$$

As previously outlined, this leads to a reduction of friction and hence fuel consumption. Furthermore market specific supplemental heating devices, e.g. PTC

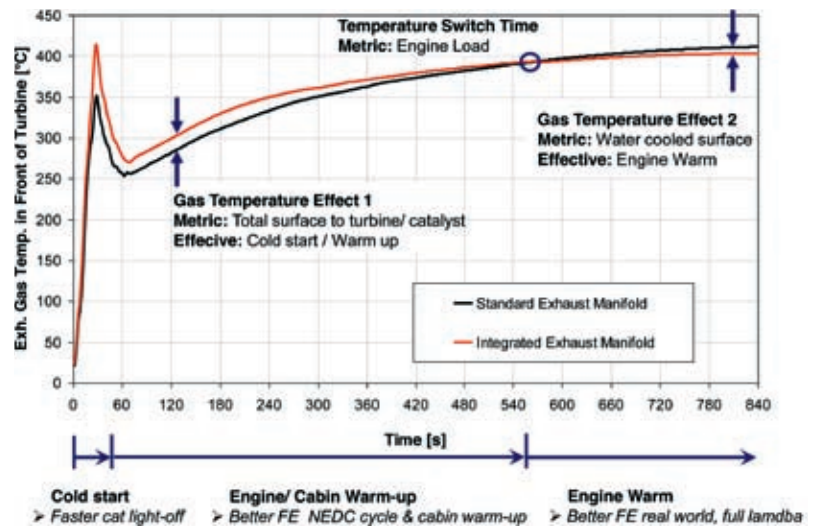


Figure 4: Exhaust gas temperature during warm-up at 1500 rpm and 1 bar bmep

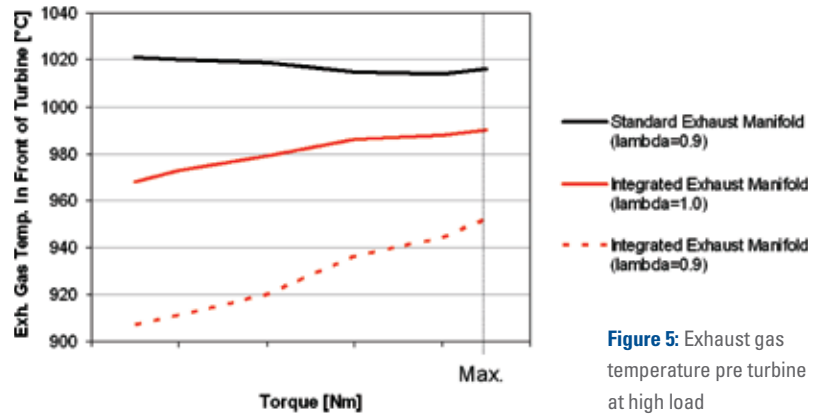


Figure 5: Exhaust gas temperature pre turbine at high load

heating elements can be deleted or combustion strategies do not have to be modified in order to achieve a quicker cabin warm-up. This could lead to further cost and fuel consumption reductions.

### 3.5 System Weight

The integrated manifold prototypes for the in-line four-cylinder head have an overall system weight advantage of 3 kg in comparison with a conventional external

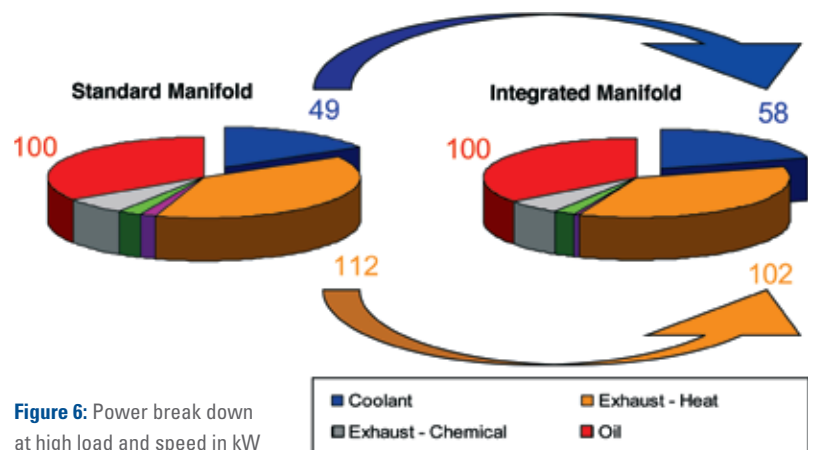


Figure 6: Power break down at high load and speed in kW

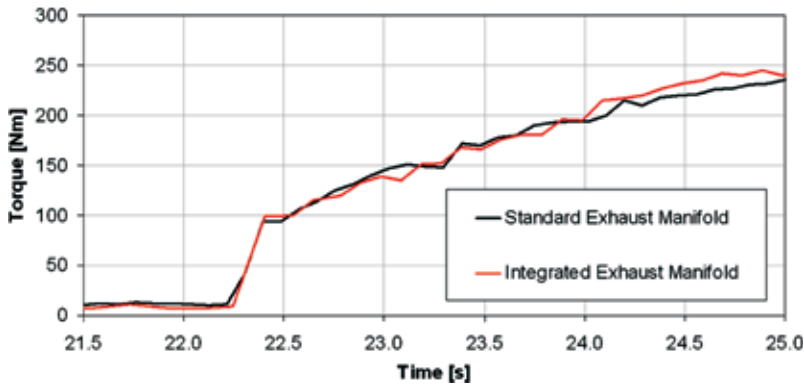


Figure 7: Transient response after full load request from 1500 rpm and 1 bar bmep

steel cast manifold. If compared with an external sheet metal exhaust manifold design there will be still an advantage of 1 kg for the engine system.

3.6 Complexity

Besides the elimination of the conventional separate exhaust manifold another advantage of the integrated design is the significantly reduced number and size of mating parts. The required amount of high-temperature-resistant studs can be reduced dependent on the amount of cylinders and design of the exhaust flange. This has not only a positive effect on part costs, but has also significant advantages in terms of logistics, assembly and service. The elimination of threaded holes in the cylinder head leads to reduced cycle time of modern CNC manufacturing. The gasket from the exhaust hot end to cylinder head, which is a remaining single gas discharge is significantly smaller and therefore cheaper. Normally conventional exhaust manifolds of turbocharged engines have to be fitted with complex heat shielding to protect surrounding components against significant heat input. Heat shielding in the area of the integrated manifold is not necessary due to less heat rejection which is relieved by cooling and thermal connection to the cylinder head. The general heat input into the engine bay and thermal requirements on surrounding devices accordingly decrease as well. This is a further contribution to a reduction of cost, complexity and demand of package space.

3.7 Full Load Characteristics

The turbocharged four-cylinder engine with integrated exhaust manifold that was

tested showed equal torque and power characteristics on the test rig, as well as the same low end engine speed where it initially reached peak torque. The lower gas temperature before turbo during steady state operation with integrated exhaust manifold has no negative impact on transient behavior after a full load request. The potential temperature effect appears compensated by the mentioned reduced heat transferring surface and smaller gas volume before turbine (hardly a smaller volume can be realized if the turbine is directly attached to the cylinder head). Similar to the situation after cold start, the exhaust gas temperature before turbo after a load step of an engine at hot running conditions is either not or only slightly reduced. Dyno measurements of the transient response characteristics after a full load request showed the same delay to maximum torque

for both tested configurations according to Figure 1, Figure 7. This shows that the integration of the manifold into the cylinder head is the preferred solution compared to a water cooled external manifold.

4 Durability

4.1 Methods

The integration of the exhaust ports and the plenum area leads to an additional heat input into the cylinder head and hence thermo-mechanical stresses which could result in local exceptional loads in the engine structure. The evaluation of the cylinder head design has been performed considering the increased load conditions applying network simulation methods, FEM (Finite Elements Method) and CFD (Computational Fluid Dynamics). Figure 8 shows the workflow of the performed simulations and their interactions.

4.2 Flow Calculation

CFD methods are commonly used during the development process to compute the flow as well as the pressure distribution in the water jacket of cylinder head and block [2]. A first calculation was done with constant coolant properties in order to avoid solving the energy equation as shown in Figure 9. This is possible because of the incompressibility of the coolant and the thermal decoupling of flow and temperature. The cylinder head gasket openings were widened to realize

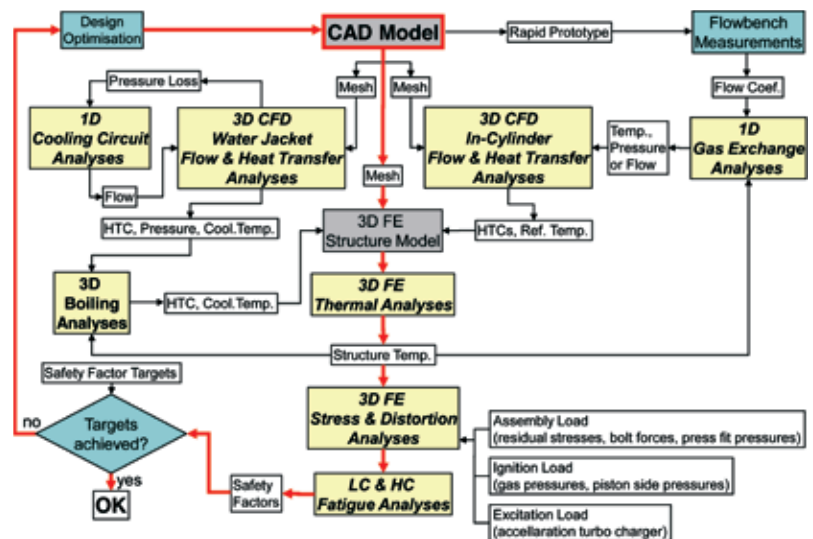


Figure 8: CAE workflow

sufficient cooling of the extended exhaust ports. On the one hand the pressure loss across the engine could be reduced and hence the volumetric flow rate through the engine increased. On the other hand the cooling of thermally and mechanically stressed areas as the exhaust valve bridges and the turbo-charger flange has been improved significantly by increasing the amount of crossflow in the cylinder head.

In order to determine the temperature distribution in the cylinder head structure the heat input from the exhaust gas needs to be known. The crank angle resolved flow distribution in the combustion chamber as well as in the inlet and outlet ports is calculated using a 3-D simulation tool. The resulting average values for gas side heat transfer coefficient and reference temperature are calculated using the following formula:

$$\bar{\alpha} = \frac{1}{720 \text{ } ^\circ\text{KW}} \int_0^{720 \text{ } ^\circ\text{KW}} \alpha(\theta) d\theta$$

$$\bar{T} = \frac{1}{720 \text{ } ^\circ\text{KW} \cdot \bar{\alpha}} \int_0^{720 \text{ } ^\circ\text{KW}} \alpha(\theta) \cdot T(\theta) d\theta$$

### 4.3 Temperature Calculation

As shown in **Figure 10** the maximum temperature can be observed in the exhaust valve bridge area, due to the heat transferred from the combustion chamber as well as the exhaust ports into the cylinder head structure and the heat conducted from the valves additionally into the valve seat area. However, not even in critical operating modes such as rated speed and full load, the maximum temperature limit for the aluminum alloy is exceeded in any location of the cylinder head. Due to the extensive mechanical load, the stiffness in the area of the turbo flange needs to be high and the temperature level low.

### 4.4 Material Fatigue Calculation

Following the calculation of the structure temperature distribution the next important step is the determination of the thermo-mechanical loads and the prediction of the resulting component fatigue life. This considers the manufacturing loads (casting residual stress and assembly loads) as well as the operating loads (thermal stresses and gas and inertia forces). Low cycle fatigue (LCF) is caused by plastic and creep strain amplitudes which arise

due to the inherent temperature gradients during cyclic heating and cooling of the engine. Lower frequency phenomena typically occur less than 10000 times over the entire component life.

The calculation of high cycle fatigue (HCF) simulates the high frequency operating loads of an engine. For purposes of the fatigue calculation, the cylinder head, in its assembled environment needs to be considered. This means all connection points, cylinder head, block, bolts, gaskets and the mounting of the turbo to the exhaust system. For final evaluation local safety factors need to be calculated which are based on a combination of local mean and amplitude stresses. In the performed cylinder head simulation the HCF and LCF safety factors were well above 2.5 in the entire integrated exhaust manifold area and lower but not critical in the cylinder head bolt areas.

## 5 Outlook

This investigation has shown that the application of a cylinder head integrated exhaust manifold provides a significant win-win step. As well as improving the at-

tributes, it also provides a great scale cost reduction especially for the turbo engine architecture. This approach can also lead to attractive downsizing opportunities for the larger vehicle segments. Areas of next level research could include testing to see whether the degree of integration used here can be extended further as well as whether this technology can also be applied in a diesel environment.

## References

- [1] Borrmann, D.; Friedfeld, R.; Pingen, B.; Stump, L.; Wirth, M.: Gasoline Downsizing, Challenges on the Path to an Attractive Powertrain. 20<sup>th</sup> International AVL Conference Paper, Sept. 11<sup>th</sup> 2008
- [2] Dilgen, P.; Mehring, J.; Meyer, J.: CAE-Methoden zur Auslegung von Wassermänteln in frühen Stadien der Motorenentwicklung und deren Einsatz zur Unterstützung der Konstruktion. Tagung CAE verstärkt die interdisziplinäre Motorenentwicklung, Haus der Technik Essen, 1998
- [3] Petutschnig, H.; Klinner, P.; Kobor, A.; Schutting, E.: Rechnerische Abbildung des Temperaturfeldes in Zylinderköpfen moderner Dieselmotoren. In: MTZ 63 (2002) S. 1010 bis 1019
- [4] Bintz, S.; Mehring, J.; Patschull, A.; Brohmer, A.: Development of a New Strategy for an Efficient Cylinder Head Temperature Analysis using the Conjugate Heat Transfer Method. Contribution to the conference 'Fluent CFD Konferenz'. Bingen, 29. - 30. Sept. 2004

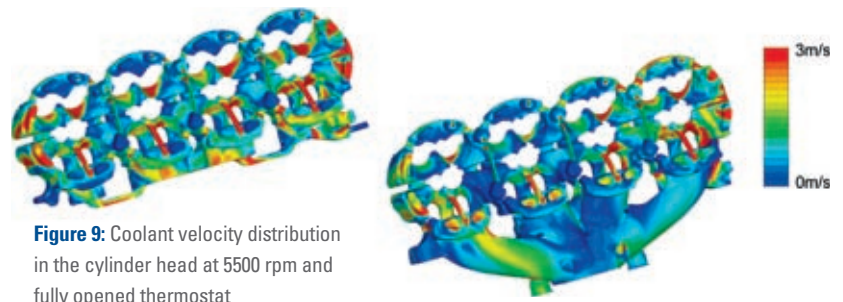


**Figure 9:** Coolant velocity distribution in the cylinder head at 5500 rpm and fully opened thermostat

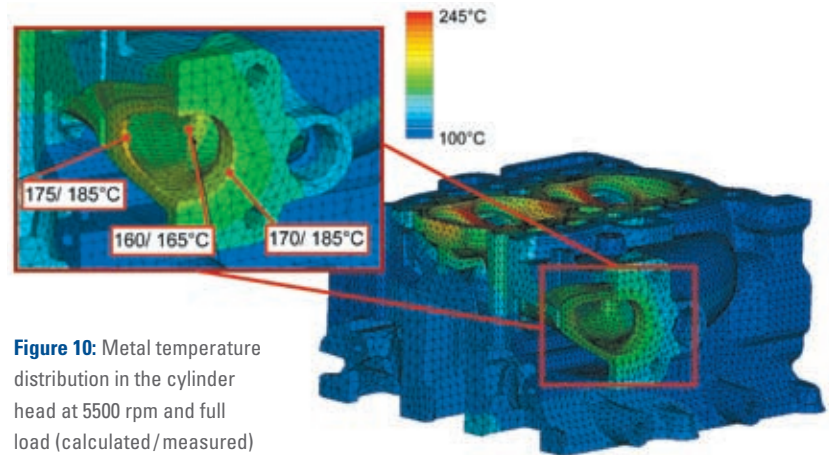
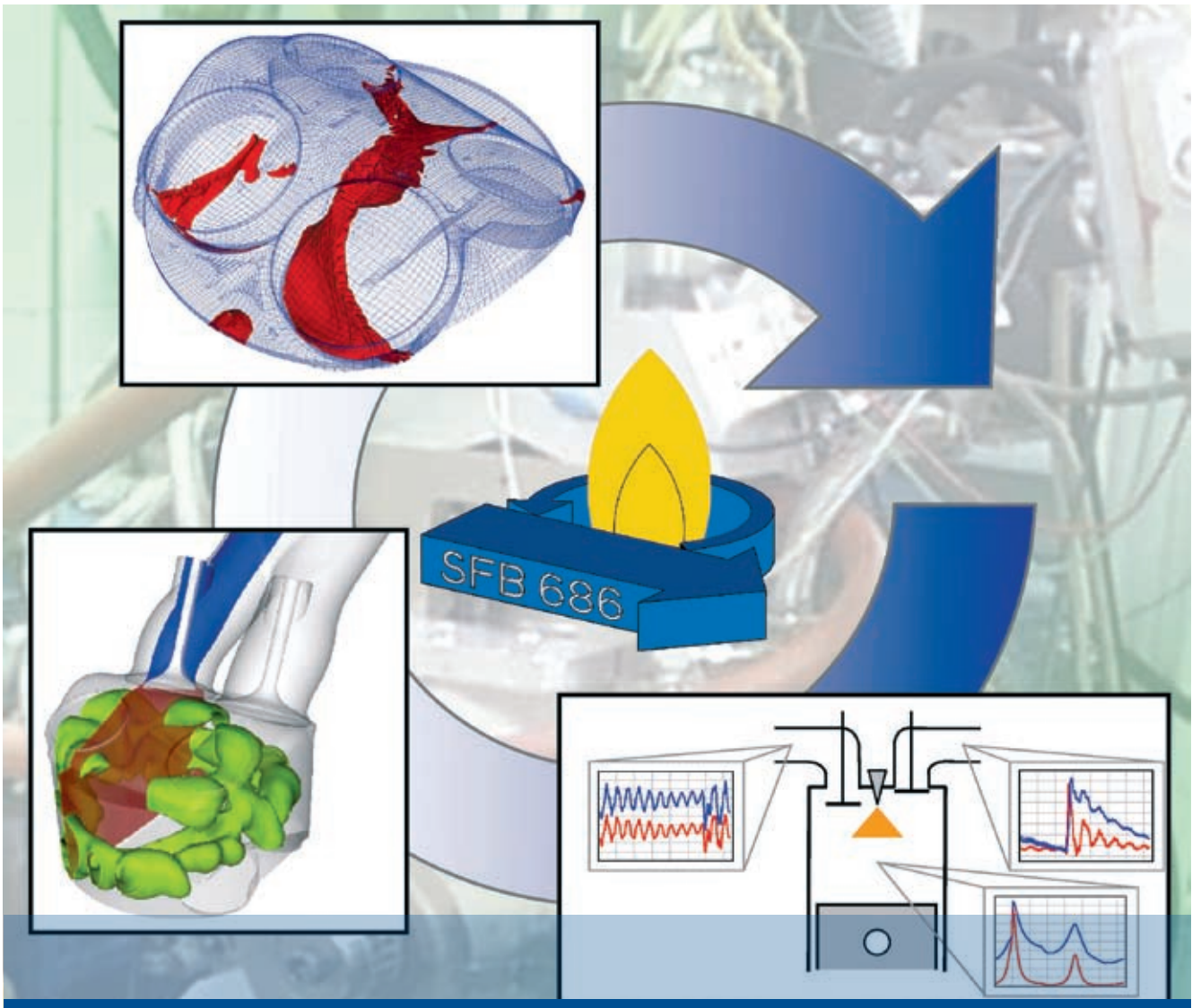


**Figure 10:** Metal temperature distribution in the cylinder head at 5500 rpm and full load (calculated/measured)



# Aspects of Gasoline Controlled Auto Ignition – Development of a Controller Concept

A promising approach to decrease emissions and fuel consumption at the same time for gasoline engines is the controlled auto ignition. The complex process is analysed and modelled within the “Collaborate Research Centre 686 – model based control of the homogenized low temperature combustion” by the Institute for Combustion Engines and the Institute of Automatic Control at RWTH Aachen University to design a future controller concept.

## 1 Introduction

Due to the ongoing discussion on CO<sub>2</sub> limitation, the fuel consumption reduction is the focus of current gasoline development. Therefore, current and future emission standards have to be taken into account.

In the past, conventional gasoline engines were characterized by throttle control, cylinder selective port fuel injection, multivalve technology and stoichiometric combustion in combination with a three-way catalyst. However, recently, good progress has been made in the area of gasoline engine development. Different technologies such as direct injection, downsizing, turbocharging and throttle-free load control with variable valve timing can decrease the fuel consumption. New combustion processes like controlled auto ignition and homogeneous lean combustion show additional fuel consumption potential.

The focus of this paper is on controlled auto ignition, which has a high efficiency and near zero NO<sub>x</sub> emissions. Therefore, expensive exhaust gas aftertreatment, as typically necessary in other lean combustion concepts, can be avoided. The self ignition is realised by extreme high residual gas fractions, in a way that the air/fuel mixture can ignite during the compression near top dead centre. In this context, the stratification of the mixture and the valve timing strategy play a central role to achieve a high efficiency. The shown test bench data are measured on a single cylinder engine with an electro mechanical valve train (EMVT) and the mixture formation can be switched between internal and external [2]. Furthermore numeric models will be introduced to get a detailed understanding of the processes in the combustion chamber and to design a future controller concept.

## 2 Experimental Investigation

### 2.1 Steady State Engine Operation

Self-ignition of the fresh cylinder charge is introduced due to exceeding the necessary thermodynamic state near top dead centre. This is mainly controlled by EGR rate, injection timing and duration as well as the mixture stratification of air, EGR and fuel. The increased fuel efficiency is a result of the de-throttling of the engine as

well as a fast fuel conversion and changed material properties. However the operation range of the controlled auto ignition is limited to part load operation. The stability limitation to low loads and the pressure gradient limitation to high loads were presented in [3]. The influence of different EGR strategies on the operation area was discussed in [2]. The operation ranges for the EGR strategies combustion chamber recirculation (CCR) and exhaust port recirculation (EPR) as well as the operation range extension to low loads with direct injection and to high loads with turbocharging are summarized in **Figure 1**. In the NEDC a fuel consumption reduction potential up to 40 % can be realised, depending on the vehicle design.

### 2.2 Transient Engine Operation

The main challenge is a realisation of a proper transient operation together with an extension of the operation range. Therefore the combustion process will be analysed and discussed in this paper. With the knowledge of this base analysis, different engine models for a setup and layout of a closed-loop controller will be investigated. **Figure 2** shows a change in operation mode at  $n = 2000/\text{min}$  and  $\text{IMEP} = 3 \text{ bar}$ . Similar steps in valve timings, injection duration and injection timing at both EGR strategies were used for identification of the control path and for the ongoing layout of the controller. **Figure 2** shows that a transient operation is possible, and simultaneously shows the challenges for highly transient operations. During the mode change from spark ignition to controlled auto ignition an advanced combustion can be observed, which results in an undesirable high peak pressure. Such operation conditions have to be avoided controller intervention, to consider the increased customer comfort awareness.

### 2.3 Flame Light Measurement

Optical flame diagnostics are an important tool to gain insight to the process in the combustion chamber and to verify numeric simulations with the test bench. **Figure 3** shows results of flame light measurements for the operation modes CCR and EPR in comparison with a conventional spark-ignited combustion process. It is to note, that the time intervals of the sequence are  $\Delta t = 0.8^\circ \text{ CA}$  for CCR and

## The Authors



Dipl.-Ing.  
**Karl Georg Stapf**  
is Scientific Assistant at the Institute for Combustion Engines (VKA) of RWTH Aachen University (Germany).



Dipl.-Ing.  
**Dieter Seebach**  
is Scientific Assistant at the Institute for Combustion Engines (VKA) of RWTH Aachen University (Germany).



Prof. Dr.-Ing.  
**Stefan Pischinger**  
is Director of the Institute for Combustion Engines (VKA) of RWTH Aachen University (Germany).



Dipl.-Ing.  
**Kai Hoffmann**  
is Scientific Assistant at the Institute of Automatic Control (IRT) of RWTH Aachen University (Germany).



Prof. Dr.-Ing. **Dirk Abel**  
is Director of the Institute of Automatic Control (IRT) of RWTH Aachen University (Germany).

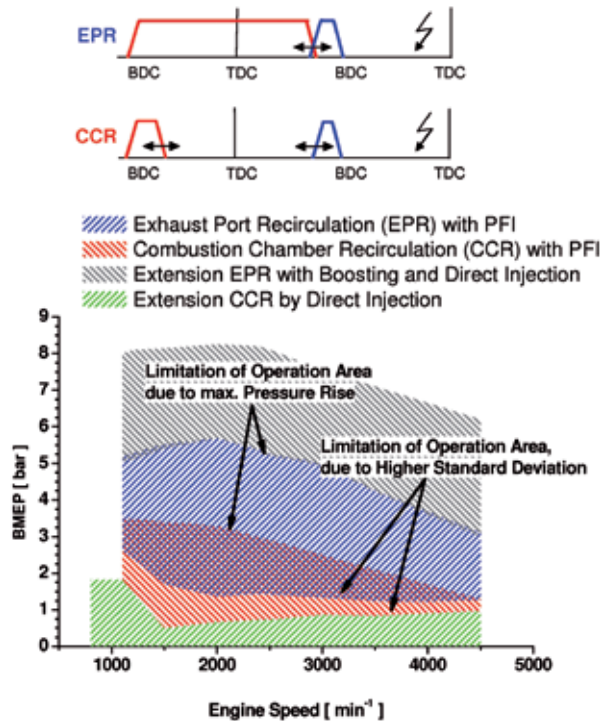


Figure 1: Operation area and schematic valve lift timings of investigated EGR strategies

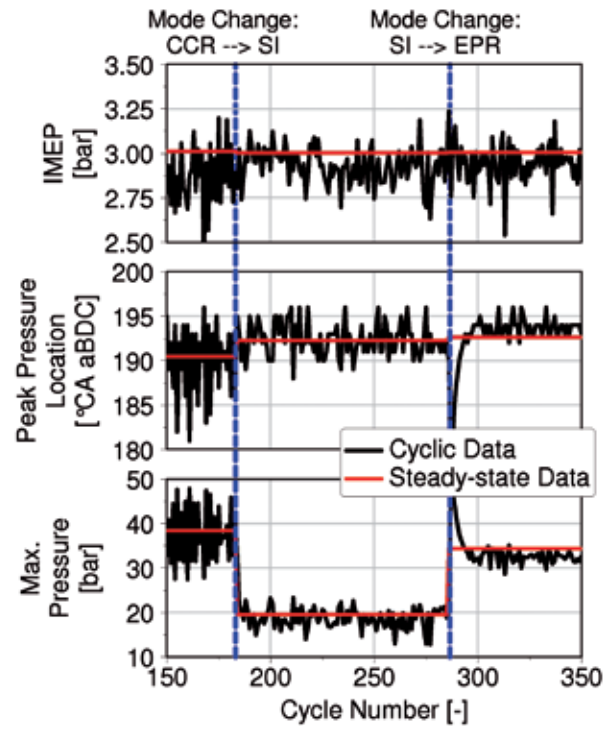


Figure 2: Operation mode change as an example of transient engine operation

EPR, whereas it is prolonged to  $\Delta t = 4^\circ$  CA for the spark-ignited combustion. In the first image for SI combustion the spark can be seen. Starting at this laminar flame kernel, the flame propagates turbulent. In the presented flame visualisation CCR and EPR are adjusted to a comparable combustion rate by individual adjustment of the residual gas content. The flame visualisation sequences with a UV sensitive intensified high-speed camera shows the simultaneous existence of several auto-ignition spots for CCR and EPR operation. From these spots the igni-

tion spreads into all spatial directions. The propagation velocity locally is small. With the short distances between ignition spots it becomes significantly higher than the flame propagation of conventional SI combustion.

### 3 Calculation Methodology

#### 3.1 Combustion Model

For the fundamental analysis of controlled auto ignition different CAE tools are used. The focus of this work is a detailed

modelling of the combustion system. Using CFD simulations (Computational Fluid Dynamics), one can investigate the flow field, injection, mixture formation and the distribution of fuel and residual gas inside the combustion chamber. Furthermore the calculation of reaction kinetics is coupled to the CFD simulation [4]. Hereby the auto ignition under engine conditions can be calculated as well as the influence on the thermodynamic state by the heat release of reaction progress during conversion of fuel. **Figure 4** shows the calculation procedure schematically.

A combustion model for the detailed calculation of gasoline auto ignition not only has to reflect the influence of residual gas mass fraction and air to fuel ratio but also the distribution of both. For this reason a multi zone reaction kinetics approach is chosen. The individual  $n$  zones are defined in the phase space. A classification in up to three dimensions is supposable. The mixture can be considered by residual gas and fuel mass fraction. Furthermore a classification by temperature is possible. Correlating distributions of the possible coordinates were verified in [3] and [5] for the consid-

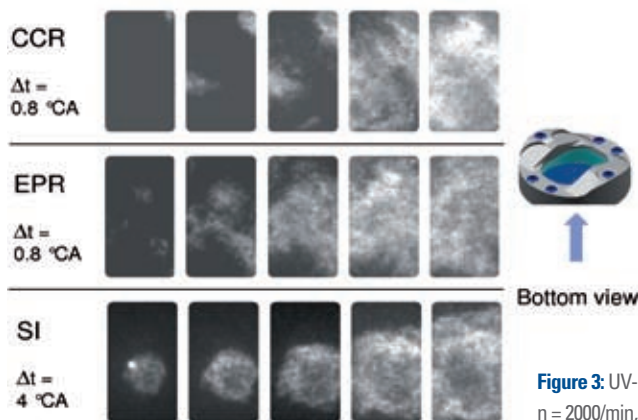


Figure 3: UV-Flame light emission:  $n = 2000/\text{min}$ , IMEP = 3 bar

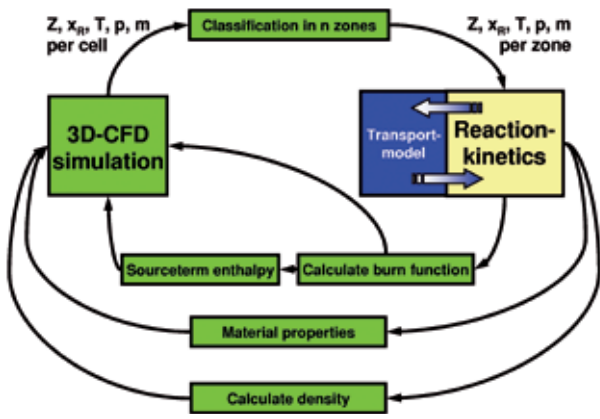


Figure 4: Modelling approach of gasoline auto ignition within CFD simulation

ered operating point. For this reason a one dimensional multi zone model is introduced here, which classifies the combustion chamber by fuel mass fraction.

From CFD calculations the information of fuel mass fraction  $Z$ , residual gas mass fraction  $x_r$ , temperature  $T$ , pressure  $p$  and mass  $m$  of all cells are analysed and transferred for every zone. The model calculates the heat release from chemical reactions according to those values. Additionally, the mass transport between the zones is considered by an attached transport model. The heat release is used to calculate a burn function and both quantities are transferred back to CFD. Furthermore the changing material properties due to combustion and the density as a function of the gas constant are committed.

The 3-D CFD calculation delivers detailed information about the thermodynamic state and the mixture inside the combustion chamber. This accompanies with the high demand for computational cost. The findings from the CFD simulations are used for the formulation of a reduced combustion model which is coupled interactively to the process design with 1-D gas exchange tools. Stationary multi cycle simulations as well as the calculation of transient operating point changes become possible. This tool conduces for the training of the designed controller and the preliminary design of the valve timings needed for auto ignition operation.

### 3.2 Model Reduction

The long-term aim of the Collaborative Research Centre 686 is to develop a mod-

el-based predictive controller (MPC) which is based on a physical pattern. This kind of controller internally uses a simplified plant model to predict the future behaviour of the process to optimise. The integration of physical knowledge in the modelling leads to a better general validity of the approach. However, an indispensable requirement for these models is a numerically low complexity with high detail level to allow a good closed loop control on a real-time basis. The development of the models can occur from two extremes. The first alternative is to begin with detailed models and to bring them to a format which is executable on the aim control device.

Outgoing from the real physical processes 3-D CFD models can be combined with models of the combustion kinetics. This combination is used for a deeper understanding of the processes inside the engine. However, with simulation times of days per cycle they are unwieldy for the development of a closed loop control. The aim is to reduce these models such that the succinct and for the regulation important characteristics of the controlled variables are preserved, while less significant details are renounced in favour of the calculation time. The first step in this reduction chain is from a three-dimensional CFD code towards a one-dimensional sim-

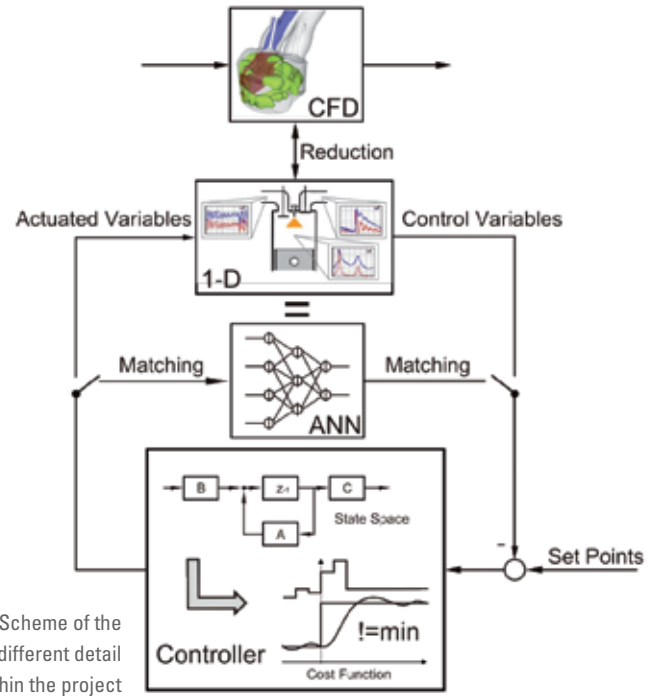


Figure 5: Scheme of the interaction of different detail levels within the project

ulation in which the combustion is already represented by mathematical function of the heat release, Figure 5.

For the controller a model is required which is reduced such that within a cycle the model can be calculated on-line, balanced with measurements, linearised and additionally the actual control algorithm is computed. For the implementation on a control unit the model must be given in a higher programming language as for example C.

An artificial neural net (ANN) fulfils the described demands of a low numerical complexity [13]. Already several times neural nets were used in engine control. Indeed ANNs are mathematically driven models which have to be fitted to a measured input/output behaviour. In contrast to the CFD models these models show no physically based understanding. However, artificial neural nets allow an integration of physical knowledge and are extendable concerning this. As soon as a reduced partial model of the whole process is available, this can be inserted by regarding it in the training process.

The first approach for the integration of physical models is their use as model of the controlled process in the closed control loop as a MIL test (model in the loop). Here the use of the already reduced one-dimensional model is promising, be-

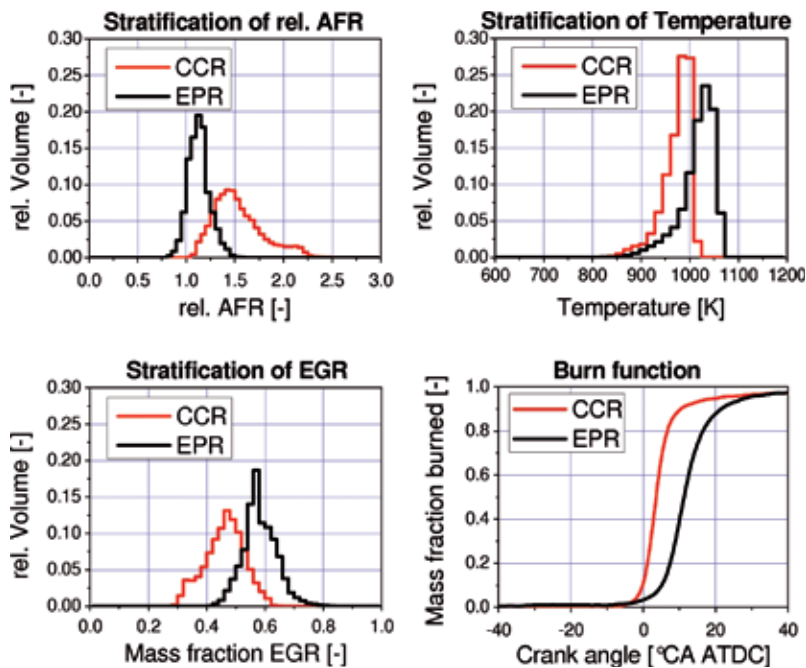


Figure 6: Distribution functions of relative air/fuel-ratio, residual gas and temperature with corresponding burn function of CCR and EPR

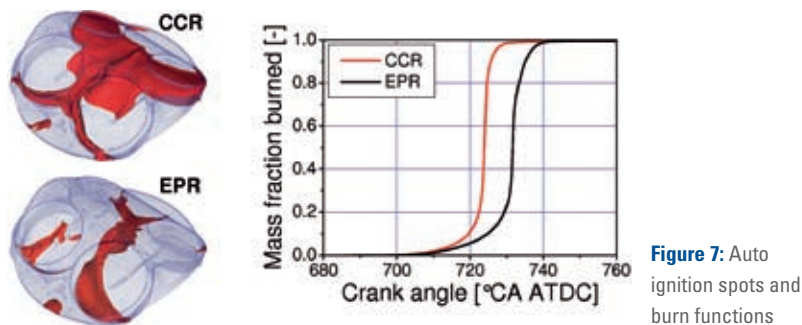


Figure 7: Auto ignition spots and burn functions

cause the calculation time per cycle is within the scope of minutes. The controller can be laid out with the help of the detailed model. Because the complexity of the model used in the controller is limited by the real-time hardware, here we have to fall back on the numerically easier neural net.

## 4 Simulation Results

In the following the results of the detailed combustion model with CFD and multi zone reaction kinetics and the reduced model with attached 1-D gas exchange calculation are presented and verified by comparison with experimental data from the considered single cylinder research engine.

### 4.1 CFD Simulation

In Figure 6 the distribution functions of relative air/fuel ratio, residual gas mass fraction and temperature can be seen together with the burn functions for both residual gas strategies Combustion Chamber Recirculation (CCR) and Exhaust Port Recirculation (EPR) at the load point  $n = 2000/\text{min}$ ,  $\text{IMEP} = 3 \text{ bar}$ . The crank angle position  $10^\circ \text{ CA BTDC}$  is shown.

In the considered operation point CCR has a bigger relative air to fuel ratio with broader distribution. Thereby the residual gas mass fraction is reduced accordingly which leads to a decreased temperature level. The noticeable earlier and faster combustion can be accounted for by stratification effects [2].

By using CFD with coupled reaction kinetics the heat release in the engine

with its influence on pressure and temperature as well as the spatial distribution of reaction zones in the cylinder can be calculated and analysed. In Figure 7 the zones are shown in which the heat release starts. For CCR, a large area beneath the exhaust valves is detected while for EPR several ignition spots are discovered, partially beneath the intake valves. Furthermore the calculated combustion functions are shown. As was shown in the experiments, the earlier and faster combustion of CCR is reflected. The late phase of combustion occurs for both strategies too fast.

### 4.2 Kinetic Analysis of Different Fuels

Current research works show the big potential of using tailor made fuels in gasoline auto ignition engines in the future [2, 6]. For this, information regarding the auto ignition behaviour of the different fuels is necessary. In the following, the ignition delay times of several energy sources already feasible today are compared. Usage of reaction kinetics shows the possibility of a preliminary fuel design by simulation.

The ignition delay time of fuel depends of the present mixture, pressure and especially the temperature in the considered reactor. Figure 8 shows a comparison of the ignition delay times of ethanol, iso-octane, methane and hydrogen for stoichiometric mixture, residual gas mass fraction of 50 % and 26 bar pressure as a function of temperature [7, 8, 9, 10].

Additionally the temperature range around 1000 K is marked. The distribution functions of temperature from Figure 6 show most of the volume fraction in the combustion chamber at  $10^\circ \text{ CA BTDC}$  for both residual gas strategies in this range. The intersection of the traces of ethanol and iso-octane is distinctive. For higher temperatures the ignition delay time for ethanol decreases more rapid than for iso-octane. For lower temperatures iso-octane shows a significantly decreased ignition delay time. With these properties, ethanol appears as an advantageous fuel for controlled auto ignition. At higher loads, the higher residual gas temperature is overcompensated with less residual gas mass fraction which leads to lower temperatures during compression and inhibits a fast ignition. Contrary for lower loads with increased residual gas

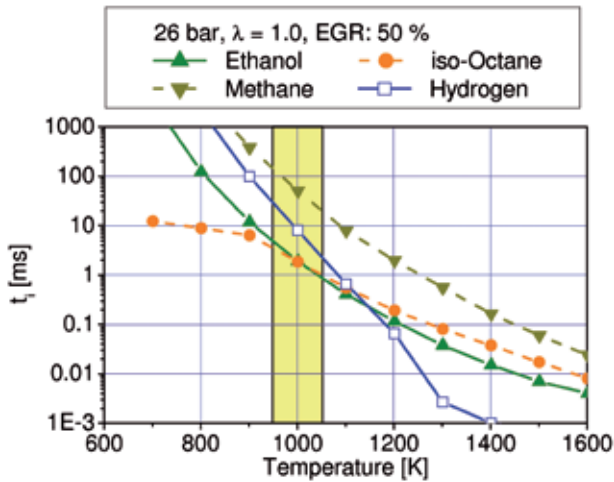


Figure 8: Ignition delay times of different fuels as function of time

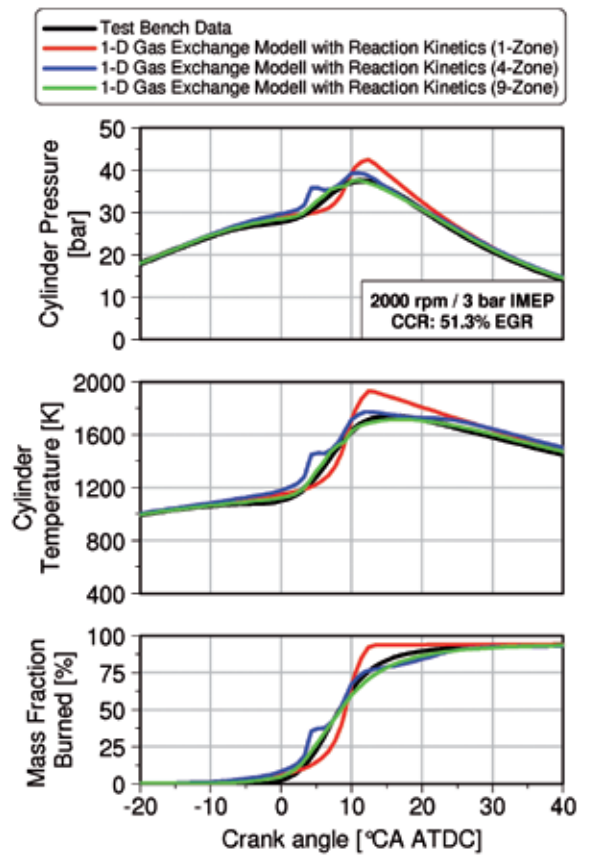
mass fraction and higher temperatures during compression the process is stabilized by shorter ignition delay [2]. From this point of view hydrogen seems to be an appropriate fuel, too for gasoline auto ignition. The positive behaviour of the ignition delay trace of ethanol is amplified. In contrast, methane has longer ignition delay over the whole range and hence does not appear as adequate fuel for the considered combustion system.

### 4.3 Reduced Model

The above described CFD model approach with interactive coupled reaction kinetics is not appropriated for a controller layout due to extreme long simulation times. In this part a first reduction step to a 1-D gas exchange simulation with different combustion models will be shown. Figure 9 compares test bench results of three different combustion models, which are coupled to a 1-D gas exchange simulation. The combustion model with one zone shows a relative slow burn rate at the combustion start. After 20 % mass fraction burned, the fuel burn rate increases rapidly and is much faster than the thermodynamic analysis of the test bench data. This fast combustion exceeds the measured peak pressure and peak temperature. However, the 50 % mass fraction burned point only slightly deviates.

An increase in number of zones to four results in a better approach to the pressure and temperature trace. For this simulation the mass is distributed equally to all zones. In the combustion trace

Figure 9: Results of the combustion simulation with the coupled 1-D gas exchange model and reaction kinetic



the burn process of each zone can be observed. The highest deviation to the thermodynamic analysis is approximately 10 % and occurs during 20 to 40 % mass fraction burned. The rest of the burn function trace fits well to the thermodynamic analysis including the 50 % mass fraction burned point, especially if the high reduction of the reaction kinetic model is taken into account.

The mass distribution at a further increase to nine zones is based on 3-D CFD simulation results. In [2] it is shown, that the EGR and A/F ratio distribution can be described by mean values and standard deviations. With this procedure, gained knowledge of the 3-D CFD simulation is implemented into the reduced model. The increased number of zones smoothes the burn function and no single zone burn process can be observed. Moreover the burn function and the location of 50 % mass fraction burned show good correlation. Only at the end the burn rate decreases slightly. Additionally only small deviations can be observed in the pressure and temperature trace compared to the test bench data.

## 5 Summary

High efficiency and near zero  $\text{NO}_x$  emissions, which exclude an expansive exhaust gas aftertreatment are the main motivation for ongoing research on controlled auto ignition. However this sensitive part load combustion process is limited to high loads and high speeds. The first part of this paper deals with experimental results from transient test bench investigations. Moreover simulation tools were shown, which allow the simulation of the complex process in different detail levels. The goal of the combustion development is to analyse the low temperature combustion and to model its process. The gained knowledge is used for the controller layout, which will be used for a transient operation, an extension of the operation area as well as a stabilisation of the combustion process.

Based on the steady state investigations, the control path is identified with several transient step response investigations. These results show that a transient operation is possible. Additionally optical investigations are performed, which

are used for a correlation of the CFD results and moreover confirm the fast combustion of the controlled auto ignition.

A coupled CFD model with reaction kinetic is presented to calculate the combustion and to identify the thermodynamic boundary conditions and stratification effects of the auto ignition. Both EGR strategies are successfully simulated and visualized. Based on these results a reduced combustion model is developed, which is coupled with a 1-D gas exchange simulation. This coupling allows a multi-cycle simulation in an appropriate time frame and can be used for future train of the controller or for a valve train layout.

## References

- [1] Sonderforschungsbereich 686 – Modellbasierte Regelung der homogenisierten Niedertemperatur-Verbrennung, RWTH Aachen University und Universität Bielefeld, <http://www.sfb686.rwth-aachen.de>
- [2] Pischinger, S.; Stapf, K. G.; Seebach, D.; Bückler, C.; Adomeit, P.; Ewald, J.: Controlled Auto-Ignition: Combustion Rate Shaping by Mixture Stratification, Wiener Motorenkongress, 24.-25.04.2008, Wien
- [3] Stapf, K. G.; Seebach, D.; Fricke F.; Pischinger, S.; Hoffmann, K.; Abel, D.: CAI-Engines: Modern combustion system to face future challenges. SIA International Conference - The Spark Ignition Engine of the Future, 28.-29.11.2007, Strasbourg
- [4] Goodwin, D.G.: California Institute of Technology. <http://www.cantera.org>
- [5] Adomeit, P.; Jens Ewald, J.; Stapf, K. G.; Seebach, D.; Pischinger, S.: Control and Prediction of the Stochastic Ignition Process for a Gasoline CAI Combustion System, 8. Internationales Symposium für Verbrennungsdiagnostik, 10.-11.06.2008, Baden Baden
- [6] Maßgeschneiderte Kraftstoffe aus Biomasse. RWTH Aachen University. [www.fuelcenter.rwth-aachen.de](http://www.fuelcenter.rwth-aachen.de)
- [7] Marinov, N.M.: A Detailed Chemical Kinetic Model for High Temperature Ethanol Oxidation. In: International Journal of Chemical Kinetics, Volume 31 Issue 3, S. 183-220, 1999
- [8] Golovitchev, V.: Chalmers University of Technology. <http://www.tfd.chalmers.se>
- [9] GRI-Mech 3.0. <http://www.me.berkeley.edu/gri-mech/>
- [10] Connaire, M. O.; Curran, H. J.; Simmie, J. M.; Pitz, W. J.; Westbrook, C. K.: A Comprehensive Modeling Study of Hydrogen Oxidation. In: International Journal of Chemical Kinetics, Volume 36 Issue 11, S. 603-622, 2004
- [11] Bückler, C.; Stapf, K. G.; Krebber-Hortmann, K.; Pischinger, S.; Mori, S.: Different Variable Valve Control Strategies for Controlled Auto Ignition Optimization. HdT-Tagung Variable Ventilsteuerung, 13.-14.02.2007, Essen
- [12] Pischinger, S.; Bückler, C.; Lang, O.; Salber, W.: Untersuchung von Ventiltriebsvariabilitäten für Brennverfahren mit kontrollierter Selbstzündung. 7. Tagung Motorische Verbrennung, 15.-16.03.2005 in München
- [13] Hoffmann, K.; Drews, P.; Seebach, D.; Stapf, K. G.; Pischinger, S.; Abel, D.: Optimized Closed Loop Control of Controlled Auto Ignition CAI. FISITA World Automotive Congress, 14.-19.09.2008, München

## Acknowledgements

The authors would like to thank the German Society of Research (DFG) for the financial funding of this project in the Collaborative Research Centre „SFB 686 – model based control of the homogenized low temperature combustion“.

## IMPRINT

**MTZ** WORLDWIDE

[www.MTZ-online.com](http://www.MTZ-online.com)

04|2009 · April 2009 · Volume 70

**Springer Automotive Media | GWV Fachverlage GmbH**

P.O. Box 15 46 · 65173 Wiesbaden · Germany  
Abraham-Lincoln-Straße 46 · 65189 Wiesbaden · Germany

**Managing Directors** Dr. Ralf Birkelbach, Albrecht Schirmacher

**Advertising Director** Thomas Werner

**Production Director** Ingo Eichel

**Sales Director** Gabriel Göttlinger

## EDITORS-IN-CHARGE

Dr.-Ing. E. h. Richard van Basshuysen

Wolfgang Siebenpfeiffer

## EDITORIAL STAFF

### Editor-in-Chief

Johannes Winterhagen (win)  
Phone +49 611 7878-342 · Fax +49 611 7878-462  
E-Mail: [johannes.winterhagen@springer.com](mailto:johannes.winterhagen@springer.com)

### Vice-Editor-in-Chief

Dipl.-Ing. Michael Reichenbach (rei)  
Phone +49 611 7878-341 · Fax +49 611 7878-462  
E-Mail: [michael.reichenbach@springer.com](mailto:michael.reichenbach@springer.com)

### Chief-on-Duty

Kirsten Beckmann M. A. (kb)  
Phone +49 611 7878-343 · Fax +49 611 7878-462  
E-Mail: [kirsten.beckmann@springer.com](mailto:kirsten.beckmann@springer.com)

## Sections

**Electrics, Electronics**  
Markus Schöttle (scho)  
Phone +49 611 7878-257 · Fax +49 611 7878-462  
E-Mail: [markus.schoettle@springer.com](mailto:markus.schoettle@springer.com)

**Engine**  
Dipl.-Ing. (FH) Richard Backhaus (rb)  
Phone +49 611 5045-982 · Fax +49 611 5045-983  
E-Mail: [richard.backhaus@rb-communications.de](mailto:richard.backhaus@rb-communications.de)

**Heavy Duty Techniques**  
Ruben Danisch (rd)  
Phone +49 611 7878-393 · Fax +49 611 7878-462  
E-Mail: [ruben.danisch@springer.com](mailto:ruben.danisch@springer.com)

**Online**  
Dipl.-Ing. (FH) Caterina Schröder (cs)  
Phone +49 611 78 78-190 · Fax +49 611 7878-462  
E-Mail: [caterina.schroeder@springer.com](mailto:caterina.schroeder@springer.com)

**Production, Materials**  
Stefan Schlott (hlo)  
Phone +49 8191 70845 · Fax +49 8191 66002  
E-Mail: [Redaktion\\_Schlott@gmx.net](mailto:Redaktion_Schlott@gmx.net)

**Service, Event Calendar**  
Martina Schraad  
Phone +49 212 64 235 16  
E-Mail: [martina.schraad@springer.com](mailto:martina.schraad@springer.com)

**Transmission, Research**  
Dipl.-Ing. Michael Reichenbach (rei)  
Phone +49 611 7878-341 · Fax +49 611 7878-462  
E-Mail: [michael.reichenbach@springer.com](mailto:michael.reichenbach@springer.com)

## English Language Consultant

Paul Willin (pw)

## Permanent Contributors

Christian Bartsch (cb), Prof. Dr.-Ing. Peter Boy (bo), Prof. Dr.-Ing. Stefan Breuer (sb), Jörg Christoffel (jc), Jürgen Grandel (gl), Erich Hoepke (ho), Ulrich Knorra (kno), Prof. Dr.-Ing. Fred Schäfer (fs), Roland Schedel (rs), Bettina Seehawer (bs)

## Address

P.O. Box 15 46, 65173 Wiesbaden, Germany  
E-Mail: [redaktion@ATZonline.de](mailto:redaktion@ATZonline.de)

## MARKETING | OFFPRINTS

**Product Management Automotive Media**  
Sabrina Brokopp  
Phone +49 611 7878-192 · Fax +49 611 7878-407  
E-Mail: [sabrina.brokopp@springer.com](mailto:sabrina.brokopp@springer.com)

## Offprints

Martin Leopold  
Phone +49 2642 9075-96 · Fax +49 2642 9075-97  
E-Mail: [leopold@medien-kontor.de](mailto:leopold@medien-kontor.de)

## ADVERTISING | GWV MEDIA

### Ad Manager

Britta Dolch  
Phone +49 611 7878-323 · Fax +49 611 7878-140  
E-Mail: [britta.dolch@gwv-media.de](mailto:britta.dolch@gwv-media.de)

### Key Account Manager

Elisabeth Maßfeller  
Phone +49 611 7878-399 · Fax +49 611 7878-140  
E-Mail: [elisabeth.massfeller@gwv-media.de](mailto:elisabeth.massfeller@gwv-media.de)

### Ad Sales

Frank Nagel  
Phone +49 611 7878-395 · Fax +49 611 7878-140  
E-Mail: [frank.nagel@gwv-media.de](mailto:frank.nagel@gwv-media.de)

### Display Ad Manager

Susanne Bretschneider  
Phone +49 611 7878-153 · Fax +49 611 7878-445  
E-Mail: [susanne.bretschneider@gwv-media.de](mailto:susanne.bretschneider@gwv-media.de)

### Ad Prices

Price List No. 52

## SUBSCRIPTIONS

VVA-Zeitschriftenservice, Abt. D6 F6, MTZ  
P. O. Box 77 77, 33310 Gütersloh, Germany  
Renate Vies  
Phone +49 5241 80-1692 · Fax +49 5241 80-9620  
E-Mail: [SpringerAutomotive@abo-service.info](mailto:SpringerAutomotive@abo-service.info)

## SUBSCRIPTION CONDITIONS

The emagazine appears 11 times a year at an annual subscription rate of 269 €. Special rate for students on proof of status in the form of current registration certificate 124 €. Special rate for VDI/ÖVK/VKS members on proof of status in the form of current member certificate 208 €. Special rate for studying VDI members on proof of status in the form of current registration and member certificate 89 €. The subscription can be cancelled in written form at any time with effect from the next available issue.

## PRODUCTION | LAYOUT

Heiko Köllner  
Phone +49 611 7878-177 · Fax +49 611 7878-464  
E-Mail: [heiko.koellner@gwv-fachverlage.de](mailto:heiko.koellner@gwv-fachverlage.de)

## HINTS FOR AUTHORS

All manuscripts should be sent directly to the editors. By submitting photographs and drawings the sender releases the publishers from claims by third parties. Only works not yet published in Germany or abroad can generally be accepted for publication. The manuscripts must not be offered for publication to other journals simultaneously. In accepting the manuscript the publisher acquires the right to produce royalty-free offprints. The journal and all articles and figures are protected by copyright. Any utilisation beyond the strict limits of the copyright law without permission of the publisher is illegal. This applies particularly to duplications, translations, microfilming and storage and processing in electronic systems.

© Springer Automotive Media |  
GWV Fachverlage GmbH, Wiesbaden 2009

Springer Automotive Media is part of the specialist publishing group Springer Science+Business Media.

# Five continents – one source of knowledge



Sean H., Manufacturing Manager  
AUSTRALIA



Daniel G., Application Engineer  
EUROPE



Vanessa P., Executive Director Product Engineering  
AMERICA

personal buildup for Force Motors Ltd.



Antony F., Director of Business Development  
AFRICA



Ming Li H., Senior Electronics Engineer  
ASIA



Drawing on the credibility and longevity of ATZ, the longest established auto trade magazine in the world, AutoTechnology has been rebranded ATZautotechnology.

ATZautotechnology delivers great value. With increased content, more issues per year and greater geographical coverage, including China and India, it is still the best source of technical information for global automotive engineering, production and management teams.

For more information, visit our website [www.ATZonline.com](http://www.ATZonline.com)



Magazine of FISITA – the world body for automotive engineers

**ATZ**  
autotechnology



# Cylinder Deactivation for Valve Trains with Roller Finger Follower

Cylinder deactivation increases efficiency of gasoline engines without negative effects in terms of exhaust gas emissions or driving dynamics. In particular, the advantageous cost/benefit ratio and great affinity to technologies currently used in gasoline engines support cylinder deactivation as the right path in meeting future market demands. The design and function of cylinder deactivation for valve trains with roller finger follower will be explained and examined with regard to functional aspects, such as stiffness, mass, and kinematic behavior. Based on initial results, design and production characteristics of this new technology are evaluated and technical control interactions in engine applications are presented by Mahle.

## 1 Introduction

Cylinder deactivation is a suitable measure, based on a cost-benefit ratio, particularly for gasoline engines with greater and even numbers of cylinders, for reducing fuel consumption without negatively affecting driving dynamics and exhaust gas emissions. The potential of cylinder deactivation for fuel consumption reduction can be seen in **Figure 1**. The data result from a driving cycle simulation – in this case, the “New European Driving Cycle” (NEDC) – which was performed on two vehicles, a sedan with an eight-cylinder engine and an SUV with a six-cylinder engine. Compared to an engine without cylinder deactivation, an 11 % reduction in fuel consumption is possible. When rating the values, it must be considered that the cylinder deactivation is activated only from the 2<sup>nd</sup> gear on, in a range from 1200 to 3500 rpm.

The advantage in fuel consumption with cylinder deactivation results substantially from shifting the operating points into a better engine efficiency range. If the engine is operated in the lower half of the engine operating map, half of the cylinders can be shut off. In order to ensure the same amount of torque, load of fired cylinders must be increased. This is accompanied by intake detuning, improved combustion conditions and residual gas tolerance as well

as reduced valve train friction, which increase engine efficiency at this operating point.

Cylinder deactivation is in competition with other measures for reducing fuel consumption, such as stratified gasoline direct injection. In order to implement stratified charge operation, injectors with piezo technology and a cost-intensive exhaust gas aftertreatment using a DeNO<sub>x</sub> catalytic converter or SCR technology are required. These costly components can be avoided with cylinder deactivation. Furthermore, with cylinder deactivation there are no requirements for fuel quality and thus ensures worldwide application of the same engine concept.

## 2 Function of the Switchable Lever

The main component of the switchable roller finger follower consists of two partial levers, **Figure 2**. The partial lever on the HLA side, which is supported on the hydraulic lash adjuster (HLA), is connected by the roller pin to the valve-side partial lever, which rests on the valve. The axis of the roller pin is also the common axis of rotation for both partial levers. The lost motion spring moves both partial levers back to the starting position after each lever collapse motion (zero lift of the valve). The coupling bolt,

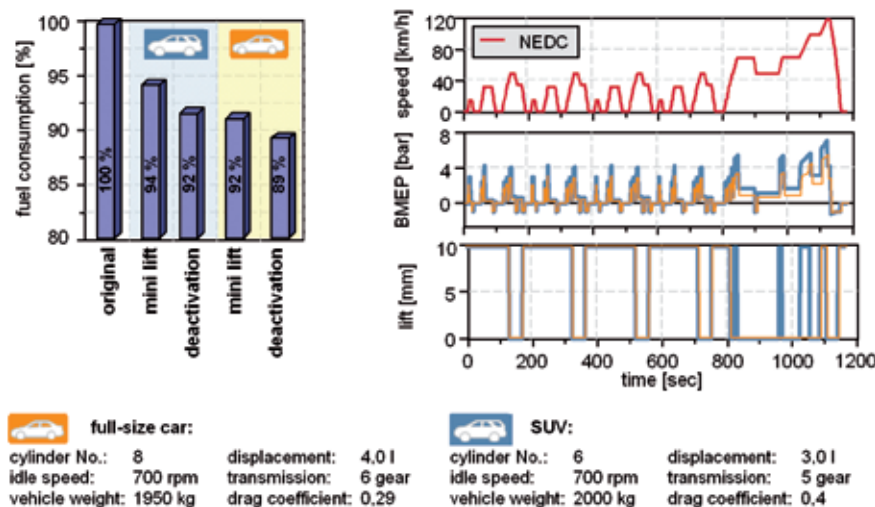


**Figure 1:** Potential for fuel consumption reduction using cylinder deactivation

## The Authors



Dipl.-Ing. Hermann Hoffmann is Head of Design and Supervisor for Variable Valve Train Technology within Mahle International GmbH in Stuttgart (Germany).



Dr. techn. Adam Loch is Project Leader in Research and Advanced Engineering of Mahle International GmbH in Stuttgart (Germany).



Dipl.-Ing. (FH) Richard Widmann is Design Engineer in Research and Advanced Engineering of Mahle International GmbH in Stuttgart (Germany).



Dipl.-Ing. Gerhard Kreusen is Project Engineer CAE in the Dynamics Department and Project Team Leader at FEV Motorentechnik GmbH in Aachen (Germany).



Dipl.-Ing. Daniel Meehsen is Project Engineer in the Mechanics and Test Department at FEV Motorentechnik GmbH in Aachen (Germany).



Dr.-Ing. Martin Rebbert is Leader of the Dynamics Department at FEV Motorentechnik GmbH in Aachen (Germany).

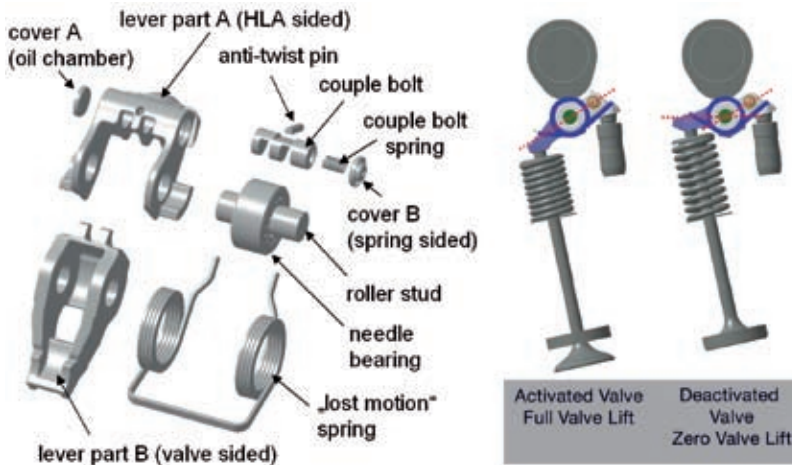


**Figure 2:** Exploded view of the lever components, switchable lever in both functional states (activated and deactivated valve lift)

which is guided in the HLA-side partial lever, provides the locking and unlocking function.

In the locked position, the partial levers cannot rotate relative to each other. The switchable lever takes on the function of a typical roller finger follower and the full valve lift is provided, Figure 2. In this position, the coupling bolt blocks both switching grooves in the HLA-side partial lever, so that the switching lugs on the valve-side partial lever rest on the coupling bolt.

In the unlocked position, the coupling bolt releases the switching grooves in the HLA-side lever. The valve-side partial lever can swing through during cam lift. No valve lift is provided, Figure 2.

The concept of the switchable lever has the advantage that there is a roller

contact between the cam and the lever in both operating modes. In contradiction to other valve deactivation systems using sliding actuation, the friction losses remain at typically low level of roller finger followers. Switching between the operating modes is done by shifting the coupling bolt against the coupling bolt spring with oil pressure. Through the HLA gallery and the oil injection bore of the HLA the oil flows into the lever and to the coupling bolt, Figure 3. The oil pressure level is controlled by a solenoid valve. When the solenoid valve is off, the oil pressure is regulated at a relative value of about 0.7 bar, to ensure the function of the HLA. The coupling bolt spring thus holds the coupling bolt in the locked position. At suitable partial load engine operating points and an oil pump

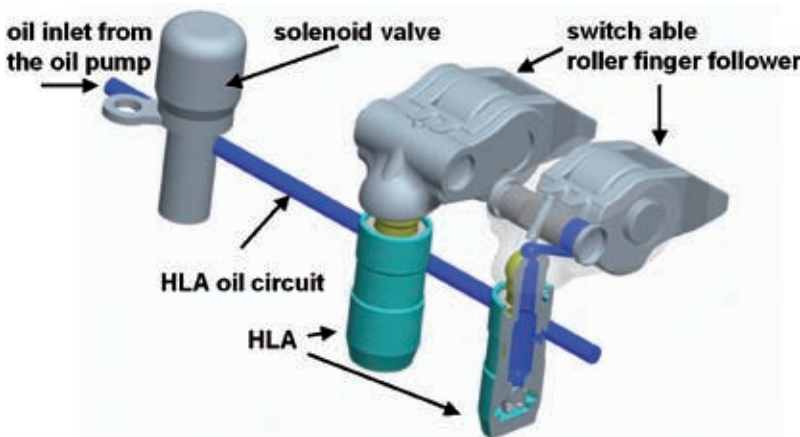


**Figure 3:** Illustration of the oil circuit for switching

pressure level of more than 1.5 bar (relative), the solenoid valve can be actuated and the oil pump pressure is applied to the HLA gallery. The oil pressure force on the coupling bolt exceeds the force of the spring and pushes the coupling bolt into the unlocked position.

### 3 Design and Computation

A V6 engine is used as an experimental platform for the development of the switchable lever. For this cylinder arrangement, one cylinder bank is shut off. Experience and results from development can be applied to other engine variants, in which only individual cylinders per bank are deactivated.

Prior to designing the switchable lever, an analysis of the original valve train kinematics is performed. The contact point movement between the switchable lever and the valve stem takes place in one direction in normal valve trains. In this switchable valve train, the contact point moves in the opposite direction in case deactivation is enabled. For both load cases, it must be ensured that the switchable lever never slides off the valve.

Using the new kinematics, which meets the requirements of the valve train, the design is detailed. Boundary conditions are package constraints, lever rigidity, mass inertia relative to the maximum rpm, and durability.

The loads and stresses are checked using FEM and MBS analyses. The stiffness of the last prototype, for example, was increased by 35 % in the individual design iterations.

### 4 Switching Strategy and Switching Tests

The switching strategy depends on the time that the coupling bolt requires to move from the locked to the unlocked position, called shift time in this context. The time available for this motion, called maximum shift time here, must also be considered. The maximum available time is prescribed by the base circle of the cam contour and the camshaft phase, and thus depends on the rotational speed.

The test for determining the shift time was carried out for different oil pump pressures and temperatures. An example for the unlocking phase (deactivation of valve lift) is shown in Figure 4. In off position, the solenoid valve regulates the oil pressure in the HLA gallery to 0.7 bar (relative) whereas the oil pump pressure is 4.5 bar (relative). After the current signal (start signal) for the solenoid valve, oil pressure increase can be detected in the HLA gallery and at the coupling bolt. Simultaneously, a slight drop of the oil pressure supply feed occurs above the solenoid valve. After a reaction time of about 9 ms and a pressure rise to about 1.1 bar (relative), the coupling bolt motion starts. The time in which the coupling bolt is in motion is defined as the shift time.

These measurements result in a characteristic map of the reaction time and shift time relative to the oil pump pressure and temperature. In order to ensure reliable switching, the switching time must be lower than the maximum available shift time. The response time can be maintained in the electronic control unit and therefore does not need to be included in the maximum switching time.

If the measured shift times are plotted against the rpm, the result is the diagram shown in Figure 5 (right). The higher the rpm, the shorter the shift time, as the oil pump pressure in the engine increases. If a safety time is added to the measured shift times, then the result is a required shift time curve over rpm (shown in green in Figure 5). The curve for the maximum available shift time must be greater than the switching time curve in order to allow switching.

When determining the switching strategy, the number of solenoid valves, and thus the maximum shift time, the following boundary conditions must be covered:

- cylinder firing sequence: Every other cylinder must be switched off
- unlocking (deactivate valve lift): Switch off exhaust valve before intake valve, so that the exhaust gas is contained in the combustion chamber; This ensures that the cylinders do not cool down and the overpressure in the combustion chamber presses the valves against their seats

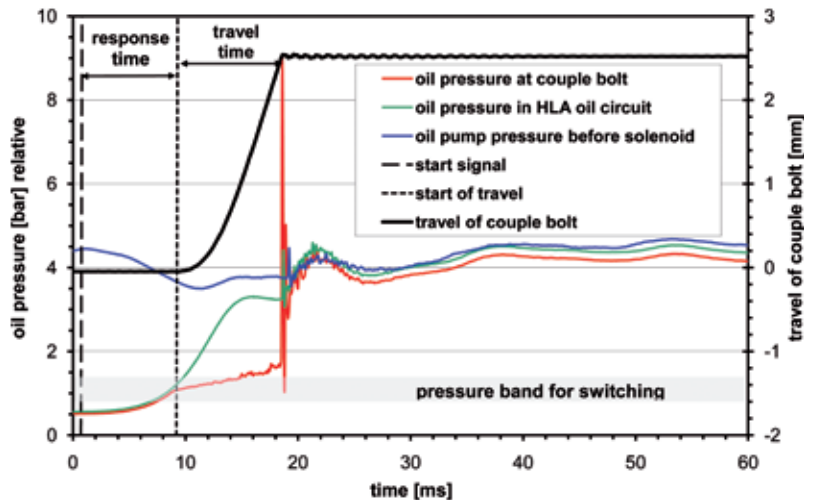


Figure 4: Shift time of the coupling bolt and oil pressure curve (90 °C oil temperature; 4.5 bar relative oil pump pressure)

- locking (activate valve lift): Engage exhaust valve before intake valve, so that the exhaust gas contained in the cylinder is first expelled into the exhaust system before fresh air is drawn in. Using the example of a V6 engine, the switching strategy with two solenoid valves is explained. In this engine design, due to the firing order, one entire bank (three cylinders) is shut off. The black bars in Figure 5 show the event duration of individual valve lifts. If the start of the shift time is placed in the initial stroke of the intake valve of the first cylinder, then the result is a maximum shift time of 414° crank angle for the first switched exhaust valve (1<sup>st</sup> cylinder). Converted to milliseconds, a curve for the maximum shift time

over rpm results (blue line in Figure 5). Using this switching strategy, a range of about 1000 rpm to 4000 rpm is possible, as the maximum shift time in this range exceeds the required shift time. The lower limit (here 1000 rpm) is determined by the oil pump pressure level. An oil pressure of about 1.5 bar (relative) is needed in order to allow switching.

### 5 Motored Test of Cylinder Head

Using the described switching strategy, switching tests were performed on a motored cylinder head. Oil flow rate, oil pressure, and oil temperature were set according to the engine operating map.

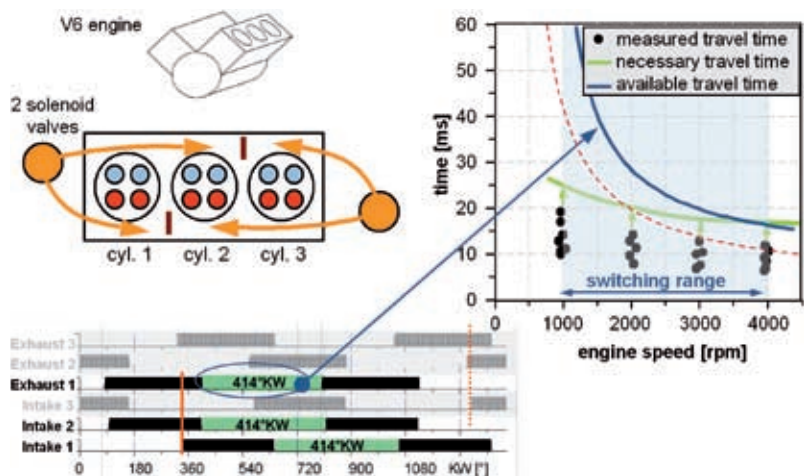


Figure 5: Switching strategy with two solenoid valves

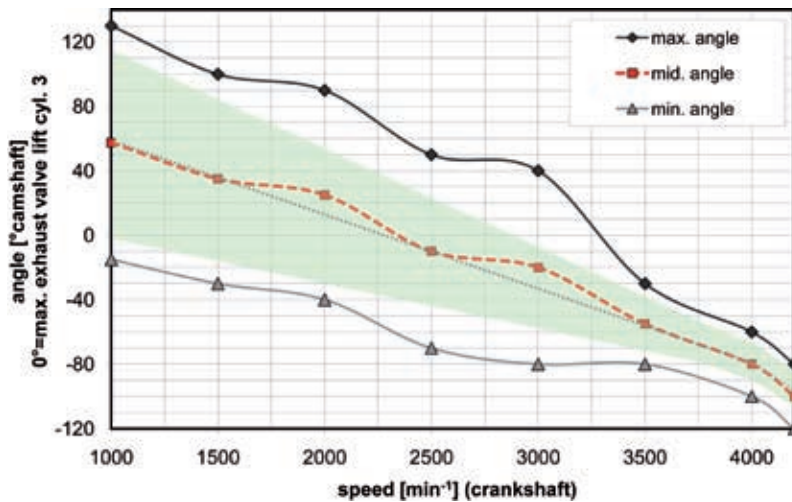


Figure 6: Control signal window over rpm at 90 °C oil temperature

Oil pressure was measured upstream and downstream of the solenoid valves.

In addition to switching function tests, an angle range for the actuation of the solenoid valve for each rpm is determined which enables successful on/off switching of the valve lifts. Therefore the actuation signal is shifted by discrete camshaft angles, until successful deactivation of the valve lift can be detected. This provides the minimum angle limit for switching. The actuation signal is shifted further, until the deactivation is no longer successful, i.e., the valve lift can still be seen. The range between the minimum and maximum angle represents the control signal window for successful switching operation. For an oil temperature of 90 °C over rpm, the control signal window test results are shown in Figure 6. The control signal window range reaches values between 280° crank angle at 1000 rpm and 80° crank angle at 4200 rpm. This leads to a safety margin of 40° crank angle, if an average value is selected for possible switching at 90 °C oil temperature.

Activation of the valve lifts, in general, shows smaller control signal windows than deactivation. Overall, the tests at 90 °C oil temperature result in successful deactivation and activation up to 4000 rpm. Lower oil temperatures increase the shift time of the coupling bolt due to higher oil viscosity, and reduce the width of the control signal window.

## 6 Summary

Pressure on engine manufacturers to introduce technologies for fuel consumption reduction is enhancing. One sensible technology for gasoline engines is cylinder deactivation and offers consumption improvements of up to 11 %.

The advantages of the Mahle system are its favorable price/performance ratio and the potential for simple application of the system in proven engine designs. Other than the switchable lever and solenoid valves, no additional components or additional oil circuit are needed.

The entire development process, from kinematic design, design, FEM and MBS analysis, to prototype building, quality inspection, and testing has been performed for a V6 engine. The boundary conditions for planned series production have also been considered for the current design. The steps indicated are contained in a development guideline that allows rapid and reliable adaptation of the switchable lever to other engines.

The article explains both the backgrounds of possible switching strategies and the successful switching function and limits by test results. The system is an attractive way to reduce CO<sub>2</sub> emissions and is being systematically adapted for other engines. ■



personal buildup for Force Motors Ltd.

# Imagine that electronics was orange ...

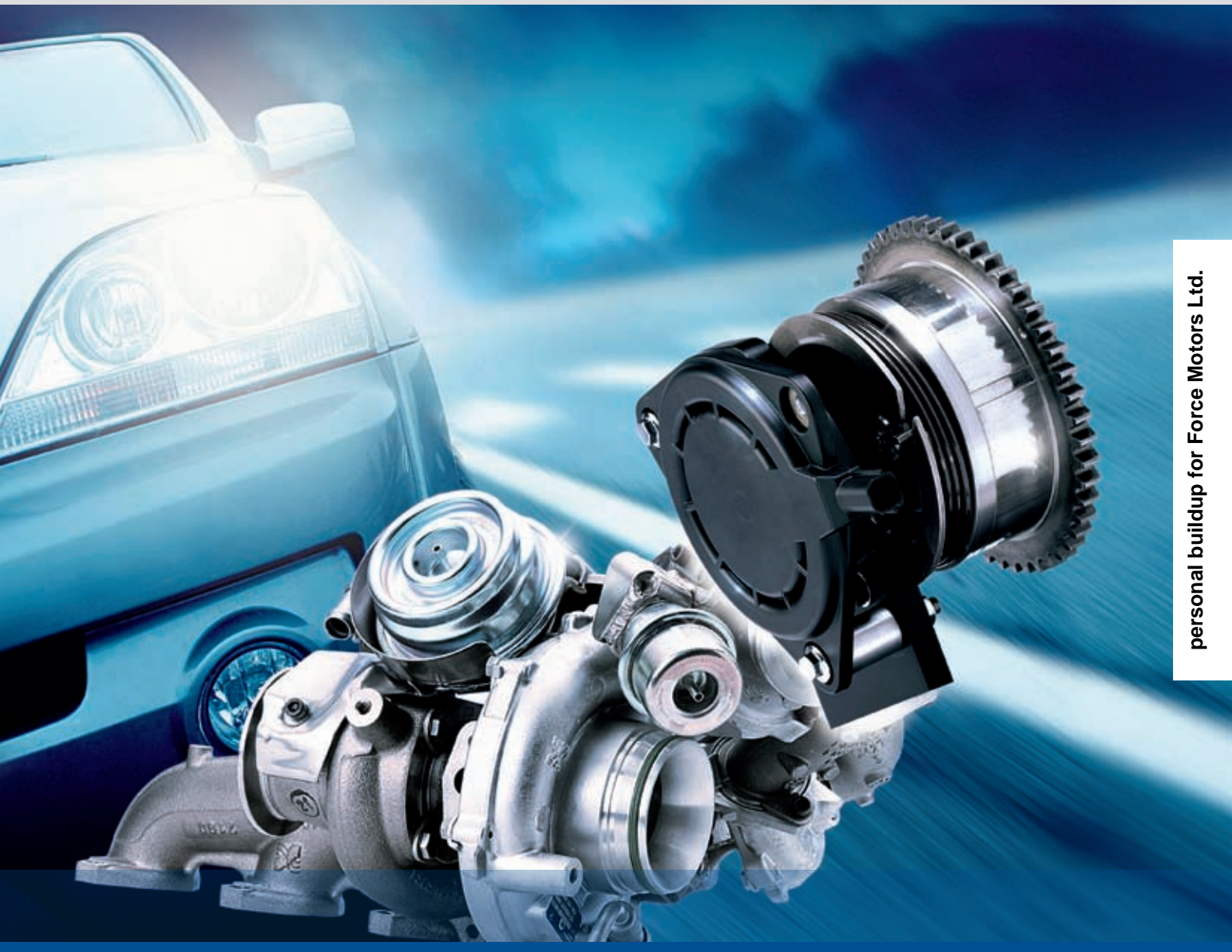


The colour orange stands for creativity and dynamic energy. And because there is hardly any other sector in which development is as active and dynamic as automotive electronics, there is now a specialist e-Magazine in orange: **ATZelektronik**.

ATZelektronik reviews the latest trends and developments in electronics and software across the global automotive industry 6 times per year. On an academic level. With a unique profoundness of information.

Find out everything you need to know about the latest developments, methods and electronic components. Read how future driver-assistance systems will change our mobile society. Monitor the progress of on-board electrical systems and energy management. ATZelektronik is an essential source of information on these and many other industry topics.

Furthermore, as a subscriber to ATZelektronik, you will benefit from our online archive of articles; an indispensable research tool that offers free downloads of the articles. Want to stay ahead of the pack? Order your free electronic sample edition today at [www.ATZonline.com](http://www.ATZonline.com).



# Variable Valve Timing Complementing Hybrid-EGR at Diesel Engines

To understand the benefits of the Atkinson cycle added to a two-stage boosting system including Hybrid-EGR, engine simulations were carried out by BorgWarner. The possible valve curves were determined by a real variable valve timing device consisting of two concentric camshafts with an integrated cam phaser. The results promise a higher degree of freedom in tradeoffs between fuel economy,  $\text{NO}_x$  emission and Particulate Matters (PM).

## 1 Introduction

The diesel engine is facing a trade-off between emission regulation and cost increase. Compared to the gasoline engine, where healthy cost/benefit ratios of exhaust aftertreatment systems have generated a reasonable atmosphere in the development processes and technology approaches, the diesel engine emissions, especially those for  $\text{NO}_x$ , are subject of both engine internal measures as well as extensive aftertreatment concepts. Besides high pressure exhaust gas recirculation (HP EGR), low pressure exhaust gas recirculation (LP-EGR) [2-7] has recently been introduced to the market [3, 11]. In addition, efficient boosting components like variable turbine geometry (VTG) and regulated two-stage turbo charging are state of the art. Diesel particulate filters (DPF) and diesel oxidation catalysts (DOC) are mandatory aftertreatment components.

To meet Euro 6 emission regulation targets, lean  $\text{NO}_x$  traps (LNT) or selective catalytic reduction systems (SCR) are being considered depending on the vehicle size in the aftertreatment environment. Today, the most favourable boosting-EGR combination consists of a two-stage boosting system with a Hybrid-EGR (HP and LP EGR) loop. In a simplified scenario, expensive  $\text{NO}_x$  aftertreatment systems like LNT and especially SCR provide excellent results within rational development and application timeframes, whereas engine internal measures combine aspects of driveability, performance and controllability, but drive up the development effort and provide a high level of uncertainty to the decision makers. Both solutions, for example to meet Euro 6, are therefore in a competition in terms of time, budgets and success.

While the application of  $\text{NO}_x$  aftertreatment will lead quickly and safely to successful Euro 6 vehicles, it's more difficult and riskier to introduce engine related measures. On the other hand engine related measures are more cost effective. One possible scenario is that exhaust aftertreatment systems for  $\text{NO}_x$  removal will penetrate the market but later, once understood, investigated and tested, engine related concepts might dominate. It has been suggested [21] that a two-stage, boosted, Hybrid-EGR equipped engine will meet the targets without  $\text{NO}_x$  reduc-

tion equipment for a broad vehicle fleet. This seems to be possible in combination with high performance fuel injection systems [8, 22]. The contribution of late intake valve closing (LIVC), also called Atkinson Cycle, to emission concepts has been investigated. To maintain performance, improved turbo charging is necessary and  $\text{NO}_x$  can be lowered down by 30 % without any disadvantage in fuel economy [9]. Nevertheless, the combination of Hybrid-EGR, turbo charging and LIVC has only been partially investigated. Sometimes results are focused on combustion in single cylinder engine (SCE) tests, in other cases EGR has been neglected, or – based on engine displacement – full load operation had priority.

This paper deals with the complex question, in how far the application of variable valve actuation (VVA), especially LIVC, may add benefits to emissions, performance or fuel economy of modern diesel engines. A well calibrated simulation model including detailed properties of today's and future breathing systems was used.

## 2 Concept Selection of Variable Valve Timing

Engine related investigations to understand variable valve trains are often run with fully variable concepts. The entire potential can therefore be explored. Transferring the investigative results to new products is sometimes difficult, especially to find the best and most cost effective product solution.

Therefore a different approach was used. Looking sideward to the gasoline engine where cam phasers have been used successfully during the past 20 years, then adding two concentric camshafts, a new VVA concept has been developed, **Table**. The first, left column in the Table explains the objective, the second column focuses on the method the third column on the required variable valve train functionality. The Table also shows that the new variable duration control (VDC) concept can be applied to the exhaust as well as the intake side. It can also be understood the new VDC concept can perform eleven out of sixteen useful functions.

In **Figure 1** the new product is illustrated in a 3D view. The two concentric cams

## The Authors



**Dr.-Ing. Olaf Weber** is responsible for Engine Systems at BorgWarner in Auburn Hills, Michigan (USA).



**Dipl.-Ing. Volker Jörgl** represents Diesel Systems at BorgWarner in Kirchheimbolanden (Germany).



**Dipl.-Ing. Wolfgang Bullmer** leads Engineering, Product Management and Business Development at BorgWarner MorseTec in Ithaca, New York (USA).



**Steve Wyatt, M.Sc.** is responsible for New Components and Systems at BorgWarner MorseTec in Ithaca, New York (USA).

**Table:** Diesel engines and their potential using variable valve trains

BorgWarner VDC* potential on diesel engines				
Goal	Method	VVA functionality	VDC location	
			Intake	Exhaust
Reduced NO <sub>x</sub> /Smoke	Lower process temperature through red. eff. CR	EIVC or LIVC	○	
	Vary swirl	Variable Intake valve Lift		
	Use Internal EGR to reduce peak process temp.	EEVC + LIVO or 2 <sup>nd</sup> valve actuation event	○	○
Improved fuel economy	Higher volumetric efficiency	optimized valve timing + lift curve	○	○
	Cylinder cut out	Valve deactivation		
Transient performance	shut off of internal EGR or Miller /Atkinson instantly	EEVC + LIVO	○	
Engine cranking*	Reduce cranking torque (fluctuations)	EIVC or LIVC	○	
Engine shut off*	Reduce torque (fluctuations)	EIVC or LIVC	○	
Effective after treatment Regeneration	Reduce air flow through red. volumetric efficiency	EIVC or LIVC	○	
	Increase exhaust gas temperature	EEVO		○
Cold starting/idling	Increase effective CR	Optimized IVC	○	
Engine warm up**	Use Internal EGR to increase exhaust temperature	EEVC + LIVO or 2 <sup>nd</sup> valve actuation event	○	○
Combustion stability	Control ignition delay /heat release (cylinder spec.)	EIVC or LIVC (cylinder specific)		
Faster Catalyst light off	Increase exhaust gas temperatures	EEVO		○
Increased low end torque	Recharge the cylinder with exhaust gas	2 <sup>nd</sup> exhaust valve actuation event during intake		
Engine braking	Use engine as compressor only	EVO at TDC (additional decompression hump)		

Possible with VDC family
 \*Variable Duration Control

personal buildup for Force Motors Ltd.

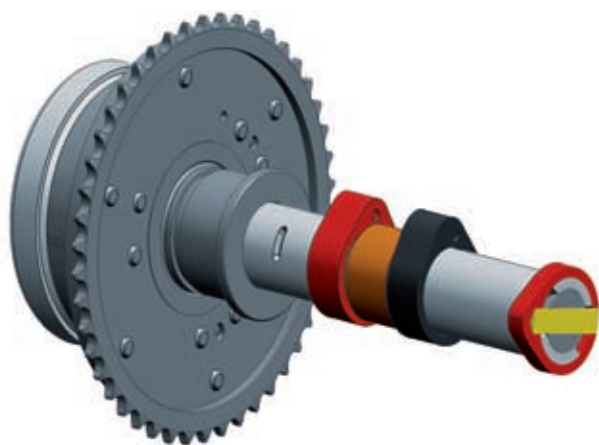


**Figure 1:** 3-D view of the variable duration control (VDC) concept

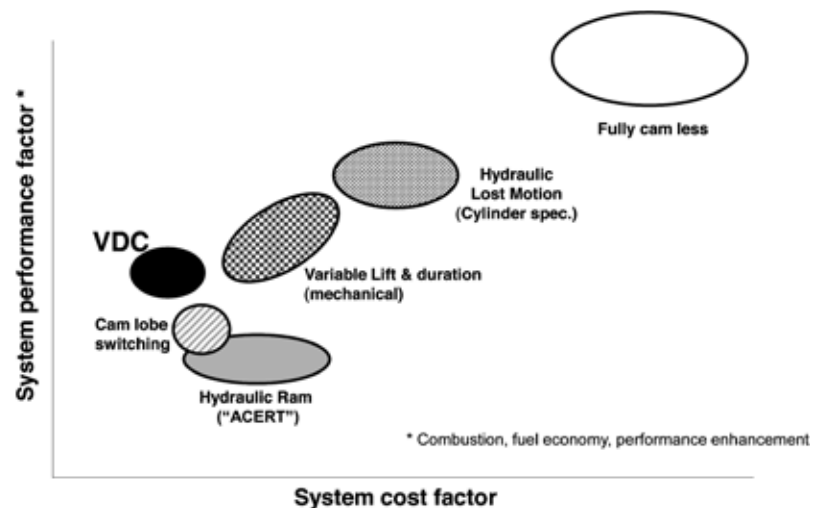


**Figure 2:** Cost/performance trade-off for different valve timing systems

are attached to a cam phaser. One of the intake lobes (red) is mounted on the inner shaft which itself is actuated by the cam phaser. The other intake lobe in this example is attached to the outer cam and is not actuated during the operation. The price/performance ratio can be seen in **Figure 2**. An average performance factor is being determined by the fact that VDC meets eleven out of sixteen different functionalities shown in the Table. The system cost factor of course is rather low because

robust, approved and rather simple technologies from the gasoline engine side are used. The fully variable VVA option of course shows the best performance but is the most expensive solution by far.

Referring to the situation in the literature, it was decided to start the variable valve actuation study with the Atkinson cycle, **Figure 3**. In other studies, which are not shown here, early intake valve closing influence and a symmetrical variable overlap between exhaust and inlet valve

for highly transient operation to control internal EGR has been investigated. The VDC concept can be exercised on different levels of complexity. VDC Type I, shown in **Figure 4**, is limited to actuating only one inlet valve so the area below the valve curves remains unchanged. VDC Type II, made possible through an additional sub component, can actuate both intake lobes and, due to that fact, enlarges the area under the valve curves. Considering high air velocities in the gap be-

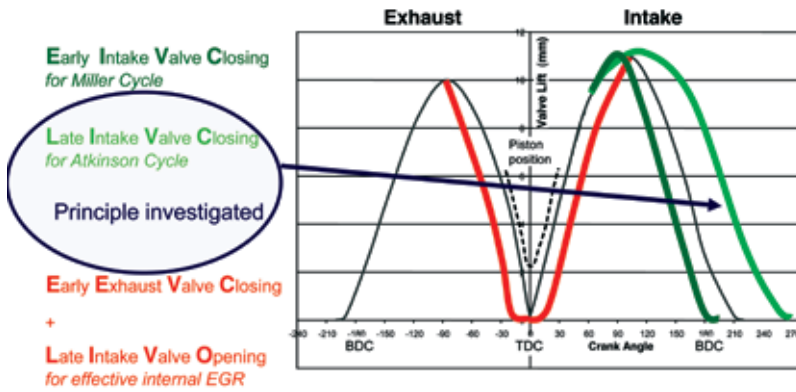


Figure 3: Identified preferred valve timing strategies

### VDC Type I

Using 1 cam phaser mounted on a concentric cam shaft to phase one valve in relation to the other:

- increasing the overall valve event duration
- maintaining the same overall open area under the valves

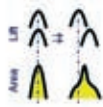


Figure 4: Variable duration control (VDC), working principle

### VDC Type II

Using 1 cam phaser and a concentric cam shaft to virtually create a "longer" cam lobe for both valves using the "handoff" principle.

- increasing the overall valve event duration of both valves
- therefore increasing the open area under the valves



tween valve and seat, VDC Type II is of course the more promising solution. The piston pushes out air into the intake port and especially at very late intake valve closing timing throttling occurs at low valve lift. This results in a higher temperature in the cylinder which is not desired because it is contradictory to the Atkinson effect. Large engines with low engine speeds and rather large intake areas will require only Type I. Type II might be preferred for engines with an engine displacement smaller than 2.0 l and engine speeds higher than 1500 rpm. All the investigations described below were therefore carried out with VDC Type II to capture all advantages.

## 3 Full Breathing System Investigation

### 3.1 System Selection

Two-stage boosting and Hybrid-EGR-systems are in the process of penetrating the market. The addition of LVC requires even higher boost pressures which led to the decision that single stage systems would not be investigated. Regulated two-stage turbo charging (R2S), Figure 5, top, and variable turbine geometry two-stage turbo charging (V2S), where the high

pressure turbine regulating valve is replaced by a VTG, are the starting points of the simulation. The selected EGR-system consist of both cooled LP-EGR and HP-EGR circuits, Figure 5, bottom, to be as competitive as possible, although the resulting complexity is quite high. To keep EGR temperatures low, therefore creating a tough competitive environment for VDC, both EGR-loops were equipped with the best conceivable cooling components.

### 3.2 Boosting System and Late Intake Valve Closing

Both the R2S and the V2S were compared directly, Figure 6, in an LVC sweep by maintaining the engine speed, load and air/fuel ratio. With increasing LVC the required boost pressure increases and the exhaust gas energy demand of the turbine rises, which can be seen in the decreasing turbine bypass mass ratios, Figure 6, bottom. The overall turbine efficiency includes the losses induced by

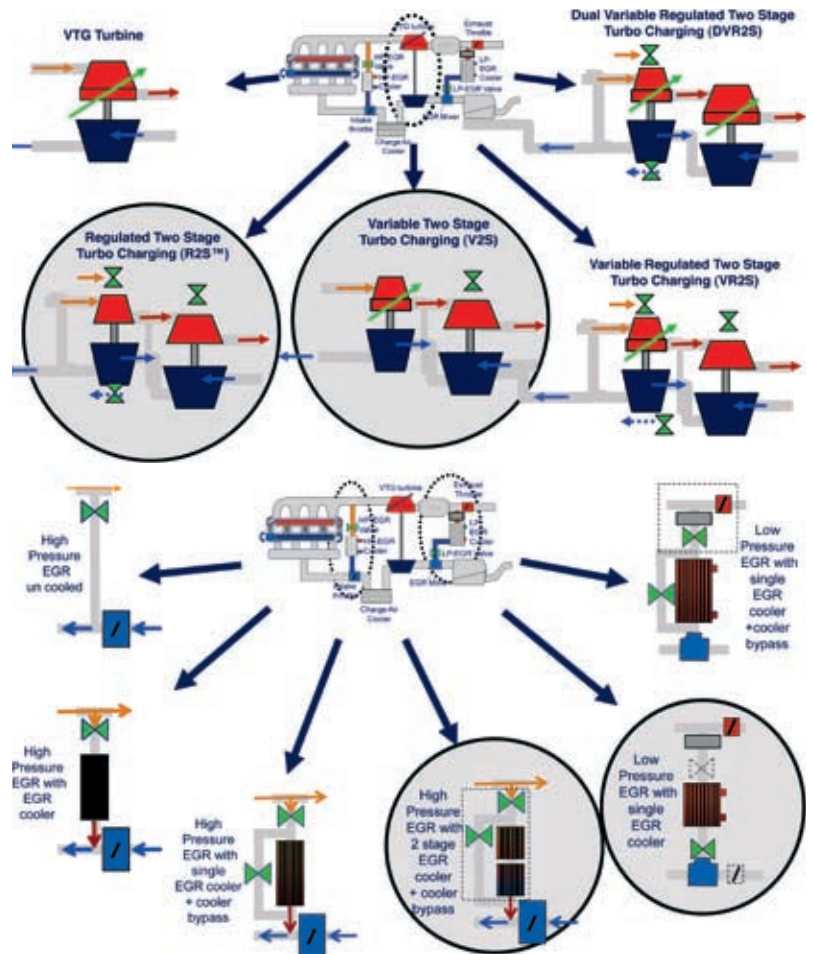


Figure 5: Considered breathing system configurations

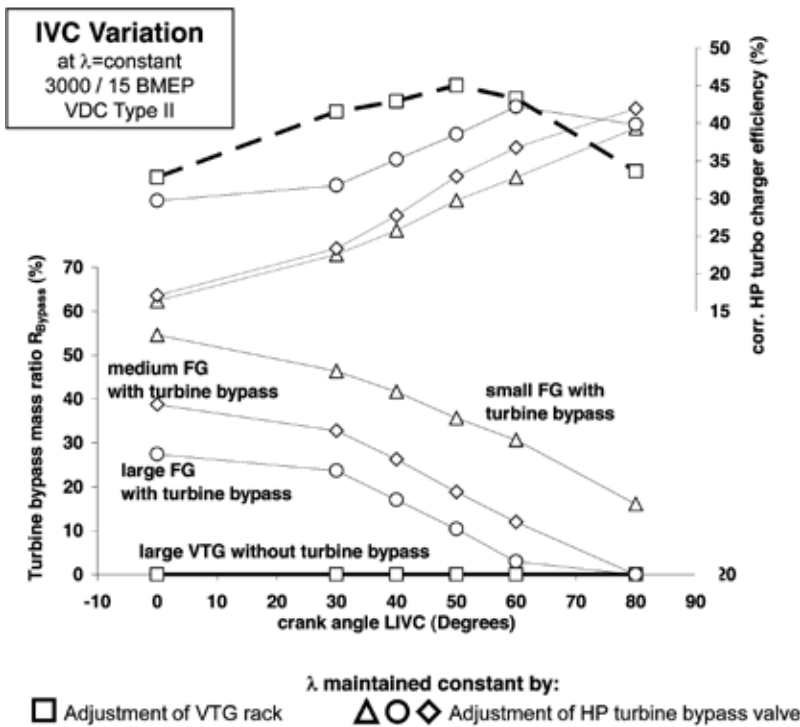


Figure 6: Marriage between turbo charging and variable valve timing

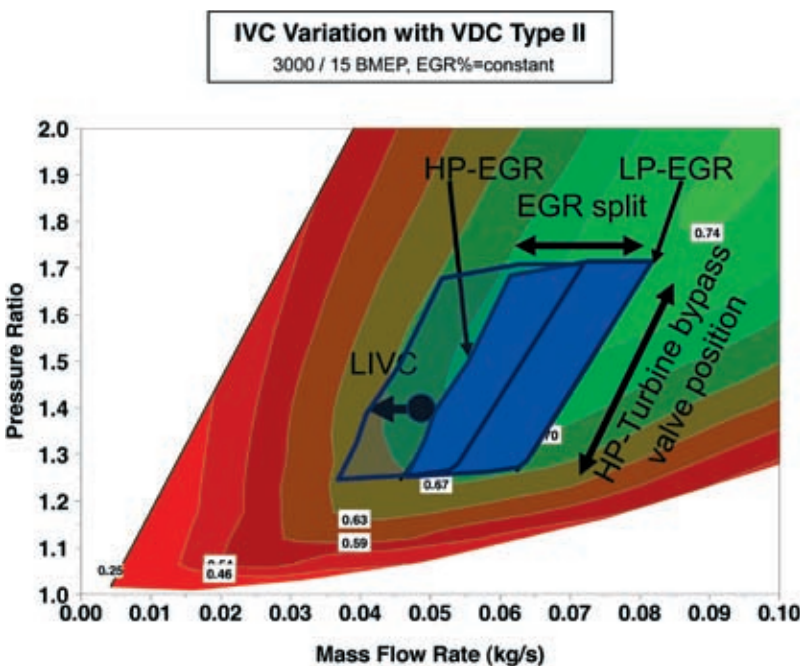


Figure 7: Engine operating points documented in the compressor map under consideration of Hybrid-EGR, turbine bypass valve and late intake valve closing

the bypass flow, increases, Figure 6, top. Higher required boost pressures would therefore not necessarily cause higher fuel consumption, if they allow more efficient use of the boosting system. The VTG version starts with much higher ef-

ficiencies but of course is inferior when the high pressure turbine bypass valve of the R2S system is closed. The fixed geometry turbines (FG), used in the R2S system, have superior efficiency throughout their flow range used. The full flow range

is needed at crank angle LIVC of more than 70°.

It has to be stated that the Brake Specific Fuel Consumption (BSFC) can be kept constant although the absolute boost pressure, the pressure drop in the piping and the throttling in the valve seat area increase the pressure losses. Nevertheless the pumping losses are lower due to higher efficiencies of the boosting system. It is just important to achieve a suitable turbo matching.

### 3.3 LIVC and Hybrid-EGR in Concert

To visualize the influence of both Hybrid-EGR and LIVC, the air system application plots (ASAP) used in [1] were enhanced, Figure 7. The solid blue field symbolizes the possible operating range when engine load, speed and EGR rate are being held constant. The split between HP- and LP-EGR is variable as well as the boost pressure and air fuel ratio. The left border is limited by the HP-EGR rate, which lowers the flow through the compressor. The right border is described by the LP-EGR rate which maintains the compressor flow. The top border is limited by the maximum boost pressure possible and the bottom border by the air/fuel ratio of one, which can certainly be seen as a combustion limit. If LIVC is applied to the engine, the compressor flow decreases due to the smaller effective engine displacement and the entire blue field moves to the left (blue shaded).

Figure 8, top, shows the results for the air/fuel ratio at constant engine speed, load and EGR-rate for the large FG high pressure turbine described in Figure 6. Keeping the load constant, the effective engine downsizing by LIVC leads to lower air/fuel ratios and a limited area of possible operation. The resulting combustion chamber temperature at 50° before top dead centre (TDC) can be seen in Figure 8, bottom. It is significantly lower by 60 K compared to that obtained with the standard valve timing. This just confirms literature data. Both NO<sub>x</sub> reduction measures, Hybrid-EGR as well as LIVC, need a highly performing boost system which provides enough energy to take advantage of their functionalities. In case of the EGR the turbocharger has to pump more EGR to keep the air to fuel ratio and engine load constant. Using LIVC, the boost pressure has to be higher to compensate

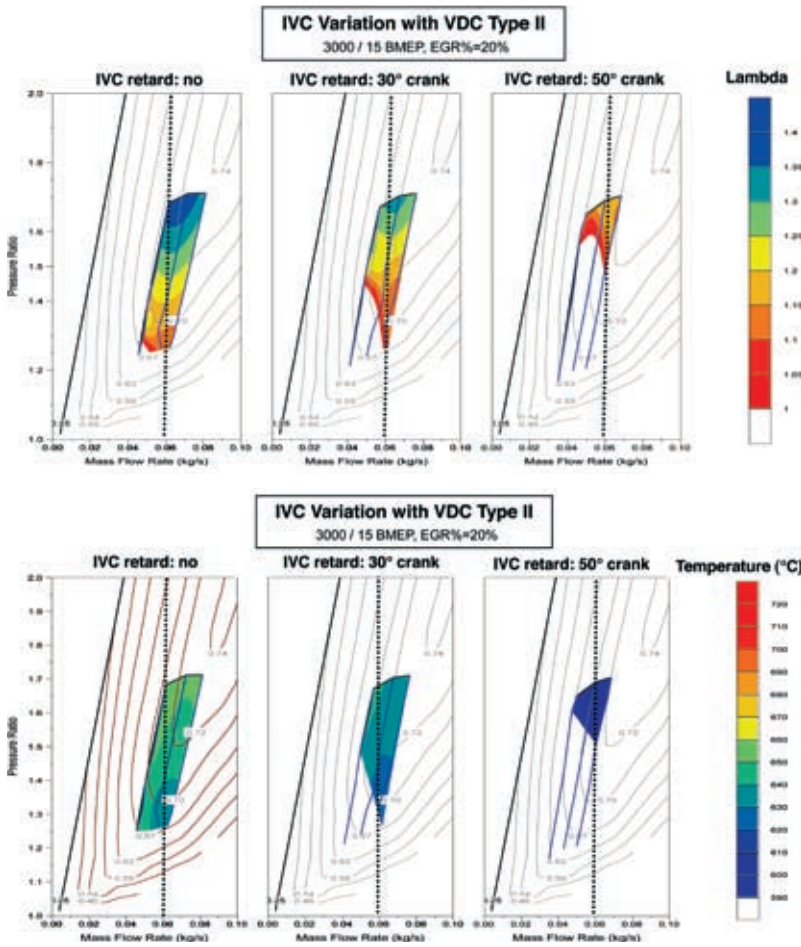


**Figure 8:** Air/fuel ratio and air temperature before start of injection, considering EGR-split and intake valve closing timing, at 3000 RPM and 15 bar BMEP

for the air mass loss to the intake port. To compare both strategies, the operation point described above was now run applying EGR rates higher than 20 %, but without LIVC. The result can be seen in **Figure 9**. Compared to **Figure 8**, the trend is the same. Of course the temperatures are higher compared to the LIVC operation. As a side result it is obvious that low pressure EGR is not worthwhile to apply in this kind of case because there is enough exhaust energy available in front of the turbine. It's also obvious that the performance limit of the turbocharger is reached at an EGR rate of 26 %. This is equivalent to a 20 % EGR rate and a LIVC time of 50° seen in **Figure 8**.

Both operating strategies can be compared in diagrams. The top of **Figure 10** shows the result where the BSFC was kept constant. We then can see the temperature advantage of 60 K in case of LIVC. On the other hand we have a higher oxygen

concentration in the combustion chamber by 1 % point. This leads, in combination with other parameters, to a higher

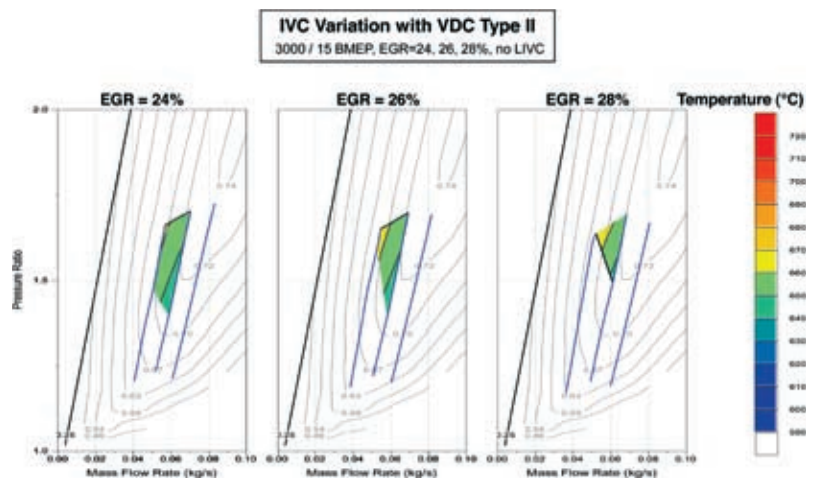


**Figure 9:** In cylinder temperature ASAP, considering EGR-rates and EGR-split at standard intake valve closing timing, at 3000 RPM and 15 bar BMEP

$\text{NO}_x$  concentration compared to the non LIVC case with a higher EGR rate of 26 %. The bottom of **Figure 10** has been created under consideration of the same  $\text{NO}_x$  emission. In this case the BSFC has been lowered by 3.5 %, which can only be explained by a more efficient gas exchange. At very similar oxygen concentrations in the combustion chamber the air fuel ratio is lower. Engine tests will have to prove the emission benefits of this additional freedom in the  $\text{NO}_x$ -PM trade-off.

#### 4 Outlook

It is now very important to understand in how far PCCI combustion concepts under the help of late intake valve closing and EGR can be used in a wider range of the engine map. A possible broader load range enabled by LIVC to run PCCI is enabled by the lower temperature before the first injection occurs. But it is unclear, in how far an optimization of EGR and fuel ratio could be used for a  $\text{NO}_x$  optimization with respectable acoustic results. Latest publications are promising [22]. Nevertheless, the most important prerequisite, a robust, cost effective designed component for LIVC, is variable duration control (VDC).

In the future, functionalities like fast transient internal EGR, an exhaust temperature control by variable exhaust valve closing or the control of the effective compression ratio to improve the cold start behaviour will be investigated.

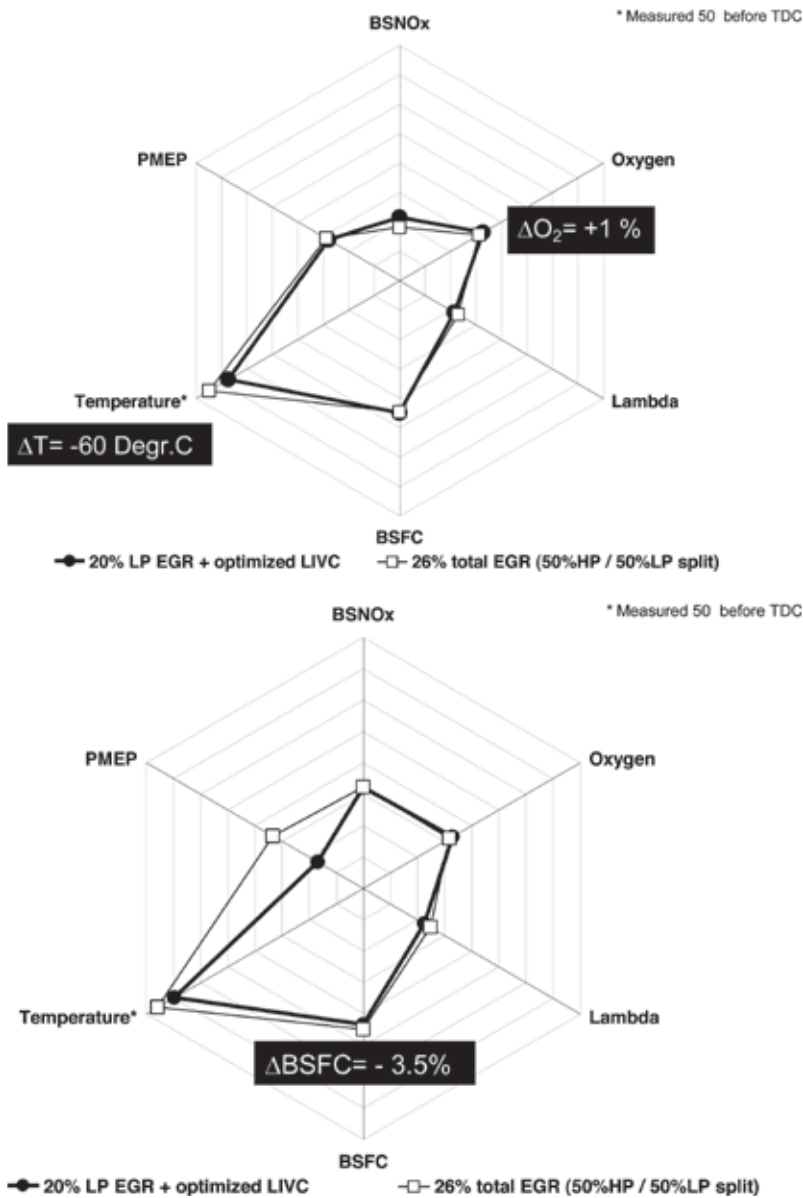


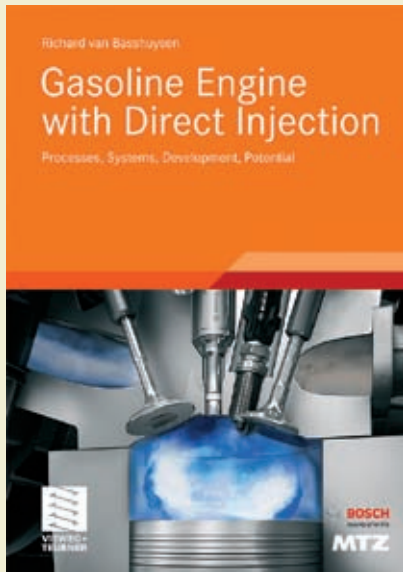
Figure 10: LIVC potential in the EGR environment

## References

- [1] Gulde, F. P.; Schmid, L.; Frieß, W.: Variable Steuerzeiten – eine Möglichkeit, die Emissionen von PKW-Dieselmotoren zu reduzieren? 4. Emission Control, Dresden, 2008
- [2] Weber, O.; Jörgl, V.; Shutty, J.; Keller, P.: Der schadstoffarme Dieselmotor und seine zukünftigen Anforderungen an moderne Beatmungssysteme. 4. Aachener Kolloquium Fahrzeug- und Motorentechnik, Oktober 2005
- [3] Münz, S.; Römuss, C.; Schmidt, P.; Schiffer, H.-P.; Brune, K.-H.: Emissionsarme Dieselmotoren mit Niederdruckabgasrückführung – Herausforderungen an die Schlüsselkomponente Turboladers. In: MTZ (2008), Nr. 2
- [4] Wenzel, W.; Joergl, V.; Keller, P.; Weber, O.: EGR Systems for Diesel Engines – The Road Ahead. SIA Diesel Conference, Rouen, Mai 2008
- [5] Weber, O.; Jörgl, V.; Shutty, J.; Keller, P.; Czarnowski, R.: Can Euro 6 Emissions be met with a Hybrid EGR System? 2nd International MinNO<sub>x</sub> Conference, Berlin, June 2008
- [6] Weber, O.; Joergl, V.; Czarnowski, R.; Keller, P.: Enabling Components for Future Clean Diesel Engines. SAE International Power Train, Fuels and Lubricants Congress, Shanghai, 2008
- [7] Joergl, V.; Weber, O.; Wenzel, W.: EGR Systems for Diesel Engines – The Road Ahead. Diesel Engines: The low CO<sub>2</sub> and Emission Reduction Challenge, Rouen, 2008
- [8] Dürnholz, M.: The Diesel System Approach – optimized concepts for the future. The 6<sup>th</sup> Advanced Diesel Engine Technology Symposium, Seoul, 25. + 26. Oktober, 2006
- [9] Paffrath, H.: Untersuchungen zum Potenzial eines regelbaren Zweistufigen Aufladeverfahrens für Nutzfahrzeugmotoren. Dissertation RWTH Aachen, 1995
- [10] Heywood, J. B.: Internal Combustion Engine Fundamentals. McGraw-Hill, 1988
- [11] Rudolph, F.; Hadler, J.; Engler, H.-J.; Röpke, S.: Der neue 2.0L 4V TDI mit Common Rail – Moderne Dieselmotoren. 16. Aachener Motorenkolloquium, 2007
- [12] Roth, D.; Sisson, J.; Gardner, M.; Wing, B.: Valve Event Duration Reduction through Ultrafast Phaser Actuation. SAE 2007-01-1281, SAE Congress, April 2007
- [13] Schutting, E.; Neureiter, A.; Fuchs, C.; Schatzberger, T.; Klell, M.; Eichlseder, H.; Kammerdiener, T.: Miller- und Atkinson-Zyklus am aufgeladenen Dieselmotor. In: MTZ 68 (2007), Nr. 6
- [14] Sommer, A.; Stiegler, L.; Wormbs, T.; Kabitze, J.; Buschmann, G.: Will We Need Variable Valve Trains for Passenger-Car Diesel Engines in the Future? SIA Conference on Variable Valve Actuation, November 30, IFP Rueil, 2006
- [15] Walter, B.; Pacaud, P.; Gatellier, B.: Variable Valve Actuation Systems Potential for HCCI or LTC Diesel Combustion. SIA Conference on Variable Valve Actuation, November 30, IFP Rueil, 2006
- [16] Millo, F.; Mallamo, F.; Mego, G.G.: The Potential of Dual Stage Turbocharging and Miller Cycle for HD Diesel Engines, SAE Technical Paper 2005-01-0221, 2005
- [17] Kook, S.; Bae, C.; Miles, P.; Choi, D.; Pickett, L.: The Influence of Charge Dilution and Injection Timing on Low-Temperature Diesel Combustion and Emissions. SAE Technical Paper 2005-01-3837, 2005
- [18] Shrivastava, R.; Hessel, R.; Reitz, R.D.: CFC Optimization of DI Diesel Engine Performance and Emissions Using Variable Intake Valve Actuation with Boost Pressure, EGR, and Multiple Injections. SAE Technical Paper 2002-01-0959, 2002
- [19] Kamo, R.; Mavinahally, N.S.; Kamo, L.; Bryzik, W.; Reid, M.: Emissions Comparisons of an Insulated Turbocharged Multi-Cylinder Miller Cycle Diesel Engine. SAE Technical Paper 980888, 1998
- [20] Ruhkamp, L.; Krüger, M.: Massnahmen zur weiteren Senkung der Rohemissionen von NFZ Dieselmotoren. 26. Internationales Wiener Motorensymposium
- [21] Weber, O.; Jörgl, V.; Keller, P.; Yang, B.: Variable Ventilsteuerung: Konkurrenz oder Ergänzung zur Hybrid-Abgasrückführung? 17. Aachener Motorenkolloquium, 2008
- [22] Otte, R.; Raatz, T.; Wintrich, T.: Homogene Dieselerverbrennung; Herausforderung für System, Komponenten und Kraftstoff. 17. Aachener Motorenkolloquium, 2008

# Gasoline Engines are the answer to the challenges of future

personal buildup for Force Motors Ltd.



Richard van Basshuysen

## Gasoline Engine with Direct Injection

Processes, Systems, Development, Potential

2009. xviii, 437 pp. With 399 Fig. Hardc. EUR 49,00

ISBN 978-3-8348-0670-3

Direct injection spark-ignition engines are becoming increasingly important, and their potential is still to be fully exploited. Increased power and torque coupled with further reductions in fuel consumption and emissions will be the clear trend for future developments. From today's perspective, the key technologies driving this development will be new fuel injection and combustion processes. The book presents the latest developments, illustrates and evaluates engine concepts such as downsizing and describes the requirements that have to be met by materials and operating fluids. The outlook at the end of the book discusses whether future spark-ignition engines will achieve the same level as diesel engines.

### authors | editors

Dr.-Ing. E. h. Richard van Basshuysen was Head of Development for premium class vehicles and for engine and transmission development at Audi. Today, he is editor of the magazines ATZ and MTZ. The editor was supported by a distinguished team of authors consisting of 22 experts and scientists from industry and universities.

### Please send me

Copies

#### Gasoline Engine with Direct Injection

ISBN 978-3-8348-0670-3

EUR 49,00

(+ shipping and handling)

### Fax +49(0)611.7878-420

Company \_\_\_\_\_ Last name | First name \_\_\_\_\_ 321 09 001

Department \_\_\_\_\_

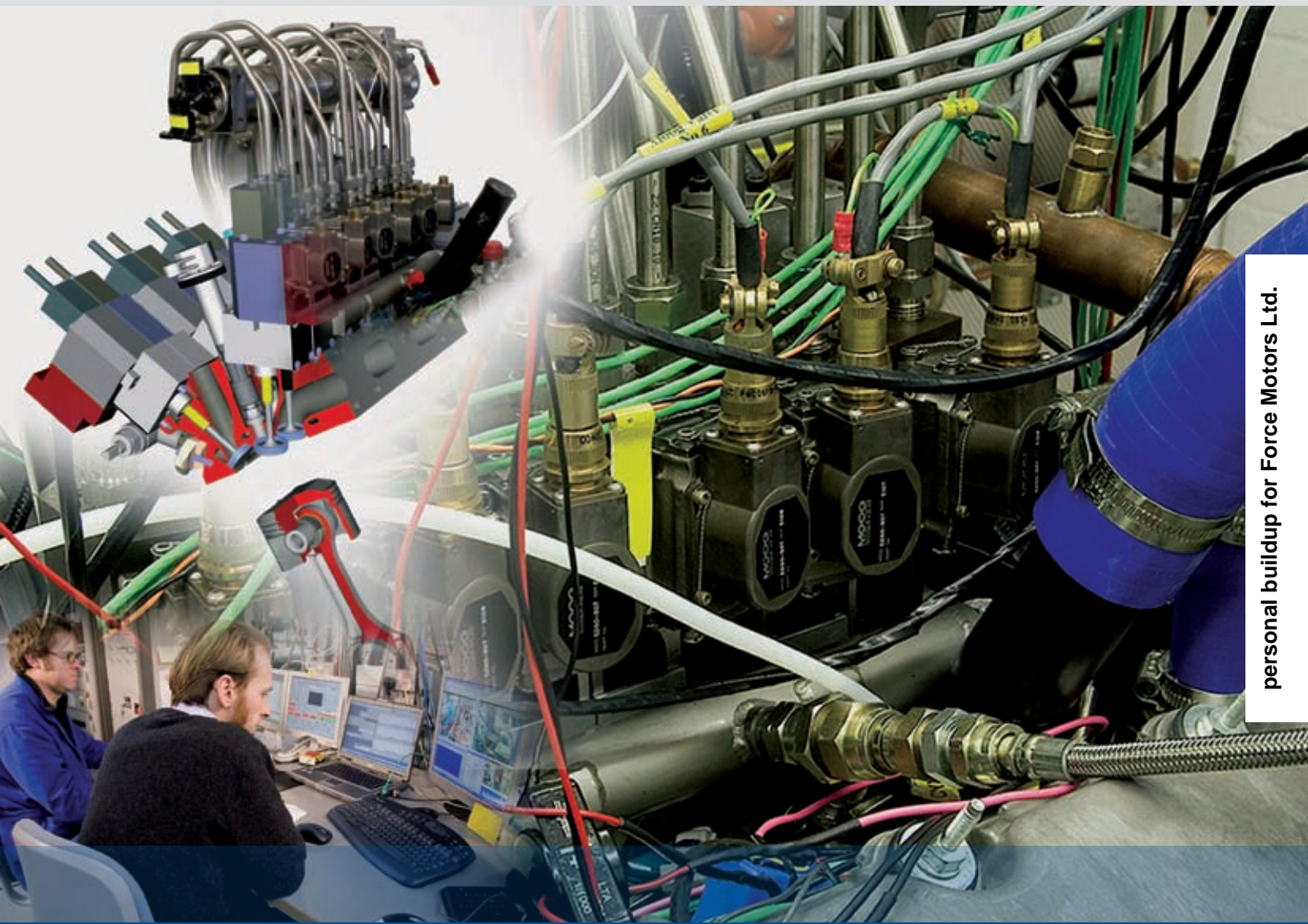
Street name \_\_\_\_\_ Postcode / Zip | City, Country \_\_\_\_\_

Date | Signature \_\_\_\_\_

Please supply at retail price via bookshop or directly from Vieweg+Teubner Verlag. Subject to change without notice. 1|2009.  
Managing Directors: Dr. Ralf Birkelbach, Albrecht F. Schirmacher. AG Wiesbaden HRB 9754

TECHNIK BEWEGT.





personal buildup for Force Motors Ltd.

# Two-stroke/Four-stroke Multicylinder Gasoline Engine for Downsizing Applications

Following the great public interest aroused by the „2/4-sight“ concept and the successful completion of the fundamental investigations on the testbed, Ricardo is now starting work on the „2/4-car“ project. This project aims to prove the combinability of two- and four-stroke operation in a single internal combustion engine within a demonstrator vehicle. The additional degree of freedom of the engine operating mode opens the potential for downsizing beyond conventional technical limits, enabling a competitive CO<sub>2</sub>/cost trade-off compared to future diesel powertrains.

## 1 The Origins of the „2/4-sight“ Engine

The end of the 1980's saw the start of work with the Flagship single cylinder engine, with which successful work was carried out to investigate poppet valve controlled two-stroke operation [1]. Since then several years have passed, in which fuel consumption and CO<sub>2</sub> emissions control have become ever more important sales factors. Following this trend, several downsizing concepts now enjoy market success, achieving fuel consumption benefits by means of an engine with reduced displacement.

The „2/4-sight“ concept marks a step to increase the fuel economy potential of downsizing still further, by combining two- and four-stroke operation in the same engine. The appropriate juxtaposition of two- and four-stroke regimes allows the engine capacity to be reduced further whilst retaining the original level of driveability. This has now been made possible by the maturity of variable valvetrain technology, improved boosting possibilities and in particular through the progress made in IC engine control.

## 2 Two-stroke Operation with Poppet Valves

For an IC engine using poppet valves to control gas exchange, combustion chamber scavenging can be achieved by the use of compressed intake air (boosting). In this way, the provision of fresh air for the next combustion cycle is combined with the displacement from the cylinder of the spent gases from the last. If gas exchange takes place by this process, then a two-stroke operating cycle can be realised with a valvetrain driven by a camshaft. **Figure 1** illustrates this point for the case of the „2/4-sight“ concept. The main difference from conventional four-stroke engine operation is that a working cycle is completed once every revolution of the crankshaft. In the ideal case at low engine speeds, the result is a doubling of the achievable torques. This opens up significant potential for downsizing, in which reductions in fuel consumption can be achieved through the use of a reduced cylinder capacity in conjunction with boosting.

## 3 Downsizing

Downsizing is regarded as a proven approach to the reduction of vehicle fuel consumption. As long as the same vehicle performance can be achieved with a smaller engine, then economy benefits result from a combination of reduced internal friction and more frequent operation at higher efficiencies. In order to compensate for the reduced displacement, compression of the intake air is also carried out.

The conventional approach to downsizing using direct injection and turbocharging has a number of limitations, as shown in the **Table**. These constraints limit the maximum downsizing to around 30 %, whereas the 2/4 concept has a number of fundamental advantages and can extend the degree of downsizing to around 50 %. This leads to an improvement in European drive cycle CO<sub>2</sub> of 10 to 15 % compared to today's downsized engines and 25 to 30 % compared to today's port fuel injection naturally aspirated engines.

Another approach to downsizing is through hybridisation of the powertrain. In this case, a reduction in engine displacement is enabled by the use of an electric motor to compensate for the resulting torque deficit. In this case too, the same mechanical and thermodynamic restrictions limit the scaling-down of the engine. Both approaches find a lower limit that is finally determined by the knock resistance of the gasoline fuel in use.

## 4 The „2/4-sight“ Engine Concept

Due to the knock limit, in gasoline engines with extreme downsizing by a high

## The Authors



Dipl.-Ing. Martin Rebhan is working as a Development Engineer on the 2/4 Sight Programme at Ricardo Deutschland GmbH in Schwäbisch Gmünd (Germany).



John Stokes is Technical Specialist Gasoline Engines at Ricardo UK at Shoreham by-Sea (Great Britain).

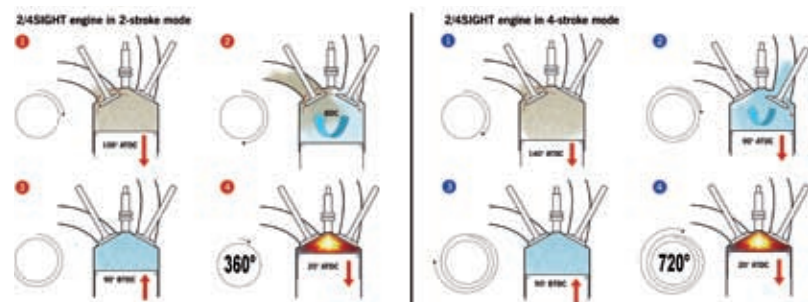


**Figure 1:** Comparison between four-stroke and two-stroke operation in the „2/4 sight“ engine

**Table:** Limiting factors of conventional downsizing

Limiting Factor	Negative Impact	2/4 Concept Advantage
Compression ratio	Indicated efficiency	For the same specific torque output, two-stroke operation gives lower cylinder pressure and temperature, enabling 1.5 to 2 ratios higher compression ratio
Maximum cylinder pressure	High structural loads lead to increased weight. Increased bearing sizes lead to increased friction and lower brake efficiency	For the same specific torque output, two-stroke operation gives significantly lower maximum cylinder pressure
High rates of pressure rise	NVH	For the same specific torque output, two-stroke operation gives lower rates of pressure rise due to lower charge mass per cycle and lower maximum cylinder pressure
High peak to mean torque output	NVH	Two-stroke operation gives reduced torque ripple due to double the firing frequency with smaller crankshaft inputs at each firing stroke
Low speed torque	Driveability	Two-stroke operation gives 150 Nm/l swept volume at 1000/min, which compares to typically 100 Nm/l for four-stroke DI turbocharged engines

degree of boosting, there exists a conflict between the joint objectives of thermal efficiency improvements and the achievable torque at low engine speeds. One route to the resolution of this conflict would be to overcome the technical obstacle posed by the knock limit by using two-stroke operation at high load. The way in which the „2/4-sight“ concept makes this possible is described in the following text.

The „2/4-sight“ engine is a multi-cylinder internal combustion engine with gasoline direct injection that can be run in either two- or four-stroke operation. In addition, it is possible to change between operating modes whilst the engine is running. The requirements of two-stroke operation are a significant influence on the inlet system configuration, as seen in [Figure 2](#).

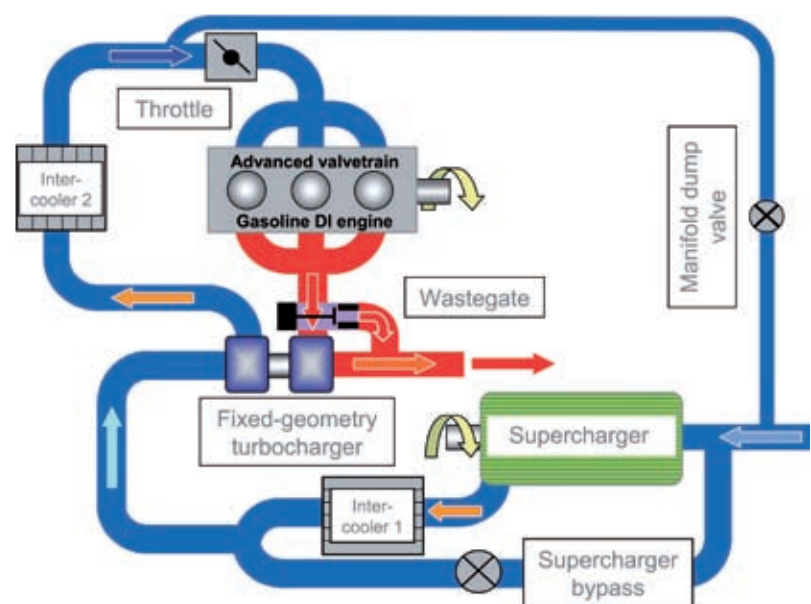
The use of turbocharging with after-cooling that is typical of four-stroke downsized applications is supplemented by a mechanical supercharger connected in series. The supercharger is necessary to provide a positive pressure difference between inlet and exhaust ports required to scavenge the cylinder in two-stroke mode. The engine could be purely supercharged, but this approach would not give as good fuel economy in four stroke mode as using the turbocharger.

Depending on the operating point, airflow is guided via the compressor or direct to the turbocharger by a controlled bypass. The differences in valve timing required between two- and four-stroke operation are realised by a variable valvetrain. The connection in series of compressor, turbocharger and charge air cooler makes it possible to realise all operating strategies currently in use with

gasoline DI concepts. The „2/4-sight“ concept is therefore based exclusively on components that are already found in production applications. The 2/4-sight Engine is conceived in such a way that during the relevant certification cycles only four stroke operation occurs. The 2/4-sight engine is conceived in such way that during the relevant certification cycles only four stroke operation occurs which, if stoichiometric, would require only three-way catalyst aftertreatment. Ricardo expects nevertheless, that off-cycle emission concerns would require an LNT for the lean engine operation which occurs in two stroke mode.

#### 4.1 The Experimental Engine

The experimental engine is based on a 2.1 l six cylinder engine, one cylinder bank of which is not used. The experimental engine carries a cylinder head that is derived from that of the Flagship engine, allowing valve-controlled operation of the engine in both two- and four-stroke modes using direct injection. The inlet ports are vertically oriented to promote efficient scavenging [2]. The switching and control algorithms for changing operation mode are implemented in a rapid prototyping control unit. This exchanges information with the main engine control unit and a valve control unit, the details of both of which are described in more detail subsequently.

**Figure 2:** Configuration of airpath system

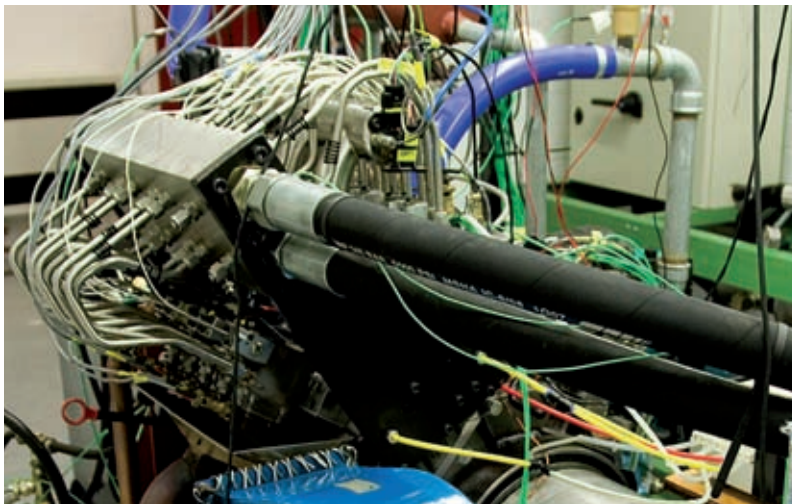


Figure 3: „2/4 sight“ engine fitted with electro-hydraulic valvetrain

The experimental engine is equipped with an external boosting system. Figure 3 shows the „2/4-sight“ engine with mounted hydraulic pressure feed.

For the development of suitable strategies for switching between engine operating modes, separate maps for two- and four-stroke operation are calibrated and stored in the engine control unit. In two-stroke mode on the testbed, the external boosting system is used for scavenging of the active cylinders.

#### 4.2 Valve Actuation in Two- and Four-stroke Operation

The requirement for different settings of valve timing and lift in two- and four-stroke operation necessitates a variable valvetrain. For the realisation of the typical lift curves for each mode shown in Figure 4, suitable variable valvetrain options are pure mechanical, electro-mechanical or electro-hydraulic.

Variable valve actuation on the experimental engine is implemented using an electro-hydraulic valvetrain developed by Ricardo. Figure 5 shows the signal flow path for this system.

Each of the active cylinders in the engine is equipped with two inlet and exhaust valves, which can be operated independently. The engine control unit (ECU) transmits the opening and closing time and the target valve lift curve to a valve control unit (VCU). The VCU then actuates the servo control valves appropriately. The current valve position is being fed back to close the control loop. The

complexity of the valvetrain is offset by its advantages of a wide range of variation of valve timing and programmable

valve lift curves. The system makes it easily possible to react to differences in the measured valve timing from the targets derived by gas exchange simulation.

#### 4.3 Combustion Chamber and Air Path

As seen in Figure 4, the available time for gas exchange in two-stroke mode is significantly shorter than that in four-stroke mode. For direct injection this shortens the time duration available for mixture preparation. Two fundamental challenges result from this that are not present in normal four-stroke operation: a sufficient supply of fresh air for the following working cycle and good mixture preparation. In order to guarantee this for over a wide operating range, the air path to and from the cylinder must be designed appropriately. Considering the requirement of sufficient scavenging efficiency in two-stroke mode of at least 85 %, a requirement to reduce the

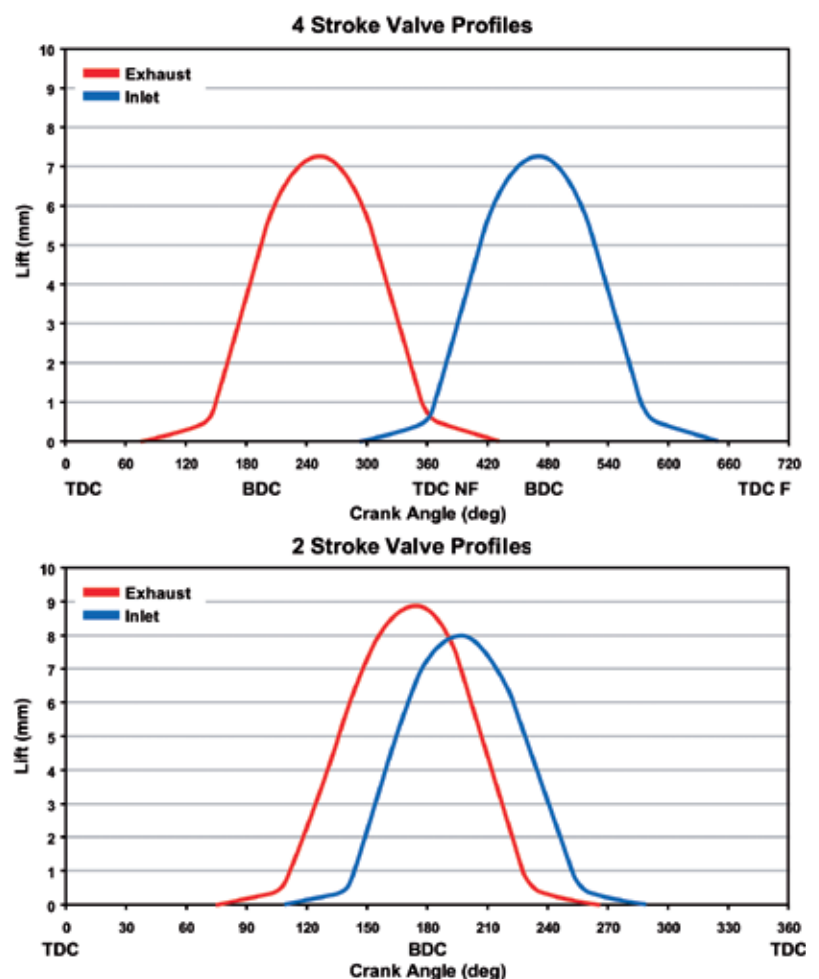


Figure 4: Difference between two and four-stroke valve characteristics

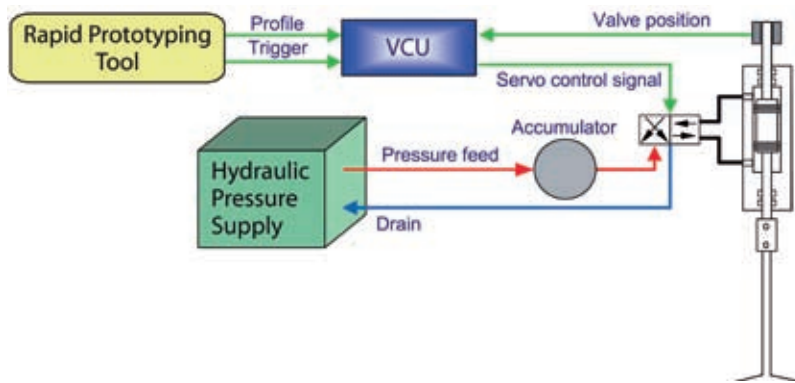


Figure 5: Schematic overview of electrohydraulic valve control

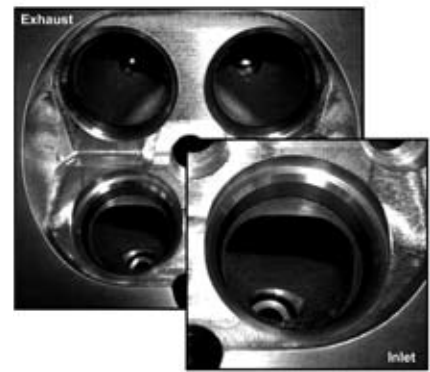


Figure 6: Closeup of combustion chamber design

tendency for auto-ignition, 3D CFD simulations led to the cylinder head design shown in Figure 6.

In general for two-stroke engines, high engine speeds and low scavenging efficiencies give rise to an increased probability of knock and other auto-ignition phenomena. For the „2/4-sight“ engine, a number of design measures were taken to counteract this. The upper, exhaust valves shown in the cylinder head in Figure 6 are larger than the inlet valves, achieving reduced flow losses on the exhaust side. In addition, each of the inlet ports opposite is fitted with an inlet valve shroud, which helps to prevent large-scale outflow of inlet air through the exhaust ports at low valve lift. This simple measure brings about a significant increase in scavenging efficiency across the entire engine operating map. The mixture preparation in two- and four-stroke operation is also supported by the high tumble in-cylinder flow regime.

An example output from a CFD study of the scavenging process made using the Ricardo „VECTIS“ code is shown in Figure 7. The results show that the in-cylinder flow is well organised and the formation of the reverse tumble scavange loop can be seen clearly. Some short-circuiting is observed, but the predominant inlet flow is confined to the non-exhaust side cylinder wall as desired. At this condition scavenging efficiency is 90.5 %. At higher speeds it becomes more challenging to maintain the target scavenging efficiency, and this is a key factor limiting poppet valve two-stroke performance at engine speeds above 4500/min.

### 5 Operating Strategy of the „2/4-sight“ Engine

The „2/4-sight“ engine is of particular interest for downsizing applications because high values of torque can be naturally achieved particularly at low engine speeds. Figure 8 shows the composite map of achievable two- and four-stroke operation ranges. The simulated value of maximum torque for two-stroke mode was confirmed by measurements on the test engine. Two-stroke operation drives the requirement for a variable valvetrain and sequential boosting with charge air cooling. These features can be used to best advantage in four-stroke operation, because the „2/4-sight“ concept permits a wide range of gasoline DI strategies.

One possible operation strategy can be derived from overlaying the two different engine maps. The decision, in

which mode the engine should run is dependent on the driver demand and the current operating point.

Up to an engine speed of 4500 rpm, the maximum torque is higher in two-stroke mode than in four-stroke mode. For the experimental engine, the achievable specific torque at 1000 rpm is 150 Nm/l, compared to 90 Nm/l for four-stroke operation.

A natural switching point between the two operation modes falls at 4500 rpm, since here the achievable torque values are identical. Driver demands for high loads in the speed range up to 4000 rpm can be served by a switch into two-stroke mode.

In order to realise the operation strategy described, it is important that switching between two- and four-stroke modes takes place sufficiently smoothly. Three types of operating mode switch can be defined, as illustrated in Figure 8. In the

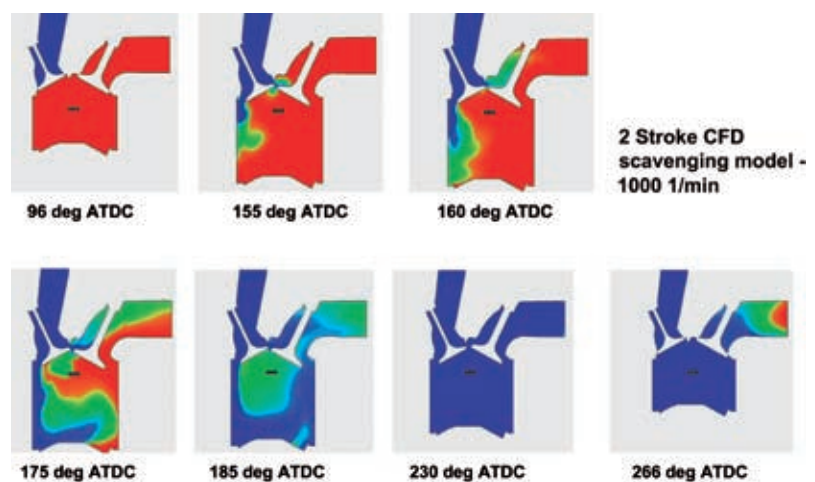


Figure 7: CFD simulation of two-stroke scavenging process

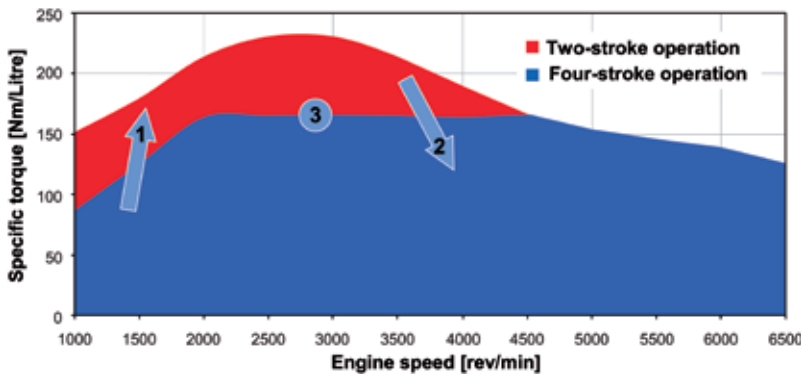


Figure 8: Two- and four-stroke engine operation maps

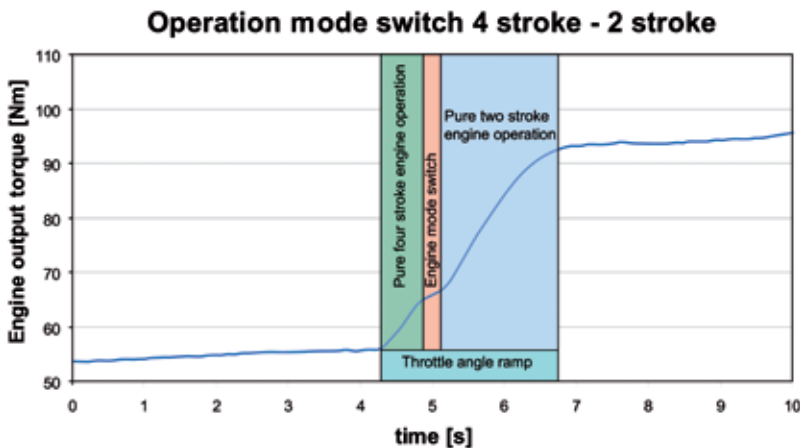


Figure 9: Transient torque response during engine operation with mode switch

case of operating mode transitions 1 and 2, the situation is one of mode switching under varying engine torque. These types of transition dominate in transient driv-

ing behaviour. A transition of type 3 takes place when a change of mode takes place but torque remains constant. This type of transition is made if it is advantageous from the point of view of fuel consumption or emissions.

Figure 9 shows test data from the 2/4-sight experimental engine for a switch from four-stroke to two-stroke operation at an engine speed of 1500 rpm. For this test the fuel quantity per injection was held constant. The result is an increase in produced torque. The operating mode transition shown was initiated as a reaction to a manual change in the throttle angle from 6° to 15° (ramp time = 2 s). The change of valve timing from four-stroke to two-stroke settings gives rise to pressure fluctuations in the inlet system, which are caused by the propagation of pressure waves through the inlet system of the test installation. These pressure waves must be accounted for in the calculation of available air for each cylinder, in order to avoid misfire due to ex-

cessively rich or lean mixtures. It has been observed that the transition between the two operating modes can be positively influenced by the use of no pre-defined cylinder switching order. In this case the transition of the first cylinder takes place selectively on the basis of the relevant air pressure upstream the inlet port with other cylinders following in firing order. The adaptation and development of such switching strategies can be carried out effectively with the rapid prototyping system employed.

## 6 The 2/4-car Programme

The successfully completed „2/4-sight“ programme has confirmed its potential for integration into a vehicle. Based on the acquired test data, vehicle simulation has shown that the CO<sub>2</sub> savings that can be realised with the „2/4-sight“ concept are competitive with future diesel powertrains in terms of a CO<sub>2</sub>/cost trade-off. To demonstrate this in a vehicle, the „2/4-car“ programme was kicked off in October 2008, with the declared aim of integrating the „2/4-sight“ concept described here into a vehicle. The layout of the inlet system will correspond to that shown in Figure 2. In contrast to the „2/4-sight“ experimental engine, the valvetrain employed will be a Ricardo-developed mechanically variable system. Currently, further investigations are underway with the experimental engine in order to develop the operating strategy. At the end of the programme, a fully-functional demonstrator vehicle will be shown to the public, whose original 4.2 l engine will be replaced by a 2.1 l unit. The vehicle performance characteristics will be maintained by a suitable combination of two- and four-stroke operation, while the downsizing potential achieved by the „2/4-sight“ concept will be utilised to realise a level of reduction in CO<sub>2</sub> emissions that lies beyond current downsizing applications.

## References

- [1] Stokes, J.; Hundleby, G E.; Lake, T.: Development Experience of a Poppet-valved Two-stroke Flagship Engine. SAE 920778
- [2] Hundleby, G E.: Two Strokes Engines. Ricardo Group. European Patent Application 89305979.0, publication No.0349149A2 published 3 Jan 1990

## Acknowledgements

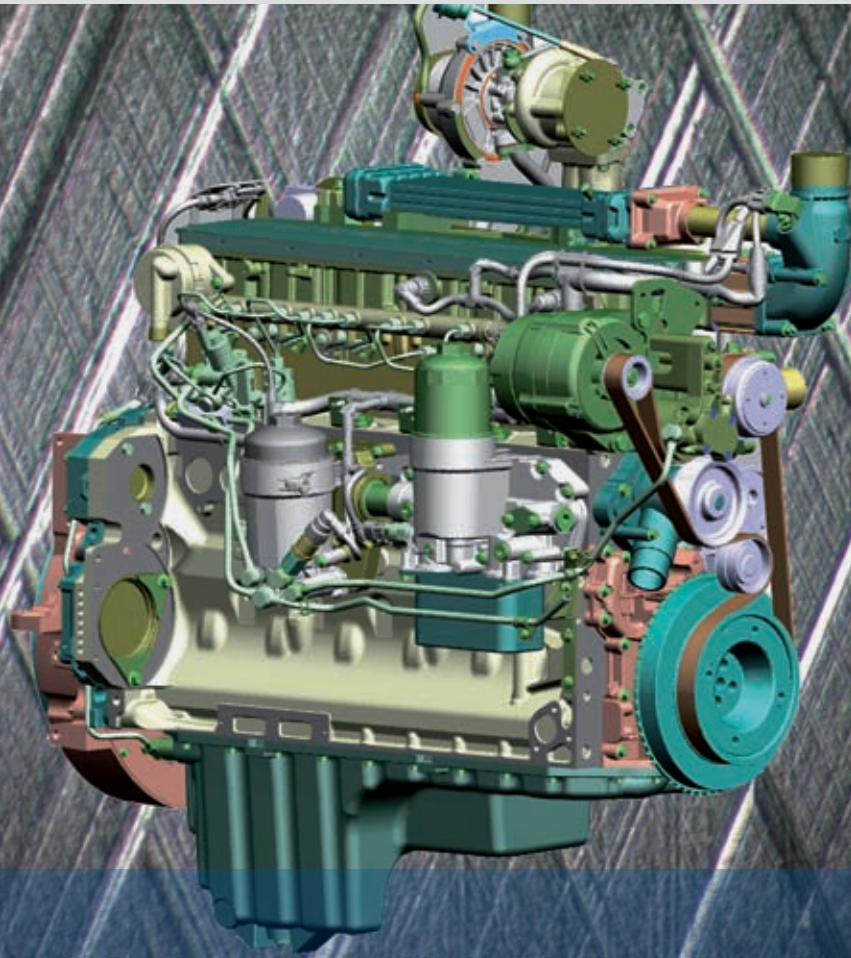
The authors would like to acknowledge the contribution of the project partners of both the 2/4 Sight and 2/4 Car programmes:

### 2/4 Sight

- UK Department of Trade and Industry
- Denso Sales UK Ltd
- University of Brighton
- Brunel University

### 2/4 Car

- UK Department for Business, Enterprise and Regulatory Reform (BERR) through the Technology Strategy Board
- Jaguar Cars plc
- Denso Sales UK Ltd
- University of Brighton



# Less Wear and Oil Consumption through Helical Slide Honing of Engines by Deutz

Within the scope of continuous development for the Deutz 2012 engines (4 l and 6 l engines) and Tier 3 emissions standards, new developments are required with regard to achieving a new maximum power requirement of 178 kW at 2100 rpm and a higher EGR rate via cooled exhaust gas recirculation. Without implementing engine design changes, the new Tier III constraints are expected to lead to higher wear in the cylinder unit (cylinder bore, piston, piston rings). Together with Deutz, Nagel found a solution for the expected cylinder unit wear on the existing engine, which not only eliminates the potential future wear problem, but also contributes to the important economic considerations of oil consumption and maintenance intervals.

## 1 The New Engine from Deutz for Tractor Application

The TCD 2012 L04/6-4V engine, **Title Figure**, was developed within the scope of Tier 3 Standards for a tractor application using a Deutz Common Rail injection system and an e-EGR (water-cooled external EGR). **Table 1** shows the technical data of the engine with a high specific power for Tier 3 engines. The liner-less cylinder unit must be redefined in order for the engine to reliably meet the high demands of service life, oil consumption, blow-by and exhaust emissions.

## 2 The Cylinder Unit

### 2.1 Piston Rings

Federal-Mogul piston rings are used for optimizing the piston ring assembly for the TCD 2012 L06-4V engine. The running sur-

face of the piston rings is coated with GDC on the keystone ring of the 1st groove. This is a hard chrome layer with ultrafine embedded diamond particles characterized by high wear and scuff resistance, and low cylinder surface wear [1]. The coating is a further development of the well proven CKS coating (chrome ceramic) of the basic engine. The tapered rings of the 2nd groove are made of a high resistant cast iron alloy and are uncoated. The two-part oil rings, which are also made of cast iron, have chrome-plated surfaces.

### 2.2 Pistons

A spray oil-cooled aluminium piston without a cooling gallery is being introduced with an enlarged compression height for reducing the bowl edge stress in the bolt axis. In order for the compression height to be increased, the connecting rod length must be shortened. This leads to an increased lateral force. The

**Table 1:** Technical data of the TCD 2012 L06-4V and TCD2012L04-4V

Motor data		Motor types	
		TCD2012 L06-4V	TCD2012 L04-4V
<b>Mechanical data</b>	<b>Unit</b>		
Number of cylinders	Qty.	6	4
Valves/cylinder	Qty.	4	4
Bore	mm	101	101
Stroke	mm	126	126
Cylinder volume	l	6,06	4,04
<b>Performance features</b>			
Power	kW	178	113
Rated speed	rpm	2100	2100
Mean effective pressure (rated power)	bar	16,8	16,0
Torque (Md max)	Nm	1070	657
Speed (Md max.)	rpm	1450	1500
Mean effective pressure (Md max)	bar	21,9	20,8
Fuel consumption (rated power)	g/kWh	213	217
Fuel consumption (best point)	g/kWh	202	202
Mean piston speed (rated power)	m/s	8,82	8,82
Engine output per liter	kW/l	29,4	28,0
<b>Special characteristics</b>			
Exhaust gas recirculation		external	external
Injection system		Deutz-Common-Rail	Deutz-Common-Rail
	bar	1400	1400

## The Authors



Dipl.-Ing. Thomas Hoen is Leader Mechanics 2012 Industry and Agri-power at Deutz AG in Cologne (Germany).



Josef Schmid is Manager R & D Process and Abrasives Development at Nagel Maschinen- und Werkzeugfabrik GmbH in Nürtingen (Germany).



Dipl.-Ing. Walter Stumpf is Application Engineer Piston Rings and Liners at Federal Mogul in Burscheid (Germany).

small top land clearance should be carried over by the basic engine.

### 2.3 Cylinder Surface

The cylinder bore running surface is the parent block cast iron material (linerless) and has previously been plateau honed. Plateau honing was accomplished in three honing stages using ceramic honing ledges at Deutz. As a result of the considerably increased external EGR rate and power, the following problems had to be addressed, **Figure 1**:

- Cylinder bore polishing: Due to the formation of hard oil-carbons, the honing structure in the middle area of the cylinder is eroded.
- Top ring reversal bore wear: This is caused by the transition from hydrodynamic friction in the mixed friction area between the piston rings and the cylinder at TDC (top dead center) during the combustion cycle.

### 3 Option for Reducing Cylinder Wear

The cylinder surface should be adapted to the increased demands with regard to wear. The options will be described in the following sections.

#### 3.1 Surface Hardening and Coating

As there are only a few material alternatives to the GG25 crankcase material for the linerless Deutz engines, potential optimization options that do not affect changes to the base material are listed in **Table 2**.

#### 3.2 Cooling of the Cylinder in the Reversal Zone

Through additional cooling of the cylinder in the upper reversal zone, a lack of lubri-

cation due to oil film evaporation in the hot (upper) zone could be prevented. On the 2012 engine model, the thickness of the crankcase cover plate is reduced from 50 mm to 15 mm in the land area between the cylinders so the temperature in the reversal zone is drastically reduced.

#### 3.3 Surface Topography

The material itself remains unchanged with the modified surface topography. The wear reduction is mainly achieved in two ways, which are interrelated:

- reduction of the run-in wear by increasing the material contact area
- reduction in friction by means of improved lubrication in the critical zones.

##### 3.3.1 Slide Honing

As a result of significant progress in the development and application of specialized honing abrasives (mainly of diamond composition), slide honing can generate a surface very close to the „ideal plateau“, **Figure 2**.

The „ideal plateau“ is close to being realized with slide honing. Especially considering that a reduction in the Rpk

and Rk values beyond what is practical in a production process is of no further advantage: Even an extremely smooth, „ideal plateau“ is roughened again to a small degree after a short running time by the piston ring and the particles contained in the oil (such as oil carbons or chips).

It is important to note, that with the optimized diamond tools of the slide honing, a very small valley width can be achieved, even in combination with the required high Rvk values. These narrow grooves are significant smaller than the surface structure of other honing processes. This formation of frequent, but narrow and sufficiently deep structured valleys, reduces friction and wear in the critical area of boundary/mixed friction. Furthermore, this results in a thin oil film and therefore less oil consumption. This has been confirmed in production with more than thirty applications in use [2].

##### 3.3.2 Helical Slide Honing

An even more consistent way of reducing wear while maintaining low oil consumption was reached by a further process development, which allows for an optimized, steep honing angle (140°) in series production. A typical (< 50°) hon-

**Figure 1:** Wear features of the cylinder surface

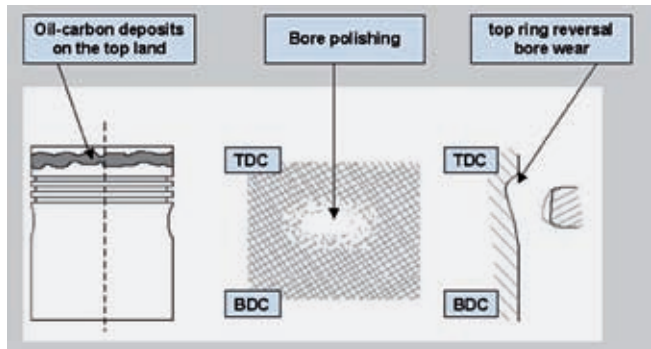


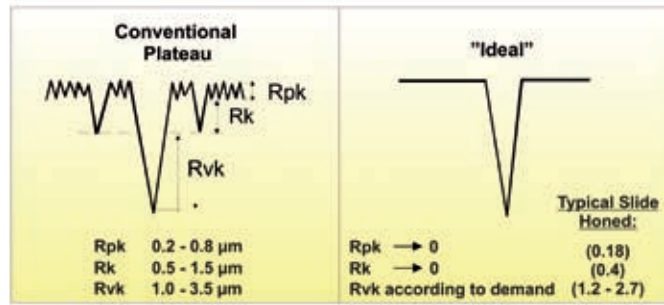
**Table 2:** Surface hardening and coating for bushless engine (parent bore)

	Inductive hardening	Laser hardening	Thermal spray coating (wire/powder methods)	Strain-hardening by lapping
Advantages	Cost effective	Reduced tendency to microcrack, Less deformation	Wear-proof Friction-favorable (depending on method)	Low investment cost
Disadvantages	Danger of microcrack formation (surface breakouts) and macrocracks (great deformation) after treatment	Expensive Reduced hardening depth than with inductive hardening	Expensive process Little knowledge regarding coating adhesion on motors operated for long periods and under extreme conditions	High production cost

ing angle promotes the floating of the piston ring with increasing piston speed (at least in theory). However, the actual problem zones for increased wear and friction are the reversal zones of the piston when piston speed approaches zero; i.e. areas with limited or no existing hydrodynamics.

### 3.3.3 UV Laser Exposure Treatment

With this process, the entire piston running surface is treated with UV laser exposure. The laser exposure produces a material modification on the cylinder surface with improved sliding properties, **Table 3**. This change allows for less oil consumption and still has a relatively fine surface



**Characteristics:**

- Minimization of the core roughness depth and plateau roughness
- Reduction of the valley width
- As much as possible, free choice of Rvk value (depending on the application, e.g. trucks or cars)
- Optimization of the honing angle
- Uniform, tribologically optimized and operation-safe surface over the entire length of the cylinder

**Figure 2:** Comparison between conventional plateau honing and slide honing

**Table 3:** Comparison table of the various cylinder surface treatments

Honing types	Inductive hardening	Laser hardening	Honing lapping	Plateau honing	Slide honing	Helical slide honing	UV laser treatment
Structured area [mm]	20	20	entire length of cylinder				
<b>Work steps</b>							
Step 1	Inductive hardening	Laser hardening					
Step 2	Coaxial honing	Coaxial honing	Pre-honing	Pre-honing	Pre-honing	Pre-honing	Pre-honing
Step 3	Honing	Honing	Lapping	Honing	Honing	Honing	Honing
Step 4	Finish-honing	Finish-honing		Finish-honing	Finish-honing	Finish-honing	Finish-honing
Step 5							UV lasering
<b>Surface parameters</b>							
Honing angle [°]	33	33	35	33	40 - 60	140 - 150	45
Rz [ $\mu\text{m}$ ]	7	7	7,5	7	2,8	2,9	4,99
Rpk [ $\mu\text{m}$ ]	0,4	0,4	0,8	0,4	0,08	0,1	0,99
Rk [ $\mu\text{m}$ ]	1,5	1,5	2	1,5	0,33	0,5	1,42
Rvk [ $\mu\text{m}$ ]	2	2	1,3	2	1,03	1,8	1,05
Topography							
<b>Evaluation</b>							
Costs	+	-	-	++	++	++	-
Proximity to current standards	+++	-	+	+++	+++	+++	+
Process reliability	+++	-	+	+++	+++	+++	+
Chances of success	+++	++	++	-	+	+++	+++

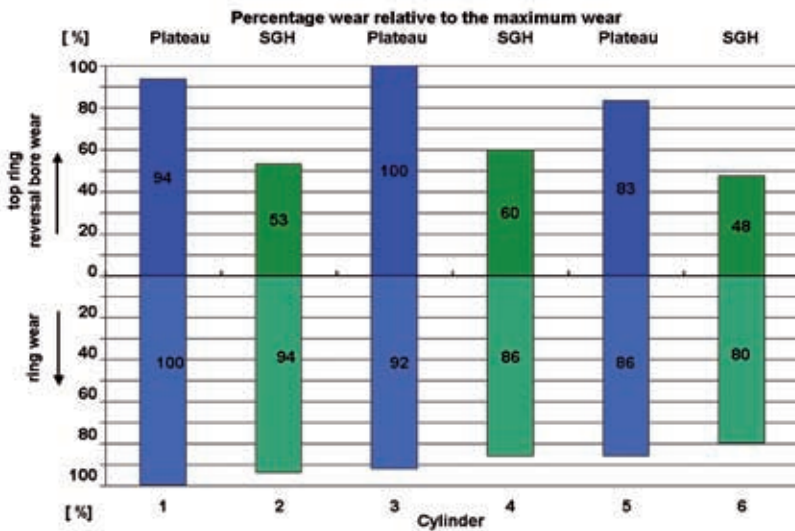


Figure 3: Cylinder and piston ring wear with plateau and helical slide honing

with low wear and friction and high operational reliability. This method has been used successfully for several years in automobile diesel engines with high specific power. However, due to economical reasons and the complex technology involved, it is not possible to carry out an engine running surface overhaul in all countries of deployment. Therefore, this process is no longer being pursued for the Deutz application.

### 3.3.4 Definition of the Cylinder Surface for Testing

After thorough consideration of the possible cylinder surface treatments available, Table 3, Deutz chose helical slide honing instead of conventional plateau honing as used before. Helical slide honing has many proven advantages and can be readily adapted to most production processes in use worldwide.

## 4 Engine Testing

### 4.1 Cylinder Wear: Plateau Honing Versus Helical Slide Honed Surfaces

To investigate the effect of the chosen hone process on wear of the cylinder unit surfaces, an engine block was plateau honed with the production process in cylinders 1, 3, and 5 and helical slide honed in cylinders 2, 4, and 6 at Nagel. The roughness values of the different honing processes were determined at Federal-Mogul Burscheid using a white light interferometer.

The engine was assembled with production parts and tested in a Deutz full-load continuous run for 500 h. After completion of the test, the cylinder wear was measured at Federal-Mogul. The wear of the piston rings was also determined. Figure 3 shows the cylinder wear in the reversal zone, averaged over the circumference, as well as the associated running surface wear of the piston rings from the 1<sup>st</sup> groove.

Clearly evident is the reduced cylinder wear (40 % less) of the helical slide honed surface as compared to the pla-

teau honed surface. Piston ring wear, due to the GDC coating, which is known to be extremely wear-resistant, there is only a slight difference between the two honing methods.

### 4.2 Cylinder Wear After 3000 h (Helical Slide Honed)

To confirm the previous positive results, a engine was subject to an additional 3000 h run test and the cylinder wear measured. The measured wear was much lower than permissible limits (specified by Deutz per 1000 hours of run time) and significantly less than the plateau honed version of the base engine.

To graphically depict the extent of the wear distribution of the cylinder running surface, the measured wear values are shown as isolines in the diagram in Figure 4. It is clearly illustrated that nowhere in the cylinder is the wear higher than 15 µm. As known from the wear evaluations of many diesel engines, this measurement is also indicative of the influence of the injection spray on cylinder wear. In the region of injection spray, the lubrication film is partially washed from the cylinder wall, increasing cylinder surface wear.

To document the optical impression and to check for the formation of bore polishing, a picture of the cylinder surface was taken by means of a scanner, Figure 5.

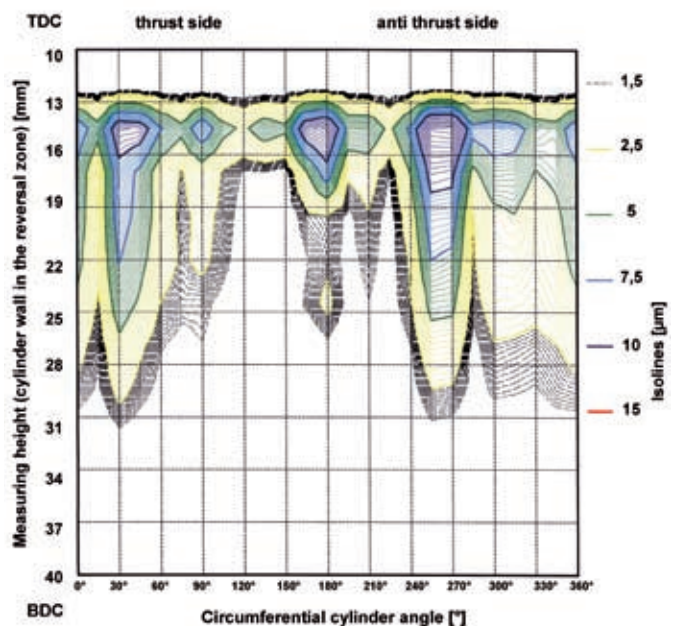


Figure 4: Isolines for the top ring reversal bore wear after 3000 h (helical slide honed)

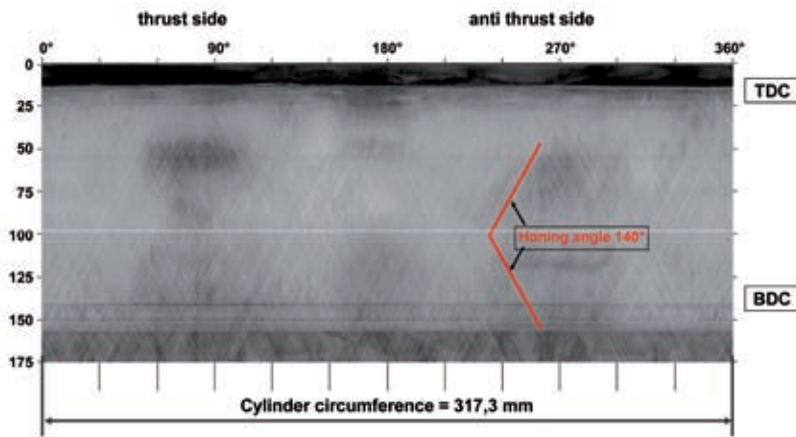


Figure 5: Cylinder scan after 3000 h of continuous running (helical slide honed)

After cylinder scanning, it can be seen that the cylinders have no bore polishing over the entire circumference and through the piston stroke, despite a narrow topland clearance. Honing valleys are still visible throughout the bore and the honing angle of 140°, typical of helical slide honing, is also clearly visible.

Lube oil consumption and blowby behaviour during the relevant engine operating conditions have been investigated using the Deutz endurance cycle test run. In the diagram, Figure 6, the results of the 3000 hour continuous run of a helical slide honed surface are compared with a 1500 hour of a plateau honed surface. The increased initial oil consumption measured is due to the measuring equipment and not attributed to either

honing quality. Over the test run time, helical slide honing is shown to have consistently lower oil consumption than the plateau honed surface due to the reduced core roughness depths and valley widths. No significant difference in blow-by behavior is noted between either honed surface.

In high and low idle running, a reduction of unburned oil in the exhaust system (slobber) could be observed for helical slide honing as compared to plateau honing. Helical slide honing, with its steeper honing angle, leads to a limitation in the oil film thickness at higher speeds, and therefore reduces oil consumption.

The piston shown in Figure 7 exhibits very low oil-carbon buildup on the top

land for the amount of run time and therefore has less of a tendency to create bore polishing. The increase in the lateral force also leads to a good wear pattern on the piston skirt with minimal wear for this long run time.

## 5 Discussion and Summary

The decision for helical slide honing was confirmed in the engine tests by:

- clear reduction in wear in the reversal zone by 40 % as compared to standard plateau honing (complying with the Deutz limit for 3000 hours of run time)
- no wear due to formation of bore polishing
- consistently low oil consumption over the entire engine run time
- reduction of oil slobber.

With the further engine development the requirement for the reduction of wear, oil consumption and friction will increase. Deutz will be well prepared for the Tier IV emissions levels with a helical slide honing process. For future research, UV laser exposure treatments could be potentially beneficial.

## References

- [1] Esser, J.; Linde, R.; Münchow, F.: Diamantbewehrte Laufschrift für Kompressionsringe. In: MTZ 2004 Nr. 7/8
- [2] Schmid, J.: Optimiertes Honverfahren für Gusseisen-Laufflächen. VDI-Berichte Nr. 1906 (2006)

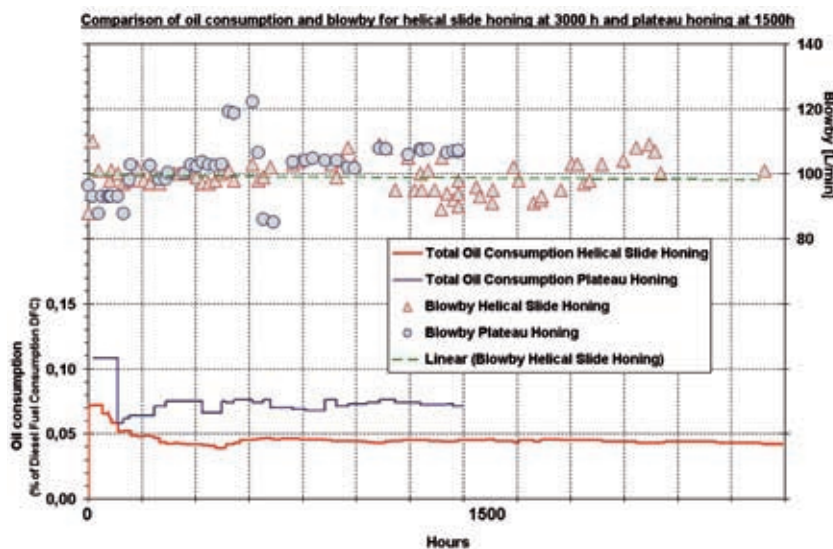


Figure 6: Oil consumption and blow-by comparison for helical slide honing and plateau honing

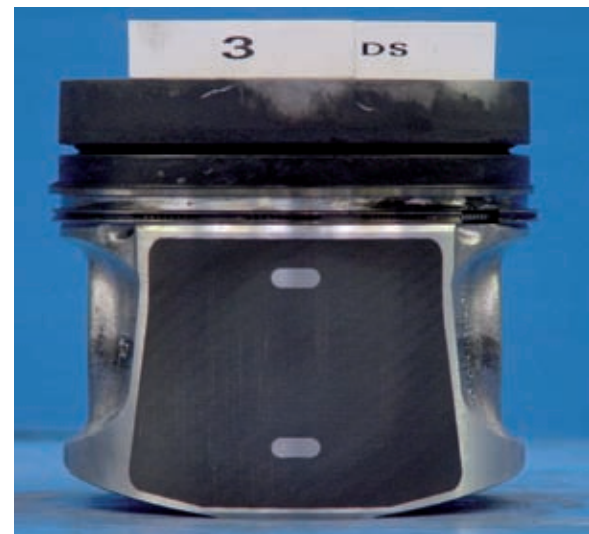


Figure 7: Piston after running for 3000 h

## Peer Review ATZ|MTZ

## Peer Review Process for Research Articles in ATZ and MTZ

## Steering Committee

<b>Prof. Dr.-Ing. Stefan Gies</b>	RWTH Aachen	Institut für Kraftfahrwesen Aachen
<b>Prof. Dipl.-Des. Wolfgang Kraus</b>	HAW Hamburg	Department Fahrzeugtechnik und Flugzeugbau
<b>Prof. Dr.-Ing. Ferit Küçükay</b>	Technische Universität Braunschweig	Institut für Fahrzeugtechnik
<b>Prof. Dr.-Ing. Stefan Pischinger</b>	RWTH Aachen	Lehrstuhl für Verbrennungskraftmaschinen
<b>Prof. Dr.-Ing. Hans-Christian Reuss</b>	Universität Stuttgart	Institut für Verbrennungsmotoren und Kraftfahrwesen
<b>Prof. Dr.-Ing. Ulrich Spicher</b>	Universität Karlsruhe	Institut für Kolbenmaschinen
<b>Prof. Dr.-Ing. Hans Zellbeck</b>	Technische Universität Dresden	Lehrstuhl für Verbrennungsmotoren

## Advisory Board

<b>Prof. Dr.-Ing. Klaus Augsburg</b>	<b>Dr.-Ing. Markus Lienkamp</b>
<b>Prof. Dr.-Ing. Bernard Bäker</b>	<b>Prof. Dr. rer. nat. habil. Ulrich Maas</b>
<b>Prof. Dr.-Ing. Michael Bargende</b>	<b>Prof. Dr.-Ing. Martin Meywerk</b>
<b>Dr.-Ing. Christoph Bollig</b>	<b>Prof. Dr.-Ing. Werner Mischke</b>
<b>Prof. Dr. sc. techn. Konstantinos Boulouchos</b>	<b>Prof. Dr.-Ing. Klaus D. Müller-Glaser</b>
<b>Prof. Dr.-Ing. Ralph Bruder</b>	<b>Dr. techn. Reinhard Mundl</b>
<b>Dr. Gerhard Bruner</b>	<b>Dr.-Ing. Lothar Patberg</b>
<b>Prof. Dr. rer. nat. Heiner Bubb</b>	<b>Prof. Dr.-Ing. Peter Pelz</b>
<b>Prof. Dr. rer. nat. habil. Olaf Deutschmann</b>	<b>Prof. Dr. techn. Ernst Pucher</b>
<b>Dr. techn. Arno Eichberger</b>	<b>Dr. Jochen Rauh</b>
<b>Prof. Dr. techn. Helmut Eichlleder</b>	<b>Prof. Dr.-Ing. Konrad Reif</b>
<b>Dr.-Ing. Gerald Eifler</b>	<b>Dr.-Ing. Swen Schaub</b>
<b>Prof. Dr.-Ing. Wolfgang Eifler</b>	<b>Prof. Dr. sc. nat. Christoph Schierz</b>
<b>Prof. Dr. rer. nat. Frank Gauterin</b>	<b>Prof. Dr. rer.-nat. Christof Schulz</b>
<b>Prof. Dr. techn. Bernhard Geringer</b>	<b>Prof. Dr. rer. nat. Andy Schür</b>
<b>Prof. Dr.-Ing. Uwe Grebe</b>	<b>Prof. Dr.-Ing. Ulrich Seiffert</b>
<b>Prof. Dr.-Ing. Horst Harndorf</b>	<b>Prof. Dr.-Ing. Hermann J. Stadtfeld</b>
<b>Prof. Dr. techn. Wolfgang Hirschberg</b>	<b>Prof. Dr. techn. Hermann Steffan</b>
<b>Univ.-Doz. Dr. techn. Peter Hofmann</b>	<b>Dr.-Ing. Wolfgang Steiger</b>
<b>Prof. Dr.-Ing. Günter Hohenberg</b>	<b>Prof. Dr.-Ing. Peter Steinberg</b>
<b>Prof. Dr.-Ing. Bernd-Robert Höhn</b>	<b>Prof. Dr.-Ing. Christoph Stiller</b>
<b>Prof. Dr. rer. nat. Peter Holstein</b>	<b>Dr.-Ing. Peter Stommel</b>
<b>Prof. Dr.-Ing. habil. Werner Hufenbach</b>	<b>Prof. Dr.-Ing. Wolfgang Thiemann</b>
<b>Prof. Dr.- Ing. Roland Kasper</b>	<b>Prof. Dr.-Ing. Helmut Tschöke</b>
<b>Prof. Dr.-Ing. Tran Quoc Khanh</b>	<b>Dr.-Ing. Pim van der Jagt</b>
<b>Dr. Philip Köhn</b>	<b>Prof. Dr.-Ing. Georg Wachtmeister</b>
<b>Prof. Dr.-Ing. Ulrich Konigorski</b>	<b>Prof. Dr.-Ing. Henning Wallentowitz</b>
<b>Dr. Oliver Kröcher</b>	<b>Prof. Dr.-Ing. Jochen Wiedemann</b>
<b>Dr. Christian Krüger</b>	<b>Prof. Dr. techn. Andreas Wimmer</b>
<b>Univ.-Ass. Dr. techn. Thomas Lauer</b>	<b>Prof Dr. rer. nat. Hermann Winner</b>
<b>Prof. Dr. rer. nat. Uli Lemmer</b>	<b>Prof. Dr. med. habil. Hartmut Witte</b>
<b>Dr. Malte Lewerenz</b>	<b>Dr. rer. nat. Bodo Wolf</b>

Seal of Approval – this seal is awarded to articles in ATZ/MTZ that have successfully completed the peer review process

Scientific articles in ATZ Automobiltechnische Zeitschrift and MTZ Motortechnische Zeitschrift are subject to a proofing method, the so-called peer review process. Articles accepted by the editors are reviewed by experts from research and industry before publication. For the reader, the peer review process further enhances the quality of ATZ and MTZ as leading scientific journals in the field of vehicle and engine technology on a national and international level. For authors, it provides a scientifically recognised publication platform.

Therefore, since the second quarter of 2008, ATZ and MTZ have the status of refereed publications. The German association "WKM Wissenschaftliche Gesellschaft für Kraftfahrzeug- und Motorentechnik" supports the magazines in the introduction and execution of the peer review process. The WKM has also applied to the German Research Foundation (DFG) for the magazines to be included in the "Impact Factor" (IF) list.

In the ATZ/MTZ Peer Review Process, once the editorial staff has received an article, it is reviewed by two experts from the Advisory Board. If these experts do not reach a unanimous agreement, a member of the Steering Committee acts as an arbitrator. Following the experts' recommended corrections and subsequent editing by the author, the article is accepted. *rei*

### MTZ Peer Review

The Seal of Approval for scientific articles in MTZ.

Reviewed by experts from research and industry.

Received .....  
Reviewed .....  
Accepted .....





personal buildup for Force Motors Ltd.

# Stop looking. Start finding.

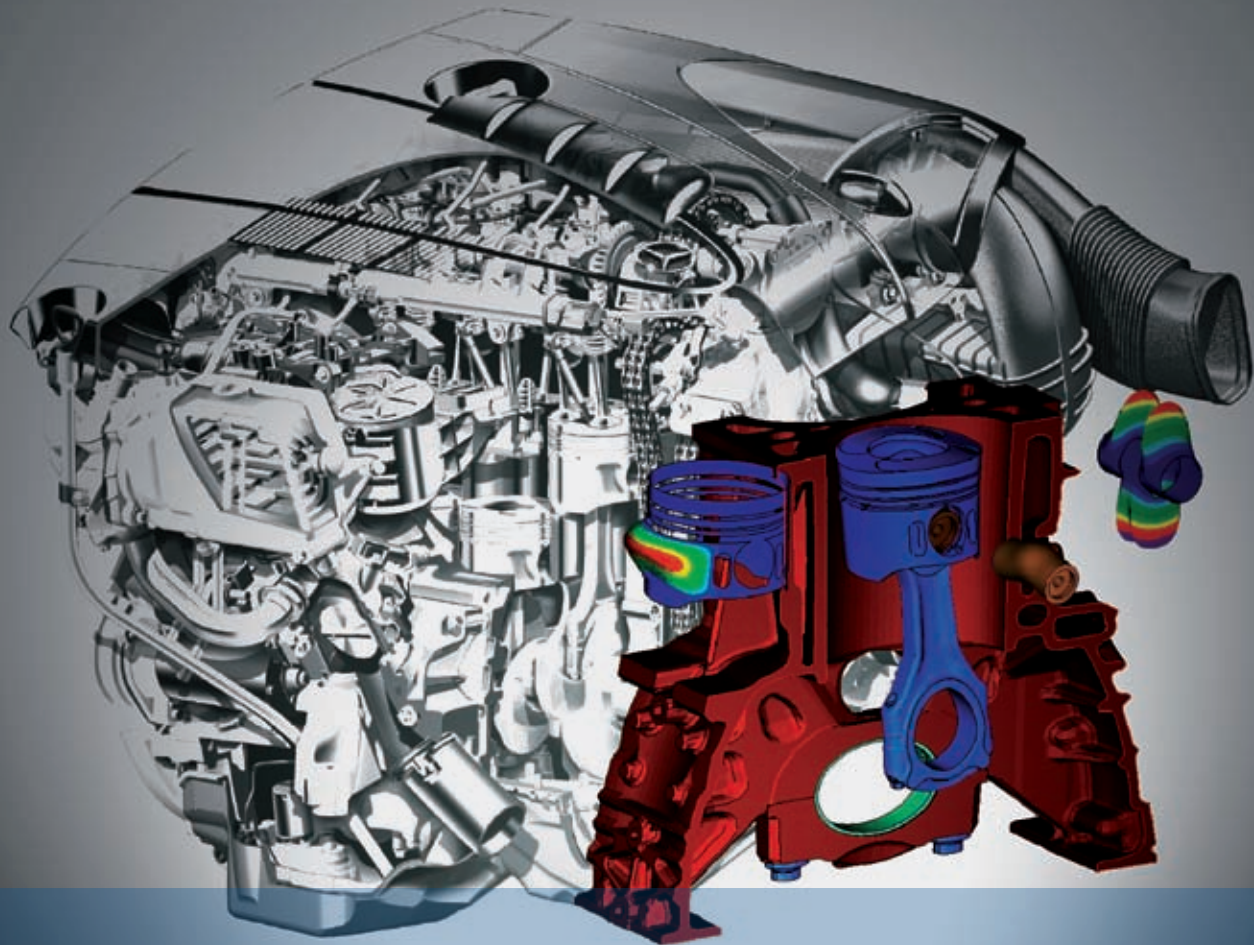
Information that inspires is the root of innovation. Staying up to date helps accelerate development. And substance is what makes knowledge valuable. ATZonline is the place to go when you want to know what's happening in our industry and to get information that is unique in its depth. ATZ, MTZ, ATZelektronik, ATZproduktion and ATZauto technology subscribers get access to a complimentary archive of industry articles as well as specials and whitepapers. All articles are well researched, with background and insider information.

No need to look any further – get your competitive advantage on [www.ATZonline.com](http://www.ATZonline.com)

**ATZonline. Know more. Go further.**

# ATZ online

Springer Automotive Media subscription service | Abraham-Lincoln-Str. 46 | D-65189 Wiesbaden  
Phone: +49 611.7878-151 | Fax: +49 611.7878-423 | SpringerAutomotive@abo-service.info | [www.ATZonline.com](http://www.ATZonline.com)



# Piston Pin in Mixed Friction Contact

## Elasto-hydrodynamic Simulation Theory for Support Analysis

Within the framework of the research project No. 868 of the FVV research association Verbrennungskraftmaschinen e. V. (Combustion Vehicles Reg.) a user-friendly numerically stable simulation tool was developed by Stuttgart University and Kassel University. The tool was validated by experiments, and offers designers and developers the possibility of system analysis and optimization of piston pin bearings. Non-linear elasto-hydrodynamic processes were included at the same time in the dynamically loaded bearing contacts of piston/piston pin and piston pin/connecting rod, with the reciprocal effects.

## 1 Introduction

Clearly rising combustion chamber pressure, downsizing and an increased specific performance density of new motor concepts lead to increased load on the bearing in the crank drive. This is particularly the case for tribological and mechanical loads on the piston pin bearing, the height of which is important in terms of function and life-span.

The solutions currently in use for a reliable design of the piston pin bearing are marked by comprehensive, frequently empirically acquired experience values of the manufacturers and seem to be no longer sufficient, because the incidents of damage in the piston hub and the small connecting rod eye are on the increase. A complete forecast for the design of this bearing system is no longer possible with simulation procedure currently available.

In terms of mechanics the dynamic system behaviour of the piston pin bearing leads to the scientific problem of the multi-body dynamically coupled elements, connecting rod, piston, piston pin and cylinder liner with elastic properties, local inertia effects and non-linear load transmission mechanisms, which are determined by elasto-hydrodynamic (EHD) effects, in which there may be temporary mixed friction conditions. Simulation techniques for a reliable design of the piston pin bearing therefore require a realistic image of the relevant influencing variables. This is the case in particular of retroactive and reciprocal effects of piston boss, piston pin and small connecting rod eye with respect to bearing deformation, mixed friction behaviour and piston pin movement.

## 2 Research Goal and Execution

The core aim of this research project is a simulation programme verified by experimental studies on a combustion engine for a reliable design and optimization of the piston pin bearing. The theoretical work is based on the programme system Pimo3D developed in a previous project to calculate the piston-cylinder dynamic [3]. The extension of the multi-body system (MBS) systematic on the connecting rod and the introduction of the double-sided EHD contact between pis-

ton pin and small connecting rod eye are important development stages. The implementation of a local mixed friction model in the pin bearing of the piston and connecting rod side is a further success. The aim is to consider the friction torque balance to calculate the pin rotation movement and its effect on the load bearing behaviour in the bearings.

The experimental studies are based on two objectives. One, they provide input variables for the calculation and serve to validate the results. Two, they provide relevant information about the tribological behaviour of the piston pin bearing using different geometric variants with regard to piston pins and form drilling of the piston hub at various stages of operation.

## 3 Model Building of the Simulation Programme Pimo3D

The construction of a simulation model for the structural or elasto-hydrodynamic system analysis of the crank drive is carried out with the main focus on the calculation of the piston pin movement. The pin displacement and rotation is determined principally by the formation of the hydrodynamic lubricant film and the solid body contact in the pin bearings and the associated frictional torques. The tribological contact situation in turn can be represented only allowing for the structural dynamic of connecting rod, piston pin and piston as well as the crank dynamic mass forces.

### 3.1 Multi-Body Dynamic Model Design of the Crank Drive

The multi-body dynamic model construction of the crank drive is necessary to ascertain the resulting forces and torques of the crank drive components and their movement state. The crank drive of the model construction under consideration is made up of the crank pin mounted counter to the bottom, connecting rod, and piston pin, piston and cylinder liner. The crank, connecting rod and piston pin move in the oscillation level of the crank drive; the crank drive can also slide in the piston pin axis direction. The cylinder liner is spatially fixed.

The MBS bodies are defined by masses, inertia moments, gravity and pin joint

## The Authors



Prof. Dr.-Ing. **Gunter Knoll** is Director at the Institut für Maschinenelemente und Konstruktionstechnik at Kassel University (Germany).



Prof. Dr.-Ing. **Michael Bargende** is Professor at the Institute for Internal Combustion Engines and Automotive Engineering at Stuttgart University (Germany).



Dr.-Ing. **Jochen Lang** is Head of Technical Analysis at the IST GmbH in Aachen (Germany).



Dr.-Ing. **Ulrich Philipp** is Department Head of NVH and Mechanics at the Research Institute FKFS in Stuttgart (Germany).



Dipl.-Ing. **Maik Lazzara** is Scientific Assistant at the Institute for Internal Combustion Engines and Automotive Engineering at Stuttgart University (Germany).

### MTZ Peer Review

The Seal of Approval for scientific articles in MTZ.

Reviewed by experts from research and industry.

Received ..... November 13, 2008

Reviewed ..... December 11, 2008

Accepted ..... January 19, 2009

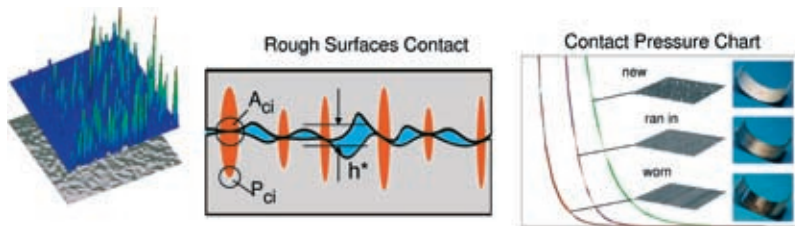


Figure 1: Contact pressure simulation to ascertain contact pressure-engine operating maps

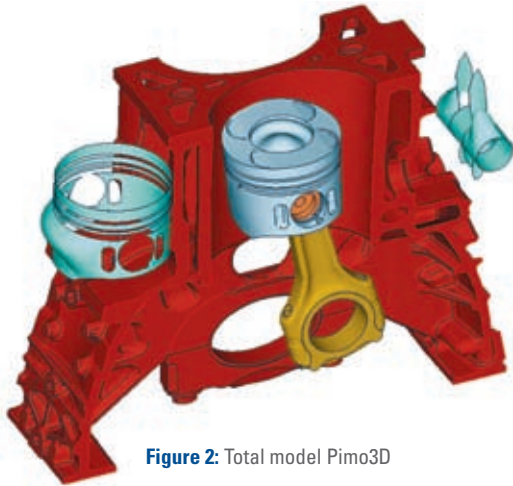


Figure 2: Total model Pimo3D

bearing. The fixed body accelerations calculated by means of the MBS algorithm [1] provide the local inertia forces because of the crank drive dynamic, which in turn represent an important determining factor in the simulation deformation of the elastic bodies.

### 3.2 Tribological Model Design of the Bearings

The load bearing pressure build-up in friction bearings is made up of an overlaying of two bearing pressure components:

- EHD-bearing pressure build-up in the lubricant film
- Solid body contact pressure between the surface roughnesses of the friction surfaces.

#### 3.2.1 Elastohydrodynamics

The hydrodynamic bearing pressure between rough elastic friction surfaces is defined by the complete Reynolds differential equation for the rough surfaces, see Eq. (1):

$$\frac{\partial}{\partial x_i} \left[ \phi_{ij}^p \frac{\bar{h}^3}{12\eta} \frac{\partial \bar{p}}{\partial x_j} \right] = u_i^z \frac{\partial \bar{h}}{\partial x_i} + \frac{\partial \bar{h}}{\partial t} + u_i^\Delta \sigma \sigma^\Delta \frac{\partial \phi_{ij}^s}{\partial x_j} \quad \text{Eq. (1)}$$

It describes the connection between the movement state of rough friction surfaces and the hydrodynamic bearing pressure that is produced as a result. The elasticity and the contouring or wear of the friction surfaces goes into the bearing pressure build-up via the sinc-function, which is aligned at each moment.

The pressure flow tensor  $\phi_{ij}^p$  and the shear flow tensor  $\phi_{ij}^s$  contain the influence of the surface roughnesses on the hydrodynamics pressure build-up. They are ascertained either via a numerical flow simulation on the basis of measured (where appropriate run-in) surface roughnesses or via synthetically produced roughnesses [4].

#### 3.2.2 Roughness Contact

With small lubricant cracks as a result of high load and/or low slippage or extrusion speeds (or low lubricant filling state) the roughness points come into contact and, in addition to hydrodynamic bearing pressure build-up, local solid body contact develops. The connection between nominal crack width and the pressure build-up through roughness contact is ascertained like the flow tensors through numerical flow simulation. The discretized roughness pairing is compacted to a prescribed nominal crack width, allowing for the deformation of the roughness points, and the local solid body contact pressure deposited in a corresponding engine operating map. In this way run-in or worn surface structures can be analysed, Figure 1. This operating map is then evaluated during the real EHD simulation in each time step [4].

The mixed friction model used in the developed simulation programme is the result of an overlay of the hydrodynamic fluid friction (made up of friction parts through shearing and extrusion) and solid body contact friction, see Eq. (2):

$$F_{Reib} = \int \eta \frac{U}{h} + \frac{h}{2} \frac{\partial p}{\partial x} dA + \mu_c \int p_c dA \quad \text{Eq. (2)}$$

Hydrodynamic      SolidBodyContact

While the fluid friction part can be reliably calculated, because it depends only on crack width, viscosity and movement state, the solid body friction part can be calculated only via a Coulomb friction value  $\mu_c$  from the contact pressure. Because in the current state of technology such friction values cannot be calculated, the friction value has to be ascertained from experimental studies and specified in the simulation as input variable.

### 3.3 Friction Torque Determined Pin Rotation

The torque balance in the piston pin is determined by the mixed friction torque in the connecting rod eye and in the piston boss as well as (to a lesser extent) in the rotation inertia of the piston pin. As a result of the different solid body contact states in both bearings, the piston pin may stick and slip changeably from time to time in relation to piston and connecting rod. This alternation between stick and slip makes demands in the numerical implementation, because in the transition phase between both states strongly fluctuating solid body friction torque may occur. To solve this problem a stable transition algorithm was developed in the simulation programme that was able to bring about stick and slip states in the piston pin bearing.

### 3.4 Structural-Dynamic Model Design of the Bodies

The calculation of the structural deformation of the elastic bodies can be done by solving the Newtonian movement equation in each time step and integrating the accelerations and bearing positions. The indirect integration of the knot-related acceleration in the present case is not practicable because of the high freedom-degree number of the FEM nets of engine components used in industry. A mixed static-modal reduction scheme is therefore used in the present simulation programme to reduce the number of integration freedom-degrees without losing the structural information necessary for the loading [2].

### 3.5 Pimo3D Total Model

The total model of the programme system Pimo3D is shown in Figure 2. It includes the crank drive from the crank to the cylinder liner, where the connecting rod, piston pin, piston and cylinder are depicted as elastic bodies. Lubricant films and mixed friction are taken into consideration in the tribological pairings piston/cylinder and piston pin/connecting rod. In the tribological pairings the local contact surface geometries can be recorded as overlay of production contour, thermal distortion and, where appropriate, wear-and-tear.

The local and global elastic deformation of the crank drive components is also included in the calculation, such as temporally and spatially changing filling state efficiency in the lubricant films. The coupling of the partial complexes, multi-body dynamics, friction surface tribology and structural dynamics, occurs via a gradually controlled step size integration scheme that is especially aligned to rigid differential equations and thus has a high numerical stability and computational time efficiency.

## 4 Experimental Validation

The experimental studies are carried out exclusively on a full engine and not an externally motorized test bed, because only in this way can marginal conditions, such as piston and connecting rod temperatures, load-dependent and thermal deformations of the bearing components, connecting rod, piston pin and piston as well as lubricant supply of the bearing positions be realistically depicted. A supercharged direct injection four-cylinder diesel engine of the series OM646 (Daimler AG) was used as the test carrier. All measurement variables were recorded synchronically on one cylinder.

To validate the simulation results the piston pin movement was investigated relative to the piston whereat movement components in axial and radial directions and the pin rotation were recorded. In addition a non-contact route measuring system was used, the distance sensors of which work according to the eddy current loss principle. In addition, mixed friction contact of the piston pin with

the connecting rod eye and piston boss is detected via an electric voltage measurement. To record these measurement variables a connecting rod- and piston-proof application of the sensors is necessary, the measurement value transmission of which is realized, grid-bound, via a pin-joint gear aligned with the test carrier.

### 4.1 Radial Movement of the Piston Pin

To determine the radial piston pin movement the distance sensors were implemented in the piston boss. In this way the relative movement between the piston boss and the piston pin, which results from both the bearing play and the dynamic components deformation, was recorded. The application of the

four sensors (total) was done in pairs on two levels and set at 90° so that the movement components in the stroke and lateral directions were recorded. With the positioning on two levels the quality of the bearing play, structural deformation and contact surface distortions were verified.

Figure 3 shows a comparison between calculation and measurement of the radial piston pin movement, as examples, at two operating points via a four-cycle working period: 1000 rpm trailing throttle and 3000 rpm full load, where in the experimental results ten individual working periods are shown superimposed on each other. The comparison shows a high level of agreement.

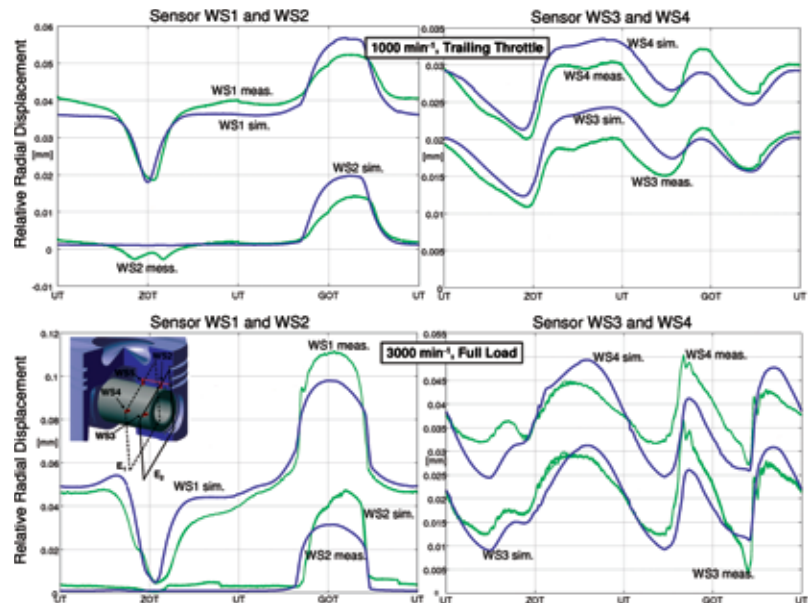


Figure 3: Comparison of radial relative movement in stroke and lateral direction

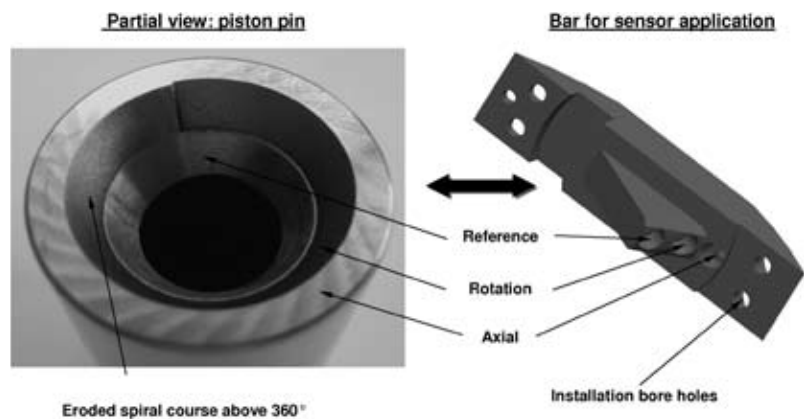


Figure 4: Measuring principle for recording the piston spin rotation movement

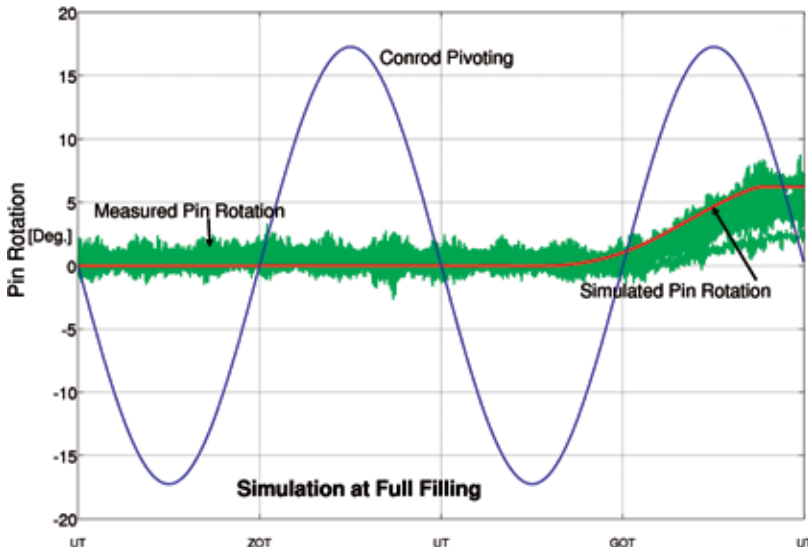


Figure 5: Comparison of the pin rotation at 1000 rpm, trailing throttle with lubricant full bore in the bearings

4.2 Rotation Movement of the Piston Pin

The recording of the rotation movement of the piston pin, Figure 4, is recorded on the front surface at the pin end on a linearly rising spiral course eroded on the surface, where the rising depicts a measure for the rotation angle. Rigidity and deformation properties of the piston pin thus continue to be unaffected. The sensor application is on a bar, which is screwed onto the piston eye. An additional reference sensor serves to compensate for the radial and axial movement and component deformation that overlay the real measuring signal of the rotation.

Figure 5 shows the comparison between the simulated and measured pin rotation at 1000 rpm trailing throttle, and lubricant full bore in the piston and connecting rod-side bearing positions. In addition, the rotation movement of the small connecting rod eye is shown for the purpose of orientation. In the area of BDC (before TDC) up to TDC the pin sticks on the piston (no pin rotation), followed by a brief rotation of the pin with that of the connecting rod eye by approximately 5° counter to the crankshaft rotation direction. The comparison of measurement and simulation shows for this operating point a high level of agreement.

The comparison of the pin rotation at 1000 rpm, full load at full bore is shown left in Figure 6. The pin rotation shows the same tendency in the simulation as in the measurement, but the amount of rotation is clearly smaller. An occasional reduction of the lubricant filling state in the connecting rod bearing leads to higher mixed friction in the connecting rod bearing and thus to an increased pin rotation that corresponds to the rotation measured (right in Figure 6).

4.3 Mixed Friction Contact Detection

The measuring procedure designed for contact detection is based on the electric conductivity between the friction partners, connecting rod, piston pin and piston. As in Figure 7 an electric circuit is produced via the bearing bush on the connecting rod, the piston pin, piston and piston-rings to the cylinder liner and/or crankcase. The bearings, connecting rod/piston pin and piston pin/piston, function according to contact as switches.

A prerequisite for implementing this measuring principle is the electric isolation of the bearing bush in the small connecting rod eye from the connecting rod bar. This function is performed by an oxide-ceramic intermediate layer.

Because of the electric series connection of the two contact pairings, connecting rod/piston pin and piston pin/piston, this measuring principle makes it possible to detect the following friction states:

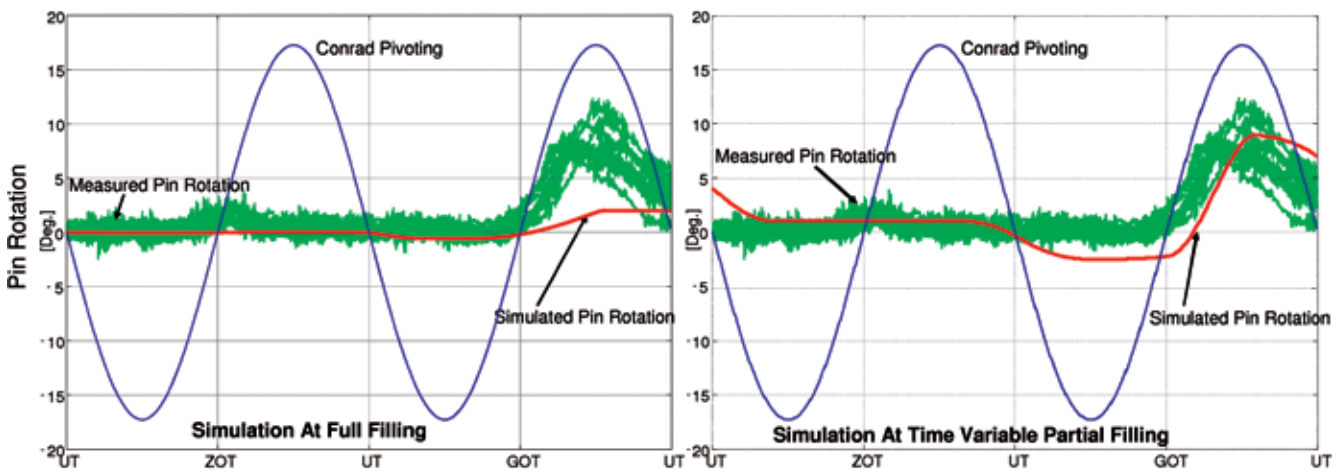


Figure 6: Comparison of the pin rotation at 1000 rpm, full load with lubricant full bore and temporally variable partial bore in the bearings

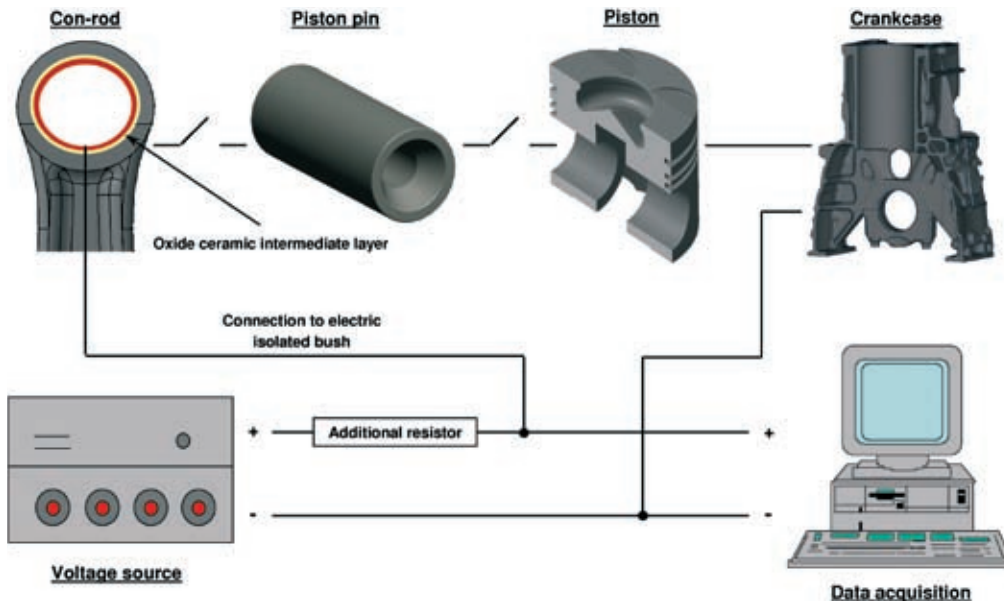


Figure 7: Measuring principle to detect mixed friction

- electric circuit closed: mixed friction in both bearings
- electric circuit open: hydrodynamics in both or in one of the two bearing positions.

To compare the mixed friction states in measurement and simulation the simulated contact pressure course in both pin bearing positions is contrasted with the measured contact voltage signal. Agreement in measure and simulation occurs when both calculated contact pressure courses are unevenly zero when the contact voltage is broken.

Figure 8 shows the comparison between the calculated solid body contact pressures and the measured contact voltage signal for the operating points 1000 rpm, trailing throttle, and 3000 rpm, full load. In the two bearings a full bore state of the lubricant was assumed. In the pointed lower area mixed friction contact appears in the simulation in both contact points and simultaneously the contact voltage breaks down. There is thus a high level of agreement with regard to the simultaneous appearance of mixed friction in both pin bearing positions.

A further comparison of the mixed friction states is shown in Figure 9, left diagram, for the operating point 3000 rpm, trailing throttle at full bore. The measuring signals show clearly more mixed friction phases in both bearings than the simulation. In the piston boss the simulation shows a lot of mixed friction, but

in the connecting rod eye there is hardly any mixed friction. The comparison indicates that at this operating point in the measurement a partial bore state in the connecting rod eye must have occurred.

In a further simulation run therefore the lubricant filling state in the connecting rod eye is clearly reduced. The calculated result is shown in the right diagram of Figure 9. Via the partial bore, mixed fric-

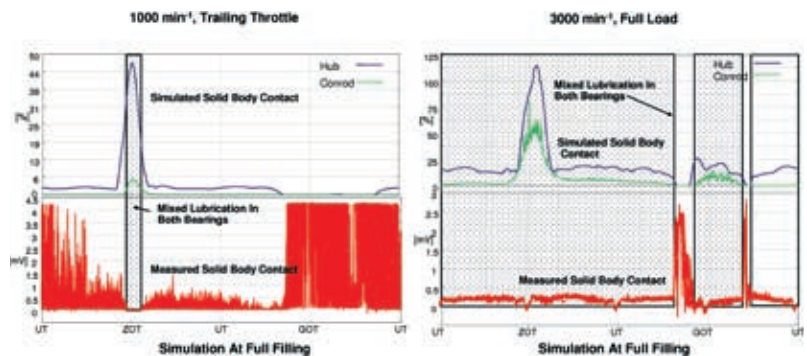


Figure 8: Mixed friction comparison at 1000 rpm, trailing throttle and 3000 rpm, full load with lubricant full bore in the bearing positions

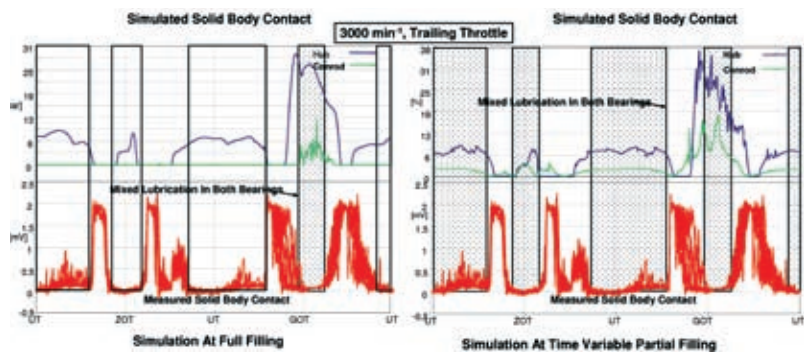


Figure 9: Mixed friction comparison at 3000 rpm, trailing throttle, dragging with lubricant full bore and temporally variable partial bore in the bearing positions

### Acknowledgements

This paper is the scientific result of project No. 868 „Piston pin bearing“, set by the Research Association for Combustion Power Machines (Forschungsvereinigung Verbrennungskraftmaschinen e. V. (FVV, Frankfurt/Main, Germany)) and carried out at the Institute for Machine Elements and Construction Technology of the University of Kassel under the direction of Prof. Dr.-Ing. Gunter Knoll and at the Institute for Internal Combustion Engines and Automotive Engineering of the University of Stuttgart under the direction of Prof. Dr.-Ing. Michael Bargende. The project was financially supported by the

Federal Ministry for the Economy and Technology (Bundesministerium für Wirtschaft und Technologie) via the Consortium of Industrial Research Associations (Arbeitsgemeinschaft industrieller Forschungsvereinigungen e. V.). The project was monitored by a working group of the FVV under the direction of Dr.-Ing. Uwe Lehmann, Federal-Mogul Wiesbaden GmbH. The authors are very grateful to the working group for generous support, especially to Daimler AG for making the test carrier available and to Federal-Mogul Wiesbaden GmbH and Mahle GmbH for providing materials at no charge.

tion states appear with greater frequency, so that a high level of agreement between measurement and simulation could be achieved.

### 5 Summary

The final result of this FVV research project No. 868, worked out at Stuttgart University and Kassel University, is a user-friendly software package for the design and optimization of the piston pin bearing with respect to tribological and structural processes. The calculation of the journal and thrust development in the elastic tribological pairings piston/cylinder, piston/piston pin and piston pin/connecting rod was made considering mixed friction conditions and temporally changing lubricant filling states. The torque friction-determined pin rotation was determined by taking the change between static and tribological friction in both pin bearings into account.

The validation of the simulation results by the experimental investigations shows in the radial piston pin rotations qualitatively and quantitatively a high level of agreement. Comparing the calculated and measured mixed friction contact states and the piston pin rotation it was also possible to achieve a high level of agreement, whereby the assumption of partially temporally changing lubricant part filling states in the bearings was necessary. Altogether the comparisons of the pin rotation movement show a strong dependency on the

bearing parameters of warming-up contour, lubricant filling state and solid body friction value. Thermal distortions can easily be considered in the simulation because they are comparatively easy to measure. The partial filling states assumed in the calculation under undefined oil supply conditions and solid body friction values are difficult to measure and simulate and have to be given at the current development stage as marginal conditions.

### References

- [1] Haug, Edward J.: Computer Aided Kinematic and Dynamics of Mechanical Systems. Allyn and Bacon, 1989
- [2] Gasch, R.; Knothe, K.: Strukturdynamik. Band 2: Kontinua und ihre Diskretisierung. Springer-Verlag, Berlin, 1989
- [3] FVV-Forschungsvorhaben Kolben-Zylinder-Dynamik. AIF-Nr. 8894, Heft-Nr. 631, FVV e. V., Frankfurt/Main, 1996
- [4] Knoll, G.; Lagemann, V.: Kontaktmodell rauher Oberflächen mit elastischen Rückwirkungen. DFG-Vorhaben Kn 266-5/3, 1995